INDIVIDUAL TUBE TRANSFER COEFFICIENTS IN A SEGMENTALLY BAFFLED SHELL AND TUBE EXCHANGER.

****
****

A thesis submitted to
The University of Aston in Birmingham
for the degree of
Doctor of Philosophy.

Peter Charles Otway Roberts.
Department of Chemical Engineering.
April 1969.

SUMMARY

A review of the literature pertaining to shellside heat transfer coefficients in segmentally baffled cylindrical shell and tube heat exchangers has been made. It is shown that this work has dealt mainly with bundle average transfer coefficients and these studies have been correlated to give empirical equations which allow similar exchangers to be designed yet do not predict the effect of the geometric parameters on the flow distribution.

A review of the literature relating to work carried out on heat exchangers using a mass transfer analogy has also been made. It is demonstrated that the mercury mass transfer analogy is the best of the methods so far developed for this approach.

Following the work of Williams (2) and Haggart (6) a reliable system of renewing a mercury transfer surface in situ has been developed. This transfer surface has been installed in an exchanger similar to that used by Williams but employing air instead of nitrogen as the shellside fluid, and the results obtained from this exchanger are compared with the results of Williams. The exchanger was of $5\frac{1}{4}$" I.D. and consisted of 80 tubes of $\frac{3}{8}$" O.D. Baffles were manufactured to give cut downs of 18.4%, 31% and 43.7% of the shell diameter at a baffle spacing of 3.86". Gaskets were employed to prevent tube to baffle and baffle to shell leakage.

A completely new analysis, using statistical methods where appropriate, has been made of the results of Bergelin et al. (1) and Williams (2) with particular reference to the individual tube results

obtained by Williams. The results of this analysis are presented in the form of tube groups which are independent of flowrate, and from this it is shown that the 31% baffle cut down gives the most even transfer of the three baffle cut downs studied.

****
****
**

TABLE OF CONTENTS.

ACKNOWLEDGEMENTS

The author wishes to express his sincere thanks to the following:-

Professor W.G. Parker, Head of the Chemistry Department, where this research began.

Professor G.V. Jeffreys, for his advice and encouragement.

Dr. B. Gay, for his help, encouragement and supervision.

The Technical Staff of the Chemical Engineering and Chemistry Departments for their help in workshop matters.

Mrs. J. Griffin for her help in using the PDS 1020 computer.

Miss W.M. Powis for her diligent typing.

****
****
**

INTRODUCTION

Economy in the utilisation of heat is extremely important in chemical processes, and depends very much upon the effectiveness of the equipment for transferring heat between fluid streams. Amongst the wide range of equipment available for heat transfer the cylindrical shell and tube heat exchanger is prominent, and accurate heat transfer data for flow on both the inside and outside of the tubes is required for the design of this type of heat exchanger.

Compared with the shellside flow i.e. the flow outside the tubes, the tube side flow is very simple and has been extensively studied with the result that the tubeside heat transfer can be reasonably accurately predicted.

The geometry of the exchanger, e.g. baffle cut down, baffle spacing and clearances, causes the shellside flow path to be extremely complex with the result that it is difficult to isolate and investigate the effect of any one geometric parameter on the heat transfer. A considerable amount of work has been carried out on shellside heat transfer, but this has dealt mainly with bundle average shellside heat transfer coefficients. The data obtained from these studies have been empirically correlated to account for the various exchanger configurations, but the correlations only allow similar heat exchangers to be designed and do not predict changes in the flow patterns due to the geometric parameters. To allow heat exchanger design to progress it is essential that the effect of these individual geometric parameters on the shellside flow should be investigated.

The most comprehensive work to date dealing with bundle average heat transfer coefficients in segmentally baffled shell and tube heat exchangers has been carried out by Bergelin et al. at Delaware University and has been summarised in a report (1). Bergelin et al. carried out an extensive programme covering a study of bundle average heat transfer coefficients in rectangular tube banks and cylindrical shell and tube heat exchangers, with and without leakage, but the complexity of the shellside flow made the development of a general shellside heat transfer correlation very difficult.

A different approach is to determine the individual tube heat transfer coefficients and from these synthesise the zonal and bundle averages. The effect of the geometrical factors on the individual tube heat transfer coefficients may be determined in this way and the flow patterns clarified. Also this method of investigation can lead to elimination of hot spots, which is of extreme importance when heat sensitive materials are being processed. Early investigations of this type were carried out using model exchangers not really representative of industrial design, and so the results, while useful qualitatively, could not be used to predict accurately heat exchanger performance. The major work to date on individual tube transfer coefficients has been carried out by Williams (2) and Gay & Williams (46). As it is experimentally extremely difficult to determine individual tube heat transfer coefficients in an exchanger Williams adopted a mass transfer technique and expressed his results in a form from which the corresponding heat transfer data could be calculated using the Chilton and Colburn analogy (3). Williams

carried out a programme which studied individual tube mass transfer coefficients in a segmentally baffled shell and tube heat exchanger without leakage, similar to the exchanger used by Bergelin, and related his individual tube coefficients to the bundle average coefficients obtained by Bergelin.

The mass transfer technique used by Williams employed mercury evaporation and had been previously used by Maxwell and Storrow (4) and Potter (5). Williams' apparatus was somewhat complicated and had a limited Reynolds number range, and so a programme was initiated in the present work to simplify the experimental techniques and also to extend the Reynolds number range. The major simplification was to use air instead of nitrogen as the shellside fluid, which removed the need to employ a closed circuit. The use of air as the shellside fluid has the disadvantage of limiting the constant rate transfer period, as the surface becomes oxidised so that the transfer surfaces must be removed from the apparatus and be renewed after each experimental run. This entails a great deal of stripping and rebuilding of the apparatus and so a system was devised whereby the mercury transfer surfaces could be renewed in situ, i.e. the mercury surface could be renewed without removal from the exchanger bundle, a technique which had been initially investigated by Haggart (6). By this means it was possible to extend the constant rate transfer period for an indefinite time. The limiting factor as far as high flowrates were concerned in Williams' apparatus was that mercury droplets tended to blow off the non-draining horizontal transfer tubes into the bundle, and thus cause erroneous results to be

obtained. The use of the in situ technique required that the transfer surfaces should be vertical and able to drain and thus there was less chance of mercury droplets being blown into the bundle. Further, if mercury droplets were blown into the bundle they were very quickly oxidised by the air stream and thus did not affect the results to any marked degree. (The vapour pressure exerted by oxidised mercury is about 5% of that exerted by a free mercury surface.)

The present work also contains an extensive analysis of the results of Williams and Bergelin. These results were available in the form of tables, or tube groupings for a given flowrate, and were thus difficult to assess. It was therefore felt that a quantitative analysis of these results, employing statistical methods where appropriate, would permit a clearer understanding of the effects of the geometrical parameters upon the shellside transfer patterns. This analysis presents groups of tubes of similar transfer characteristics which are independent of flowrate. These tube groups indicate the transfer patterns and hence the flow patterns on the shellside of the model exchanger, and show very clearly the effect of baffle cut down on exchanger performance at the baffle spacing studied.

****
****
**

HEAT TRANSFER TERMINOLOGY

It has been found that a certain confusion exists in the terminology used in discussing heat transfer coefficients. In the present work the following terminology is used, and is presented as being more self-explanatory and less ambiguous than that previously used.

(a) Bundle Average Transfer Coefficient.

This is the average value of the transfer coefficient for the entire baffle compartment. This value was previously referred to as the average transfer coefficient.

(b) Zonal Average Transfer Coefficient.

Bergelin et al. (1) divided the shellside into two flow zones:- the cross flow zone and window zones. The cross flow zone is that region enclosed between planes through the baffle edges. The remaining region, enclosed between alternate baffles, the shell wall and a plane through the central baffle edge, constitutes the window zone. These zones are shown in Figure 1 (page 7).

The cross flow and window zone average transfer coefficients may be defined similarly to the bundle average transfer coefficient.

(c) Individual Tube Transfer Coefficient.

This is the average value of the transfer coefficient for a particular tube of length equal to the baffle spacing.

(d) Local Transfer Coefficient.

This should really refer to a point value, or more practically to the transfer coefficient for a length of a particular tube very

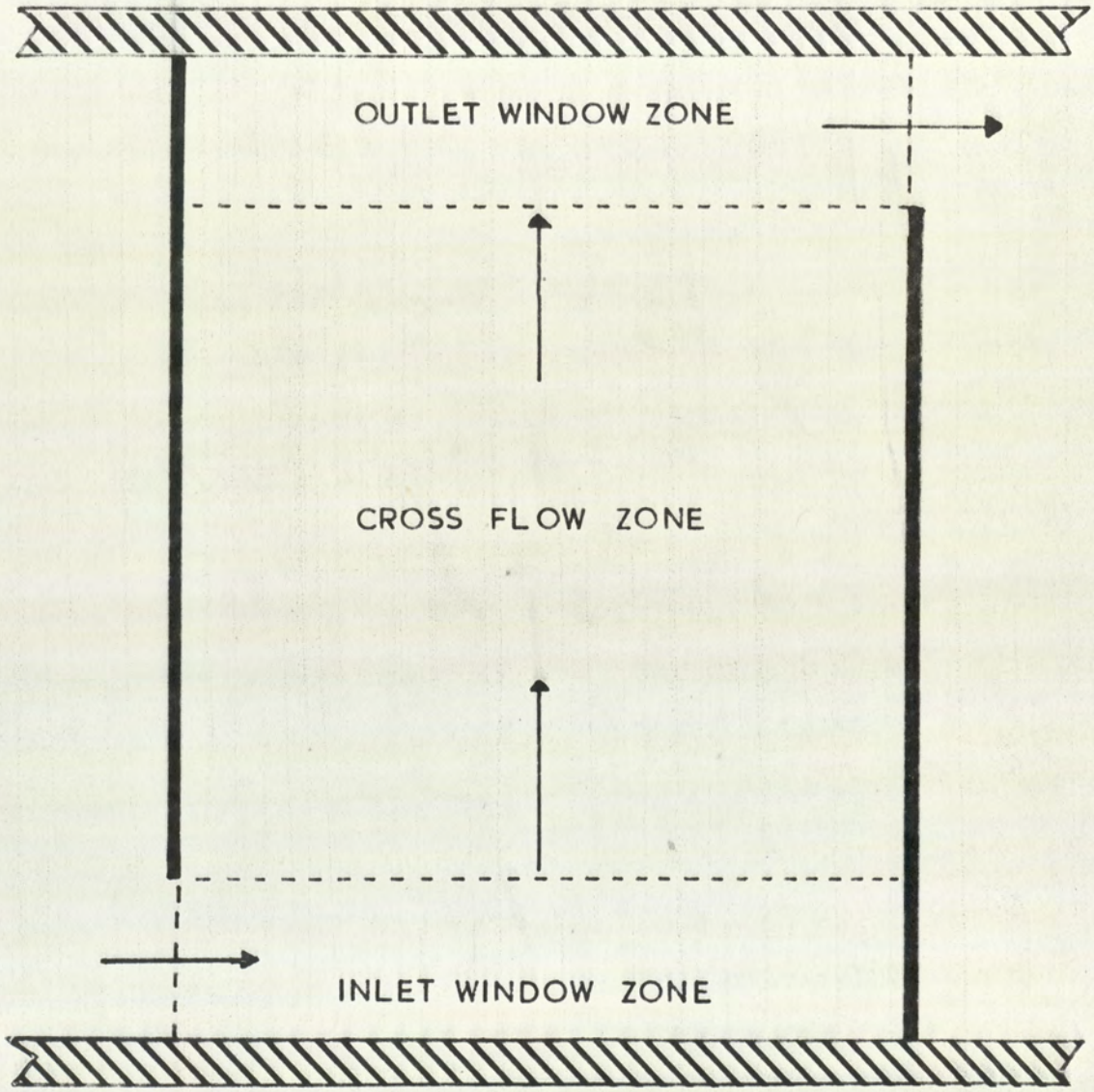

FIG. 1. – FLOW ZONES.

much less than the baffle spacing.

In the previous literature the "local coefficient" often referred to what is called in the present work the individual tube coefficient, and so a certain ambiguity resulted.

****
****
**

CHAPTER I.

PREVIOUS WORK ON HEAT TRANSFER IN RECTANGULAR TUBE BANKS AND SEGMENTALLY BAFFLED SHELL AND TUBE HEAT EXCHANGERS.

A. Flow normal to rectangular tube banks.

Heat transfer for flow normal to unbaffled rectangular tube banks provides basic information from which baffled cylindrical shell and tube heat exchangers may be studied. The effect of tube bank variables, i.e. tube size, tube spacing and tube arrangement, have been investigated by several authors (7, 8, 9, 10, 11, 12, 13, 14) over a wide range of Reynolds numbers. It is of interest to note here that one of the earliest workers in this field, Thoma in 1921 (15) used a mass transfer analogy, as have several other workers (14, 16, 17)since. These mass transfer analogies will be fully discussed in Chapter II. Colburn (8) correlated the data for rectangular tube banks, up to 1933, for a range of $1{,}000 < Re < 10{,}000$ and showed that the data for in line tube arrangements fell 40% below the data for staggered tube arrangements. The data for staggered square and triangular tube arrangements correlated on one curve. It was further shown that straight parallel lines represented the viscous flow data whereas there was a distinct curvature in the lines representing the transition and turbulent zone data. An increase in tube size and spacing was found to lower heat transfer, and it was also observed that the in line tube arrangement data were lower and more scattered than the staggered tube arrangement data. Bergelin, Brown and Doberstein (13) then linked the data for viscous and turbulent flow, and showed that the discrepancy

between in line and staggered tube arrangements disappeared at a Reynolds number of 5,000 and the data became coincident.

Weisman (18) correlated the results of several workers (7, 11, 12, 13, 14) to a deviation of less than 10% for staggered tube arrangements, and 15% for in line tube arrangements, by incorporating a void volume factor in the j - factor correlation.

Other workers (14, 19, 20, 21) have investigated transfer from individual tube rows within a tube bank, and all publish similar results for the heat transfer variation from row to row. The transfer from the first row was found to be 40% less than the average value. The transfer then increased to a maximum value at the third row, fell slightly to the fourth row and thence remained constant through the tube bank.

B. Flow in segmentally baffled shell and tube heat exchangers.

(i) Tubeside flow.

Because of its relative simplicity, compared with shellside flow, tubeside flow is much more clearly defined than shellside flow, and all workers have published similar results.

The flow in tubes is usually maintained in the turbulent region because higher heat transfer coefficients are obtained under these conditions.

For tubular flow conditions inside pipes Colburn (8) recommends:-

$$\frac{hd}{k} = 0{\cdot}023\ (Re)^{0{\cdot}8}\ (Pr)^{0{\cdot}4} \quad \text{for} \quad Re > 4{,}000$$

For high viscosity oils, where turbulent flow conditions cannot be employed because of the resultant high pressure drop across the equipment, Seider and Tate (22) recommend:-

$$\frac{hd}{k} = 1{\cdot}86 \left[Re.\ Pr.\ \frac{d}{l} \right]^{\frac{1}{3}} \left(\frac{\mu}{\mu_S} \right)^{0{\cdot}14} \quad \text{for} \quad Re < 2{,}100$$

For the range $2{,}100 < Re < 7{,}000$ the effect of the ratio $\frac{d}{l}$ diminishes to zero.

For high viscosity oils in turbulent flow Seider and Tate recommend:-

$$\frac{hd}{k} = 0.027 \ (Re)^{0.8} \ (Pr)^{0.33} \left(\frac{\mu}{\mu_s}\right)^{0.14} \quad \text{for } Re > 2,100$$

(ii) Shellside flow.

(a) Bundle average heat transfer coefficients.

The extreme complexity of the shellside flow in a baffled cylindrical tube bundle causes the heat transfer coefficients to be extremely difficult to predict. The geometrical parameters affecting the flow are:- the cylindrical shell, baffle cut down, baffle spacing, tube diameter, pitch and arrangement, clearances or leakage paths. Clearances, required by mechanical construction considerations, allow flow between baffle and shell, and between tube and baffle hole. A third source of leakage is by-passing of the flow between the bundle and shell. Bergelin et al. (1) defined the effect of these parameters, as summarised below:-

Baffle height:- The larger baffle height, i.e. smaller baffle cut down increases the fluid velocity at the baffle and the distance that the fluid moves towards the next baffle. The result is an increase in transfer rate.

Baffle spacing:- An increase in baffle spacing:-

(a) Decreases the fluid velocity across the tubes between the baffles and thus tends to decrease the heat transfer.

(b) Allows a longer mixing time following the flow of fluid through the baffle opening, thus tending to increase the heat transfer.

(c) Prolongs the turning over the baffle resulting in a poorer sweep of the transfer surface, thus decreasing heat transfer.

As the velocity of the fluid across the tubes is the most important factor the net effect of increasing the baffle spacing is to decrease the heat transfer.

Tube pitch:- A wider tube spacing:-

(a) Increases the width of the stream flowing between the tubes and thus decreases the heat transfer.

(b) Allows a longer mixing time following the flow of fluid over the tube surface, and thus increases the heat transfer.

Tube size:- The tube diameter directly affects the turbulence of the fluid on the trailing side of the tube. A smaller tube increases the heat transfer, since the fluid sweeps more of the trailing side of the tube for a given fluid velocity.

Clearances:- On economic grounds it is not possible to construct a commercial exchanger without leakages. The leakage paths are:-

(a) Baffle hole to tube clearance. In this case the leakage stream is in contact with the heat transfer surface, and thus the heat transfer is increased.

(b) The baffle to shell clearance. In this case the leakage stream is not in contact with the heat transfer surface, and thus the heat transfer is decreased.

The tube bundle to shell clearance may also be accepted as leakage, and in this case the leakage stream is not in contact with the heat transfer surface, and thus the heat transfer is decreased.

Several workers (23, 24, 25, 26, 27) have obtained design methods for calculating the bundle average shellside coefficient, in which an attempt has been made to allow for the geometrical factors by the use of an effective mass velocity. The resulting equations from these methods allow similar exchangers to be designed, but the fact that constants dependent on exchanger design, and complicated calculations, for which all the data may not be obtainable, are incorporated, leaves doubts as to the validity of these design methods for a wide range of exchangers.

The major work on bundle average transfer coefficients for shell side heat transfer has been conducted by Bergelin et al. (10, 11, 12, 13, 27, 28) at Delaware University. The work started with rectangular

tube banks, and then progressed to cylindrical shell and tube heat exchangers, with and without normal leakage streams. This work has been summarised in a report (1) and also by Bell (29). The shellside flow was simplified by eliminating or reducing the leakage paths and entrance and exit effects; thus removing the factors which had been of unknown magnitude when considering heat exchanger performance. Gaskets were used to eliminate tube hole leakage and baffle to shell leakage, and the tubes were spaced as close to the shell as possible to reduce the bundle to shell by-pass stream. The narrow side clearance was further reduced by the use of spacer bars, and entrance and exit effects were minimized by using large rectangular ports. The heat transfer performance of the model heat exchanger was then compared with the performance of the model heat exchanger without gaskets over a range of $2 \cdot 5 < Re < 14{,}000$ for various baffle spacings and cut downs. A considerable spread of the data was found to exist due to the effect of baffle configurations. An attempt was made to introduce a correction factor into the j - factor to allow for exchanger configuration, and to relate the results obtained from the cylindrical investigation to those of the rectangular tube bank study. This factor will be mentioned again in the discussion on bundle averages in Chapter II.

It was also found from this study that leakage affected pressure drop rather more than it affected heat transfer, and accounted for half the flow in commercial exchangers. The results obtained confirmed the 0·6 design factor given by McAdams (30) for correcting heat transfer coefficients so that they apply to baffled heat

exchangers with the usual leakage streams.

The results of Bergelin et al. were expressed in terms of the j - factor of Chilton and Colburn (3) and Reynolds number. The fluid velocity was based on the minimum flow area at the centre row of tubes.

However, although a great deal of work has been carried out on the shellside heat transfer in cylindrical heat exchangers, nearly all of the work has been concerned with bundle average heat transfer coefficients. The data obtained from these investigations have then been empirically correlated to allow for the different exchanger geometries. These correlations allow similar heat exchangers to be designed but give no indication of the fluid flow patterns inside the shell, neither do they indicate how the flow patterns are changed by different exchanger configurations.

These flow patterns and the effect on them of the various geometrical factors can be clarified by studying the individual tube heat transfer coefficients and synthesizing the bundle average heat transfer coefficient from the individual tube coefficients. Several workers have conducted investigations on this basis and their work is summarised and discussed in other sections of the present work.

****
****
**

(b) Individual tube and local heat transfer coefficients.

The present work is concerned with individual tube heat transfer coefficients rather than local, in the sense of point, heat transfer coefficients. As will be shown in this discussion, a considerable part of the previous work was carried out on model heat exchangers not entirely representative of commercial design practice. The application of results obtained from these models to actual exchanger design is therefore of doubtful validity.

Gupta and Katz (31) used a single pass gasketted cylindrical glass heat exchanger and studied the range $500 < Re < 10,000$. They observed the motion of coloured glass beads introduced into the fluid stream and made visual observations of the flow. They divided the flow into three streams:- the longitudinal zone, the cross flow zone and the eddy zone. Coefficients of heat transfer for the eddy zone were computed from the experimental data by means of known equations for longitudinal and cross flow. A considerable scatter of the eddy region data was found to exist.

Ambrose and Knudsen (32) measured local heat transfer coefficients in a baffled cylindrical exchanger with leakage, for five baffle spacings and two tube spacings at one shellside flow rate. The heat transfer coefficients were determined by use of an electrically heated sensing probe first developed by Giedt (33). Eddy zones were detected between the baffles and it was found that the heat transfer rates in the eddy and cross flow zones were almost equal and about 15% below the average in longitudinal flow. The size of the sensing probe allowed only 4 and 14 tubes to be fitted into a shell of 6" internal diameter.

This technique of replacing a section of tube by an electrically heated probe does not allow representative models of industrial heat exchangers to be made. The experimental problems of fitting in large enough electrical leads to carry the required current precludes the use of small diameter tubes.

Gurushankariah and Knudsen (34) extended the previous work and measured local heat transfer coefficients at intervals between the two central baffles of a segmentally baffled cylindrical heat exchanger with leakage. Two baffle spacings and three flow rates were used for a bundle of fourteen 1" O.D. tubes in a 6" I.D. shell. The heat transfer coefficients were found to be high at the baffle hole, decreasing rapidly along the length of the tube until they reached a minimum value midway between the two baffles, this minimum value being approximately 25 - 50% of the value at the baffle hole. Unfortunately the effect of leakage could not be determined as the amount of leakage could not be measured. The results indicated the existence of three flow zones in the baffle space with the average Nusselt number for the eddy zone being generally higher than those in the cross flow or longitudinal zones.

Stachiewicz and Short (35) investigated local heat transfer coefficients in a baffled rectangular exchanger without leakage. Three baffle spacings at one baffle cut down were studied for $5{,}500 < Re < 26{,}000$ using a heat probe technique. From their results they correlated the local heat transfer coefficients in both zones by the same type of equation by using a geometric mean mass velocity.

The major study of individual tube coefficients in a baffled

shell and tube exchanger without leakage has been carried out by Williams (2) using a mass transfer technique. Before discussing Williams' results and their relationship to the foregoing heat transfer coefficients, the mass transfer analogy will be discussed, and the validity of applying mass transfer results to a heat transfer problem will be demonstrated.

****
****
**

CHAPTER II

A. The Mass Transfer Analogy.

The main disadvantage of using a heat transfer technique to measure individual tube heat transfer coefficients is the bulk of the measuring equipment. This has resulted in other methods being examined so that transfer coefficients may be obtained from models similar in design to commercial products.

Chilton and Colburn (3) have demonstrated that mass transfer coefficients may be related to heat transfer coefficients and it is therefore possible to construct a model and obtain mass transfer coefficients from which the heat transfer coefficients may be predicted.

Two main systems for the mass transfer analogy seem to have emerged. Firstly, there are methods which employ transfer of a solute from a surface into a solvent stream which is then analysed and hence the transfer rate obtained, e.g. benzoic acid into water, naphthalene into air, and secondly there are electrochemical methods. For a model exchanger it is extremely difficult to eliminate short circuits occurring in an electrochemical system and so this method seems not to have been used.

There are several criteria for the first system to work successfully:-

(1) There should be a low solution rate requiring a low energy transfer rate, to ensure that the transfer is mass transfer and not energy transfer controlled.

(2) The required shapes should be able to be fabricated easily.

(3) The solvent stream containing the vapour from the transfer surface should be capable of accurate, quick and easy analysis.

Several workers (2, 4, 6, 15, 16, 17) have constructed model heat exchangers employing a mass transfer technique and they have presented their results in the form of Reynolds numbers and j - factors on similar bases to the heat transfer results discussed previously.

As mentioned in Chapter I A, one of the early investigators of heat transfer from rectangular tube banks, Thoma (15), employed a mass transfer analogy in 1921. In his experiments he passed an ammonia-air mixture over model tube banks fabricated from filter paper soaked in a known quantity of phosphoric acid. The amount of ammonia absorbed by the filter paper was then determined by titration.

Winding and Cheney (16) used another mass transfer analogy in 1948. They fabricated tubes in a tube bank from naphthalene and then passed air over them. The amount of naphthalene sublimed from the rods was determined by weighing the rods before and after each experimental run. Measurements of the change in diameter of the rods through the bundle indicated the local transfer coefficients.

Leadley and Oliver (17) used this method to investigate transfer from plain and finned tube banks.

However, the above methods have several disadvantages:-

(a) They do not lend themselves to the fabrication of fragile and/or complicated shapes.

(b) The change in clearances in a naphthalene tube bank, due to sublimation of the naphthalene, affects the flow paths and may affect the flow patterns.

Because of these disadvantages other methods were investigated and Maxwell and Storrow (4) experimented with the evaporation of mercury vapour from amalgamated copper rods to air flowing parallel to the surface. The results obtained from their experiments were in agreement with the accepted mass and heat transfer equations. They also demonstrated that the transfer from the surface of a mercurised sphere agreed with the accepted equations.

Maxwell (see 2) set up the transfer boundary layer equations for a body of revolution and solved them for the case of evaporation from bands on a sphere. He then experimentally verified these derived equations, using the mercury transfer technique.

Potter (5) then studied ellipsoidal shapes, placed with their axes of revolution parallel to the air flowpath, using the method and equipment of Maxwell and Storrow.

From the above results it was concluded that the mercury evaporation method was more sensitive and versatile than other methods for determining mass transfer coefficients.

There were, however, several disadvantages with the experimental technique used by the above workers. The major difficulty encountered was that the rate of transfer from the amalgamated surfaces decreased with time, and the results had to be calculated by plotting an ageing curve and extrapolating this back to zero time. This falling rate period was due to two defects. Firstly, the mercury surface was obtained by chemically cleaning the required copper shape, amalgamating in a mercuric salt solution, immersing in liquid mercury and finally lightly polishing with tissues. The mercury surface

obtained in this way did not "wet" with liquid mercury, i.e. a true free mercury surface did not exist and so the full vapour pressure of liquid mercury was not exerted. Secondly, the airstream oxidised the mercurised surface, further aggravating the falling transfer rate. By plotting an ageing curve the zero time transfer rate (i.e. when the full liquid mercury vapour pressure was exerted) was obtained, but this was a tedious procedure of somewhat doubtful validity.

Williams (2) instigated a development programme to obtain a mercurised surface which would give a constant transfer rate period for a considerable time. This was achieved by using an electroplating mercurisation technique which gave a mercury surface that would "wet" with liquid mercury, i.e. a free mercury surface existed. By this method of deposition a much thicker mercury film could be obtained which was much more stable, both chemically and mechanically, than the galvanically deposited mercury film. The substitution of nitrogen for air also assisted in obtaining a constant rate transfer period, and by these two means constant rate transfer periods of up to an hour were obtained by Williams.

The analysis of the mercury vapour/gas streams was carried out by using an ultraviolet absorptiometer. Williams much improved the stability and sensitivity of this instrument by fitting a constant temperature controller within the instrument casing, and by incorporating a constant voltage transformer in the mains electrical supply to the instrument.

The advantages of the mercury mass transfer system, as compared

with other mass transfer systems of this type, are:-

(a) The low vapour pressure of mercury results in low evaporation rates so that there is a negligible change in surface area and in the shape of the transfer surface. This is important when considering model tube bundles which have small clearances for the shellside flowpath.

(b) The low evaporation rate of mercury requires a low energy transfer rate thus ensuring that the transfer is mass transfer, and not energy transfer, controlled.

(c) A gas stream containing mercury may be very quickly and easily analysed by the use of an ultraviolet absorptiometer. In the work discussed above, and in the present work a HANOVIA instrument was employed (modified as in Chapter III (vii) page 58 and Appendix 5 page 183).

(d) The required shapes can be fabricated in copper and then mercury plated (see Appendix 4 page 180). This is especially useful in the case of fragile shapes e.g. if transfer from gauzes is to be investigated.

Having developed and improved the mercury mass transfer technique Williams (2) investigated individual tube mass transfer coefficients in a segmentally baffled cylindrical shell and tube model heat exchanger. This model was essentially similar to that used by Bergelin et al. (1) in the Delaware project and consisted of a bundle of eighty $\frac{3}{8}$" O.D. tubes in a $5\frac{1}{4}$" I.D. shell. As in the Delaware

investigation the model incorporated large rectangular entrance and exit ports to minimize entrance and exit effects on the fluid stream. Also tube to baffle and baffle to shell leakage w eliminated by means of gaskets and bundle to shell leakage (or by-passing) was minimized by placing the tubes as close to the shell as possible and using spacer rods. The investigation studied the effect on individual tube mass transfer coefficients of three baffle cut downs, at one baffle spacing, over a range of $54 < Re < 2,173$. The method used was to replace one tube at a time, in the third baffle compartment from the inlet port, with a mercurised copper rod. Nitrogen was used as the shellside fluid, there being no tubeside fluid in this investigation. The results obtained were presented in the form of j - factor and Reynolds numbers on the same basis as used by the Delaware workers.

The heat transfer data calculated from the mass transfer results are those that would be obtained if the equivalent heat transfer surface under consideration was isothermal. This is not strictly representative of actual practice where there are temperature variations along and around the tube, but nevertheless the method is comparable with other methods that have been used for studying local heat transfer coefficients. Also the driving forces are somewhat different from those encountered in actual practice, as there was no transfer from the upstream tubes.

Williams (2) investigated baffle cut downs of 18.4%, 31% and 43.7% of the baffle diameter at a baffle spacing of 3.89 inches. The investigation by Bergelin et al. (1) had only studied the 43.7% baffle cut down at this baffle spacing, and so Williams compared his

43.7% cut down data with the Delaware data so as to determine the validity of the mass transfer analogy in this investigation. This was done in the following manner:- from the individual tube transfer coefficients, the bundle average transfer coefficient was calculated. A simple arithmetic average was employed as there was no justification for a more complicated weighting procedure. When this bundle average was compared with the corresponding values from the Bergelin et al. investigation very good agreement was found (see Fig. 2 page 27), Williams' results falling between those of the two Delaware investigators who had worked in that particular Reynolds number range.

This demonstrated the validity of the mass transfer technique for obtaining heat transfer data, and also the use of the arithmetic average for calculating the bundle average coefficient from the individual tube coefficients. Chapter II B of the present work covers a study of the various zonal averages and bundle averages, calculated from the individual tube coefficients by Williams, and compares these results with the results obtain by Bergelin et al.

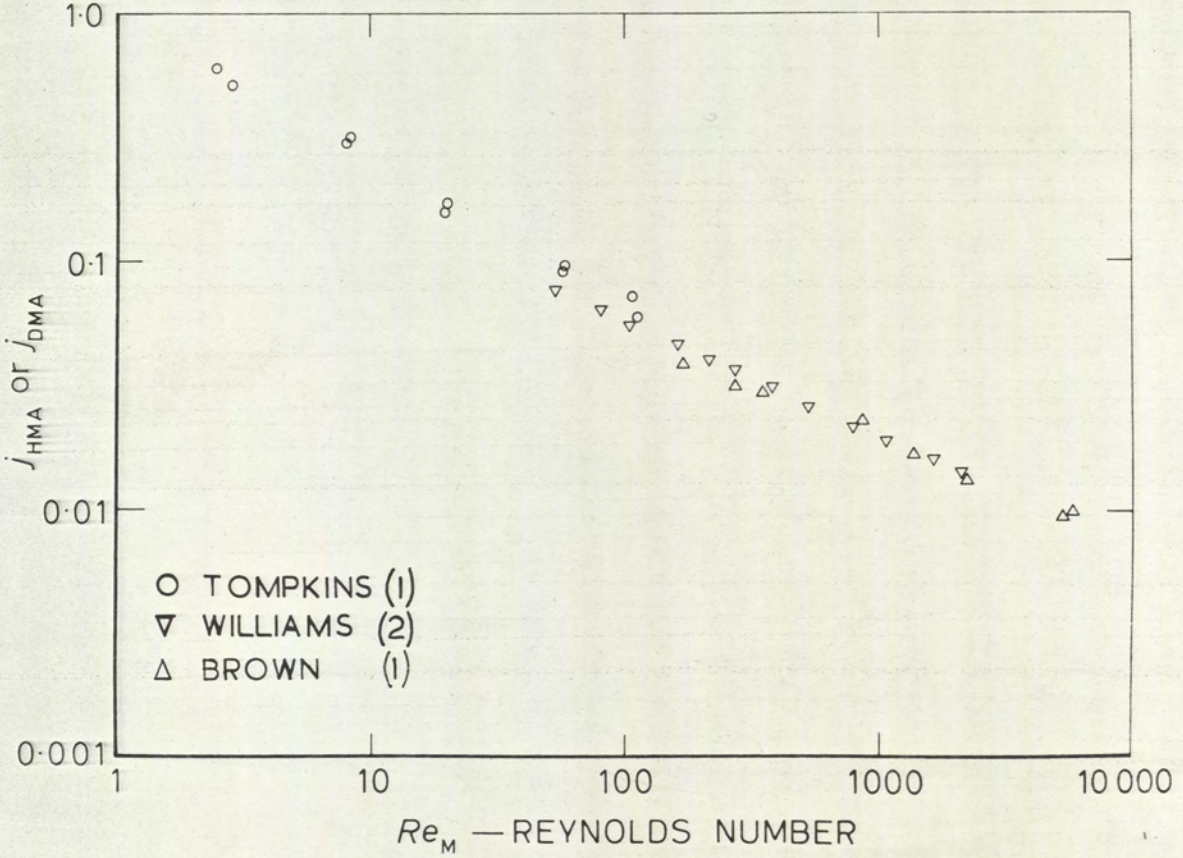
1·0
0·1
0·01
0·001
j_{HMA} or j_{DMA}
O TOMPKINS (1)
∇ WILLIAMS (2)
Δ BROWN (1)
1
10
100
1000
10 000
Re_M — REYNOLDS NUMBER

FIG. 2.

B. Comparison of the Results of T.A. Williams (2) and Bergelin et al(1)

From his individual tube data Williams calculated the bundle average coefficients for the three baffle cut downs studied. When these bundle average coefficients were plotted three distinct lines were found to exist. The choice of fluid velocity based on the minimum flow area at the centre row of tubes did not therefore allow for the effect of variations in the baffle cut down. As will be mentioned later in this section Bergelin et al proposed a correction factor to allow for baffle cut down. Application of this factor to Williams' data reduced but did not eliminate the separation between the lines. The further correlation of bundle average coefficients will be considered after the zonal averages have been discussed.

(i) Zonal Average Coefficients of Heat Transfer.

Bergelin et al. (1) divided the shellside flow into two zones: the cross flow zone and the window zones (see Fig.1 page 7). Williams (2) further divided the shellside into the inlet window zone and the outlet window zone. The inlet window zone is that part of the window zone between adjacent baffles on the inlet side of a baffle compartment, and the outlet window zone consists of the corresponding region on the outlet side of a baffle compartment. As the tubes in the baffle edge could be in either the cross flow or window zones, they were considered separately. The average coefficients for these zones were calculated from the individual tube coefficients by arithmetic averaging.

(ii) Baffle Edge Zones.

The data for the outlet baffle edge zone agreed with the data for the cross flow zone for all baffle cut downs studied and was therefore included in the cross flow zonal average. For the 18·4% and 43·7% cut downs the inlet baffle edge zone values agreed with the inlet window zone data and cross flow zone data respectively and were therefore included in the appropriate zonal averages. For the 31% cut down the inlet window zone, inlet baffle edge zone and cross flow averages all coincided and the inlet baffle edge data was included in either zone as convenient.

(iii) Cross Flow and Window Zones.

For all three baffle cut downs studied the outlet window zone gave the lowest data, the outlet window zone for the 43·7% baffle cut down giving the lowest data of all. The inlet window zone data was 50% higher than the cross flow zone data for 18·4% cut down, coincided with the cross flow zone data for 31% cut down and fell 10% below the cross flow zone data for the 43·7% cut down. The cross flow and window zones will be further discussed separately.

(a) Cross flow zone.

For the three baffle cut downs studied the average data for the cross flow zone fell on one line. This line was found to be a curve on logarithmic coordinates, and hence the data was not represented by a simple equation of the form:-

$$j_{DMC} = C\,(Re_M)^{-n}$$

White and Churchill (36) had proposed that heat transfer data for

flow across a single cylinder should be correlated by the equation:-

$$Nu_O = A \left(Re_O\right)^{\frac{1}{2}} + b\, Re_O \qquad (1)$$

This equation was obtained by summing the contribution of heat transfer through the boundary layer on the forward portion of the tube and turbulent heat transfer through the wake on the rear portion.

Assuming $Nu \propto \left(Pr\right)^{\frac{1}{3}}$ equation (1) may be rewritten:-

$$Nu_O = \left\{ a \left(Re_O\right)^{\frac{1}{2}} + b\left(Re_O\right) \right\} \left(Pr\right)^{\frac{1}{3}}$$

$$\text{or} \quad j_{HO} = \frac{a}{\left(Re_O\right)^{\frac{1}{2}}} + b \qquad (2)$$

When the cross flow data of Williams were plotted according to equation (2) (see Fig. 3 page 31) a striking resemblance to Fig.6 in White and Churchill's paper (36) was obtained, especially at low Reynolds number. White and Churchill attributed the behaviour at low Reynolds number to natural convection. Williams cross flow data for Reynolds number greater than 200 were correlated by the equation:-

$$j_{DMC} = \frac{0{\cdot}5}{\left(Re_M\right)^{\frac{1}{2}}} + 0{\cdot}0037 \qquad (3)$$

which is of the same form as equation (2). Although this correlation was subject to scatter, nevertheless its coordinates were linear not logarithmic.

Corresponding to equation (3) the following equation was fitted to the linear portion of Whites' and Churchills' correlation:-

$$j_{HO} = \frac{0{\cdot}508}{\left(Re_O\right)^{\frac{1}{2}}} + 0{\cdot}00142$$

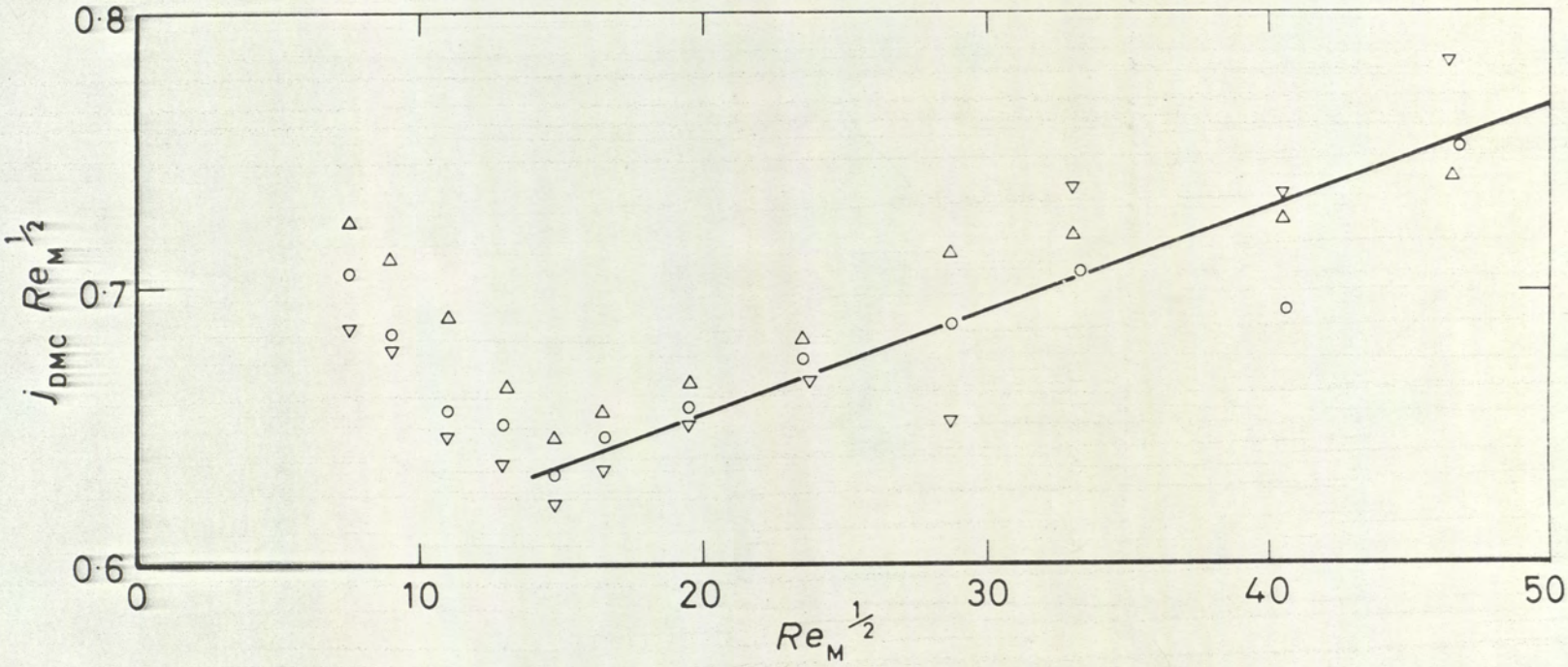
0·8
0·7
0·6
0
10
20
30
40
50
$j_{DMC}\ Re_M^{1/2}$
$Re_M^{1/2}$
▽ 18·4%
○ 31%
△ 43·7%
BAFFLE CUT-DOWN.

FIG. 3.

As this equation was very similar to equation (3) the cross flow data for $Re_M > 200$ were considered to be correlated by equation (3).

(b) Window zones.

From the inlet and outlet window zones results the average transfer coefficients for the entire window zone were calculated. When these data were plotted in the form j_{DM} versus Re_M it was found that separate lines were obtained for each baffle cut down. It could therefore be seen that the velocity based on the minimum flow area at the centre row of tubes did not eliminate the effect of baffle cut down in this case.

In the window zone a more representative velocity would be that based on flow through the free area available at the baffle window i.e. the area of the baffle window less the area of the tubes through it.

The data for the window zone were therefore replotted using this velocity in the calculation of j - factor and Reynolds number. The separation of the lines was slightly reduced but the important fact was that the order of the lines was reversed. It was therefore obvious that a velocity between the previous two might eliminate the separation.

Donohue (25) had proposed the use of the geometric mean of the cross flow and window velocities, and the window data were therefore recorrelated on the basis of this geometric mean velocity. The data correlated on one line in this case, thus indicating that the use of this geometric mean velocity eliminated the effect of baffle cut down. The equation of the straight line obtained from this correlation of

the window zone data was:-

$$j_{DZW} = 0{\cdot}45 \left(Re_Z\right)^{-0{\cdot}46} \qquad (4)$$

It can therefore be seen that for this design of heat exchanger, with a baffle spacing of 3·89 inches, the cross flow and window zonal average data may be correlated for all baffle cut downs likely to be encountered in practice by equations (3) and (4).

Having now discussed the zonal averages the bundle average coefficients will be considered in the light of the above results.

(iv) Bundle Average Coefficients.

The bundle average coefficient was related to the zonal average coefficients by the equation:-

$$j_{DMA} = (1 - r)\, j_{DMC} + r \cdot j_{DMW} \qquad (5)$$

By substituting equations (3) and (4) into equation (5), and by use of the relationships

$$j_{DMW} = \left(\frac{A_C}{A_W}\right)^{\frac{1}{2}} \cdot j_{DZW} \quad \text{and} \quad Re_Z = \left(\frac{A_C}{A_W}\right)^{\frac{1}{2}} \cdot Re_M$$

the following correlation was obtained:- (6)

$$j_{DMA} = \frac{0{\cdot}58\ (1 - r)}{\left(Re_M\right)^{\frac{1}{2}}} \left\{1 + 0{\cdot}0064 \left(Re_M\right)^{\frac{1}{2}} + \frac{0{\cdot}78r}{1 - r} \left(\frac{A_C}{A_W}\right)^{0{\cdot}27} \left(Re_M\right)^{0{\cdot}04}\right\}$$

This equation was the final correlation of the bundle average data in terms of Reynolds Number (greater than 200) and baffle cut down.

For the Reynolds Number range of Williams' results, equation (6) could be approximated to:-

$$j_{DMA} \simeq j_{DMC} \left\{ 1 - r + 1{\cdot}025\, r. \left(\frac{A_C}{A_W} \right)^{0{\cdot}27} \right\} \qquad (7)$$

Since $\left(Re_M\right)^{0{\cdot}04} \simeq 1{\cdot}315$ over the range $200 < Re_M < 2000$.

Thus equation (7) related the bundle average coefficient to the cross flow zonal coefficient.

Bergelin et al. (1) used a coefficient of $1 - r + r.\left(\frac{A_C}{A_M} \right)^{0{\cdot}30}$ to relate the bundle average coefficient to the coefficient for the corresponding rectangular tube bank for Reynolds number greater than 200.

The similarity between the Bergelin et al. factor and that obtained from equation (7) by Williams is interesting, the former having to attempt to fit a coefficient to their bundle average coefficient results, whereas Williams was able to proceed much more readily from his individual tube results. This illustrates how the determination of individual tube coefficients greatly simplifies the investigation of shellside heat transfer, and also allows the flow patterns in the various zones to be isolated and studied.

Williams only carried out a limited qualitative analysis of the individual tube transfer coefficients, as he was chiefly concerned in illustrating that bundle average coefficients could be synthesised from individual tube coefficients. From this limited examination Williams concluded that the 31% baffle cut down gave the least

variation in transfer factors and hence the best fluid distribution across the bundle. The 18·4% baffle cut down gave the highest overall j - factor of the three baffle cut downs studied but it was considered to be uneconomic for commercial exchangers on the grounds of excessive pressure drop, and also there seemed to be a tendency towards channelling of the fluid stream. The largest variations in transfer factors occurred with the 43·7% baffle cut down, indicating the greatest likelihood of hot spots in the exchanger. Tube 80 (see Fig.4 page 36) was found to give the lowest transfer coefficient, i.e. this tube would be the most likely to be a hotspot. For all three baffle cut downs a wider variation in transfer factors was found at the low Reynolds number due to the large bundle to shell by-pass stream, particularly around tube 37.

Williams presented his results in the form of contour map diagrams of the baffles which showed the values of the $j_D \times 10^3$ factors for a given value of the Reynolds number. A further set of diagrams indicated the high and low transfer areas at various values of the Reynolds number range studied for each baffle cut down. As each diagram is for a specific Reynolds number it is somewhat difficult to assess the overall pattern of the transfer factors with this method of presentation. An example of each form of diagram is given in Fig. 5 and Fig. 6 (pages 37 and 38).

A new analysis of the individual tube results of Williams, together with comparisons with the Bergelin et al results, is presented in Chapter V of the present work.

****
****
**

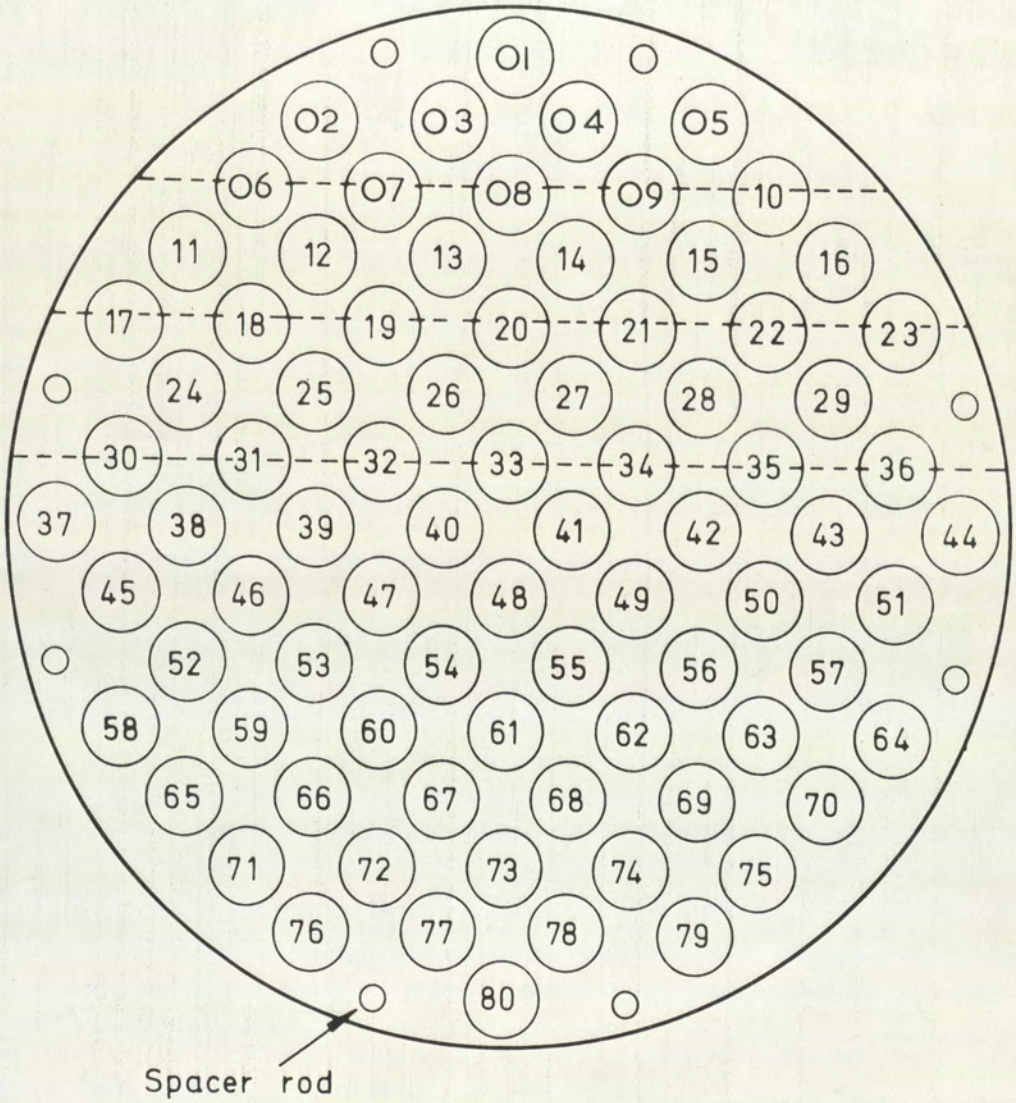

— — — INDICATES BAFFLE CUT-DOWN.

FIG.4. TUBE LAYOUT

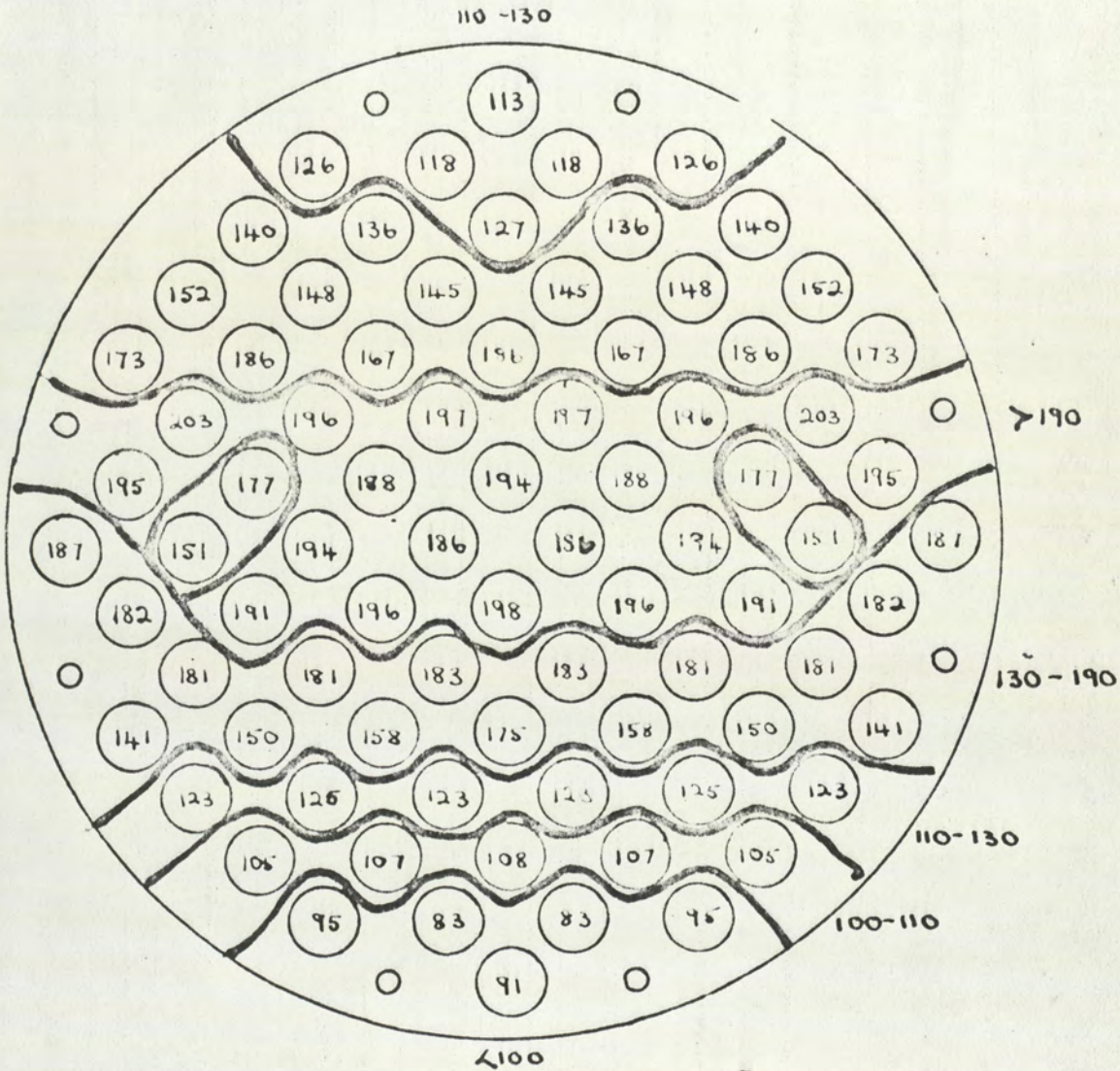

CUT-DOWN 43·7%

Re_M 1625

(WILLIAMS (2) FIG. 47.)

FIG. 5.

HIGH TRANSFER AREAS

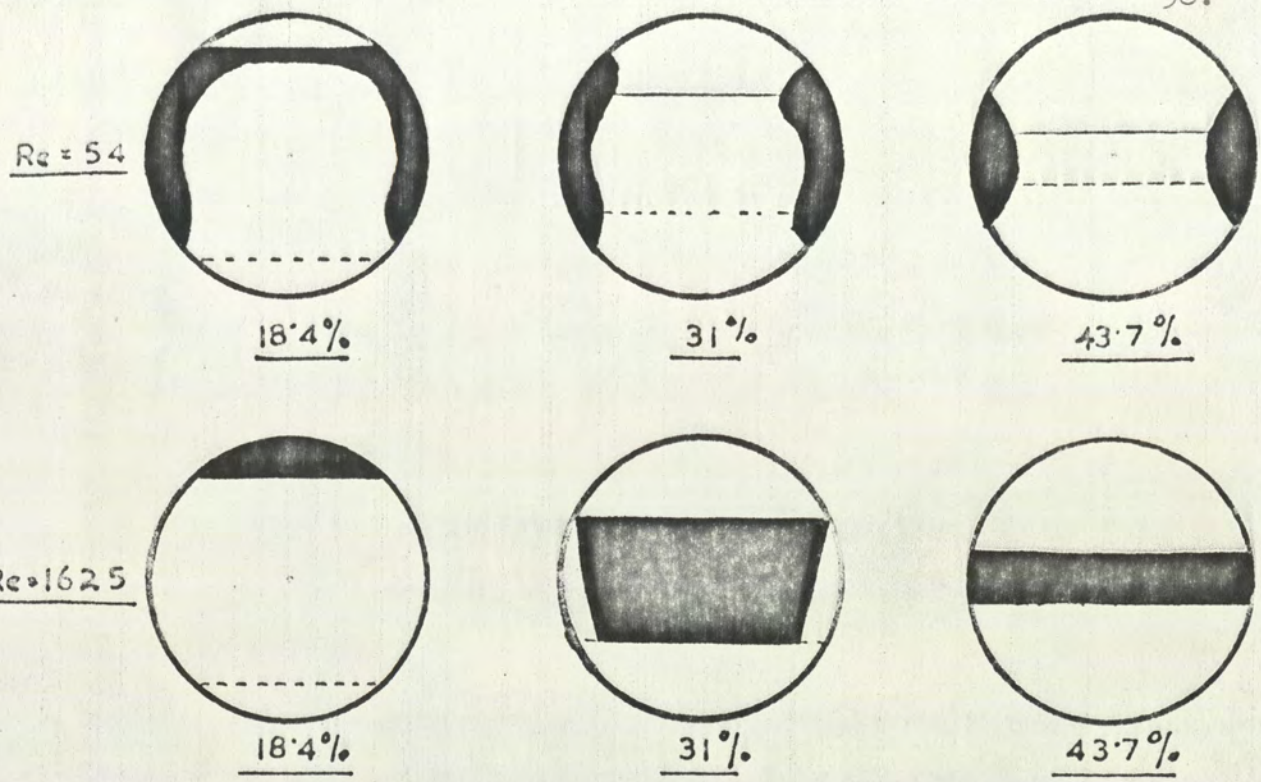

LOW TRANSFER AREAS

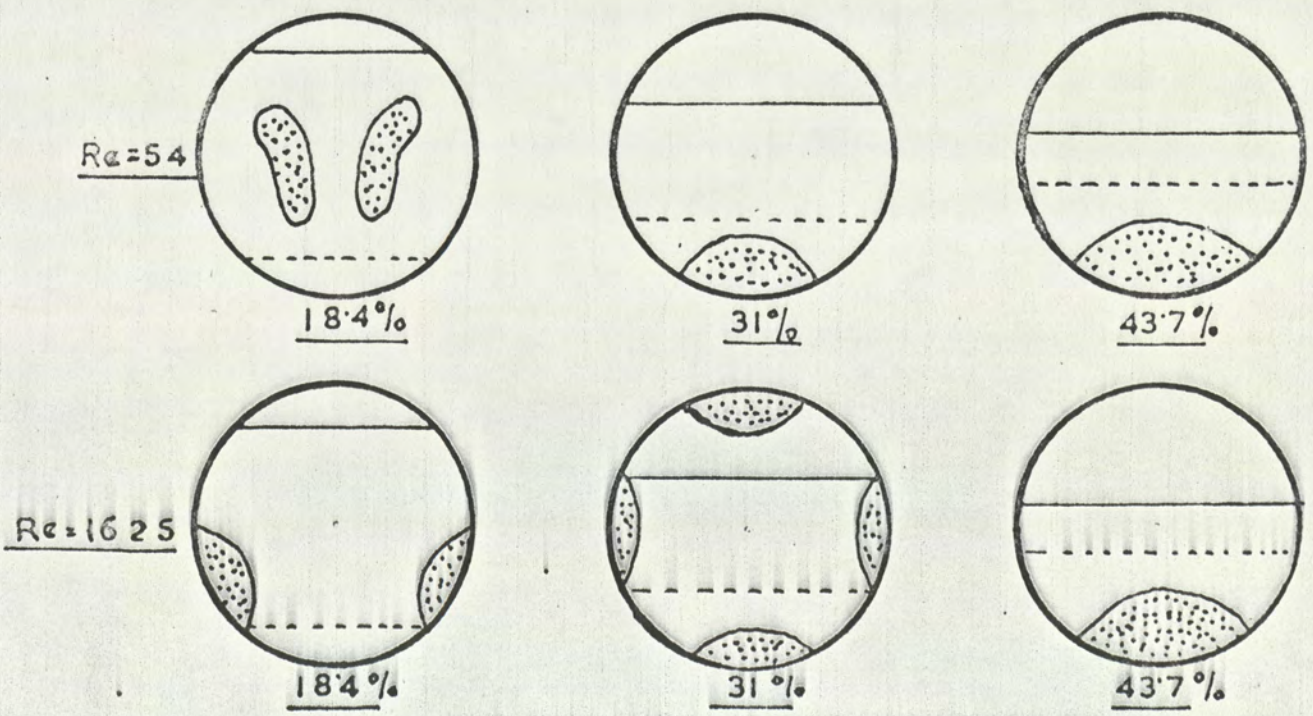

(WILLIAMS (2) FIG. 48)

FIG. 6.

CHAPTER III

A. Experimental Apparatus.

The object of the experimental apparatus was to obtain the salient factors necessary to determine the transfer factor for each individual tube position in the exchanger bundle. This entailed obtaining values of the Reynolds number and the mass transfer factors. It was therefore necessary to incorporate flow meters in the main gas circuit to determine the flowrate through the exchanger and hence the Reynolds number.

The gas stream through the exchanger picked up mercury vapour from the transfer surfaces and the amount of vapour picked up was measured by the absorptiometer which had previously been calibrated with gas/mercury vapour streams of known proportions. Due to the steeply rising calibration curve of the absorptiometer it was necessary to dilute gas streams containing large concentrations of mercury vapour so as to obtain a more accurate result. It was therefore necessary to incorporate flowmeters in the sample line from the exchanger to the absorptiometer meter to determine the sample flowrate, the dilution flowrate and the flowrate through the meter. It was also necessary to incorporate a mixer in the exit part of the exchanger to ensure a homogeneous gas/mercury vapour stream to prevent unrepresentative samples of this stream flowing to the absorptiometer.

With the above criteria in mind the apparatus used by Williams(2) was investigated with the intention of simplifying this where possible.

Williams used nitrogen as the working fluid in his investigation of individual tube shellside transfer coefficients in a segmentally baffled cylindrical model exchanger (see Chapter II page 24). In order to conserve the nitrogen a closed circuit had to be employed, resulting in a somewhat complicated apparatus, the main points of which are outlined below.

Nitrogen was circulated through the closed circuit by means of a centrifugal blower. The work of pumping caused the temperature of the circulating nitrogen stream to rise and hence a cooling coil had to be incorporated in the circuit. A HOPCALITE filter in the circuit removed the mercury vapour from the circulating nitrogen stream. (HOPCALITE is a granulated mixture of cobalt, iron, manganese and nickel oxides which has the property of absorbing mercury vapour). A vacuum pump was employed to suck the mercury vapour/nitrogen sample stream through the absorptiometer. As any leaks of air into the system would have affected the absorptiometer reading frequent checks of the oxygen content of the circulating nitrogen stream had to be carried out with an Orsat apparatus.

This nitrogen circuit was somewhat complex and so it was proposed in the present work to simplify the experimental apparatus and use air as the working fluid on a single pass basis. The use of air removed the need for a recycling pump, cooling coil, HOPCALITE filter, vacuum pump and Orsat analyses. The disadvantages of using air, together with details of how these disadvantages were removed or rendered insignificant, are discussed in Chapter IV. The final experimental circuit used in this work, together with its various

components, is described below.

Air from the laboratory compressed air supply was metered by rotameters and then passed to the shellside of the model heat exchanger where it picked up mercury vapour from the transfer surfaces in the model tube bundle. This air/mercury gas stream was then sampled before passing to the laboratory extraction system. The sampled gas stream was analysed by means of an ultraviolet absorptiometer, which was calibrated to give the mercury vapour concentration in the air/mercury stream.

(i) Air flow rig.

A flow diagram is presented in Fig.7, page 42 , and general views of the apparatus are shown in Plates 1 and 2, pages 43 and 44.

The air supply was taken from the laboratory ring main, using $1\frac{1}{2}$" nominal bore mild steel pipe, via an Aerox filter and an AEI - Birlec dryer (model AB.30) and was then regulated to 10 psig with a diaphragm regulator. The air then went via a tee piece and a $1\frac{1}{2}$" Saunders diaphragm valve V 1 to the main flow line, and a $\frac{1}{2}$" Saunders diaphragm valve V 2 to the dilution/saturator circuit.

The main flow line was constructed of $1\frac{1}{2}$" bore Vulcathene pipes and fittings. The sampling, dilution and saturating circuits were constructed from $\frac{1}{2}$" bore Vulcathene pipes and fittings together with some $\frac{1}{2}$" bore flexible P.V.C. tubing. Vulcathene plumbing, which is manufactured from high density polythene has the advantages of not absorbing mercury, lightness and ease of jointing. Jointing is done by fusion welding using a simple brass spigot tool heated in a gas

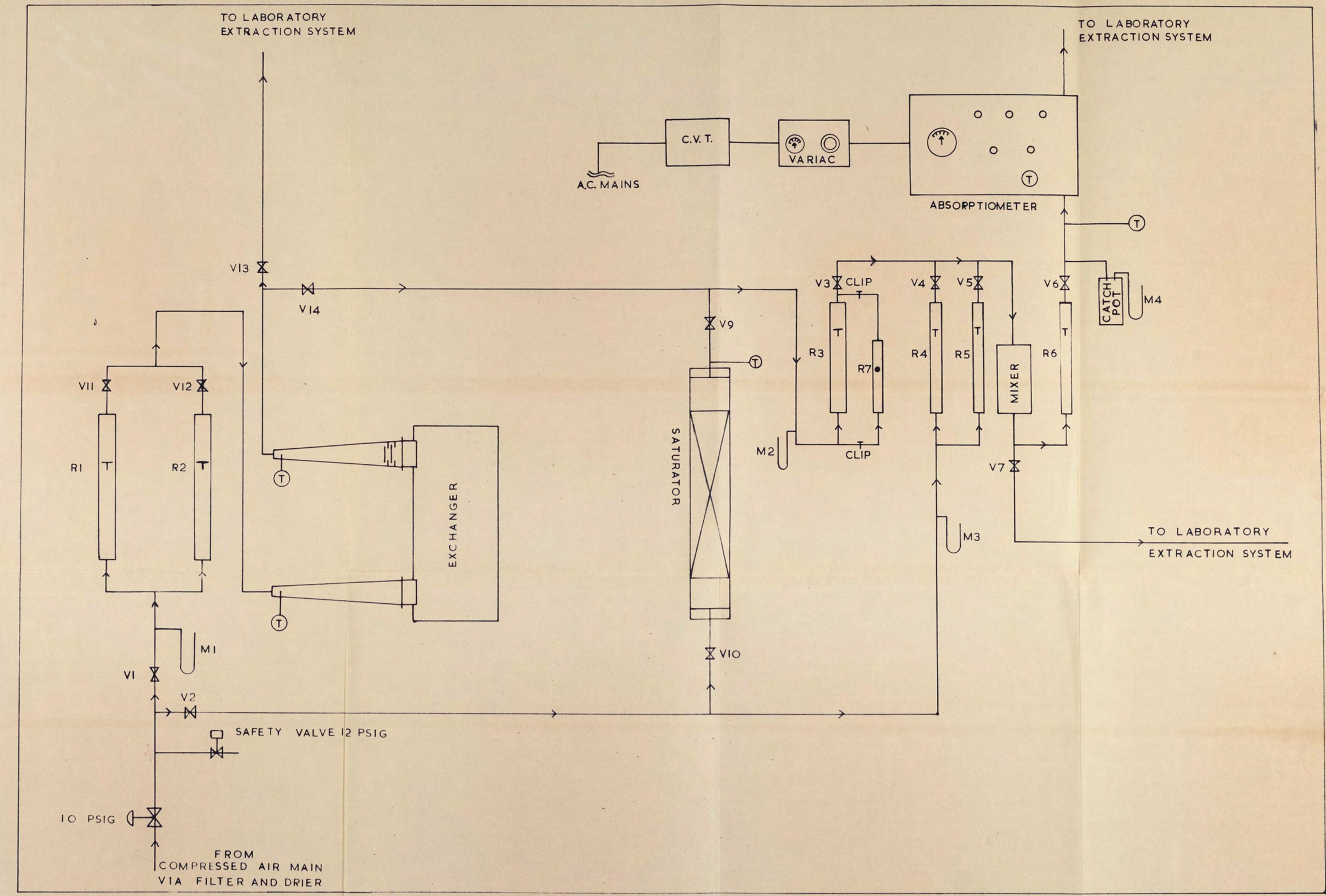

FIG. 7. – FLOW CIRCUIT.

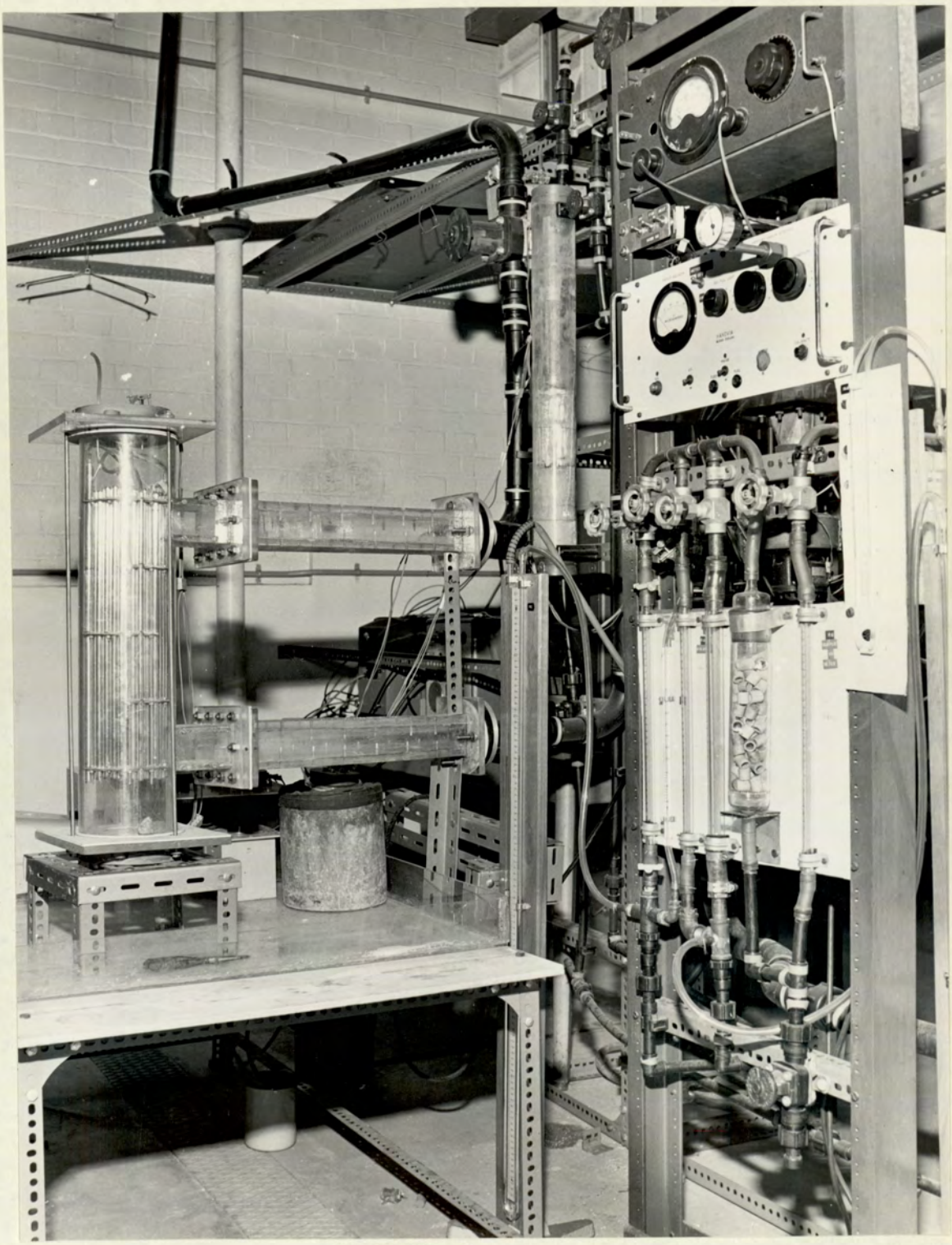

PLATE NO. 1.

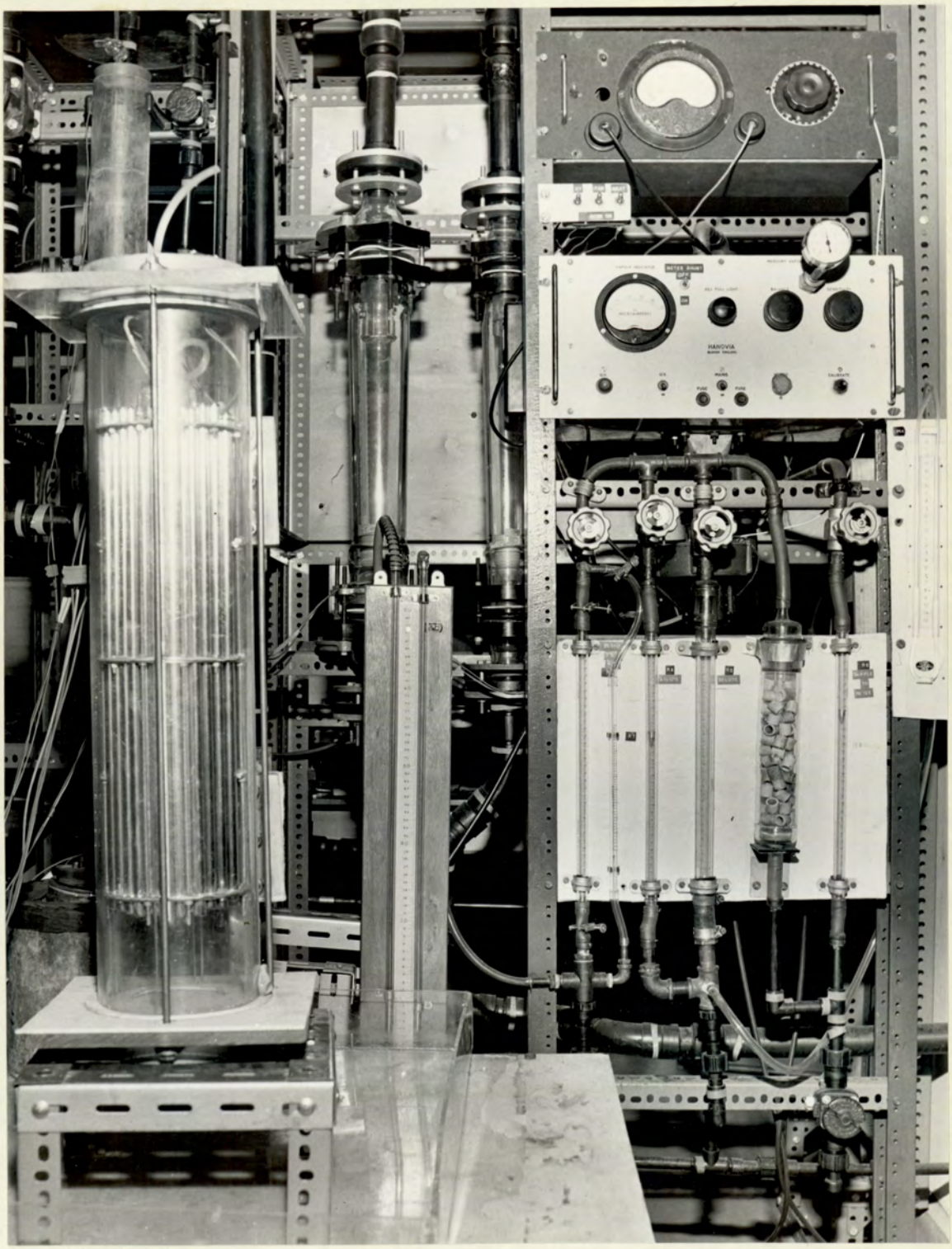

PLATE NO. 2.

flame, any leaks being sealed by hot nitrogen welding. All unions were sealed with neoprene O rings of 60°Shore hardness. P.V.C. tubing is also resistant to surface attack by mercury. It is important that red rubber tubing and galvanised mild steel pipes and fittings are not used in apparatus of this type as both absorb mercury.

The valves were of the Saunders diaphragm type fitted with Vulcathene bodies and cast aluminium mounting brackets, except for the valves controlling the sample and dilution rotameters to the absorptiometer which were stainless steel Clockhouse needle valves.

The flow of air to the exchanger was metered by either rotameter R 1 (100 - 1000 litres/min), or rotameter R 2 (200 - 2000 litres/min), by opening the appropriate valve V 11 or V 12. Beyond the rotameter the air passed to the model exchanger via a perspex expander (see Chapter III A (ii)b page 47). From the model exchanger the air/mercury stream flowed via a perspex contracting section incorporating a disc and doughnut baffled mixer to ensure that the air/mercury stream was homogeneous. A $\frac{1}{2}$" sample line was taken from the exit section of the model exchanger and the main stream passed, via valve V 13, to the laboratory extraction system.

With valve V 9 closed the sample stream flowed via valve V 14 to the inlet rotameter R3 (2 - 20 litres/min), and after dilution via rotameter R4 (2 - 20 litres/min) and/or R5 (5 - 50 litres/min) through a packed bed mixer. This mixer consisted of a 2" diameter glass column, 8" long packed with $\frac{1}{2}$" ceramic Raschig rings, and ensured that the air/mercury sample stream was completely mixed with the diluting air stream. If the sample stream flowrate after dilution

was greater than 15 litres/min part of it was by-passed round the absorptiometer, via valve V 7, to the laboratory extraction system. The sample stream flowed through the absorptiometer via rotameter R6 and thence to the laboratory extraction system.

To enable the flowrates indicated by the rotametes to be converted to free volumes mercury manometers M_1, M_2 and M_3 were connected to the inlet flowlines of the main rotameters R_1 and R_2, the sample rotameters R3 and R7 and the dilution rotameters R4 and R5 respectively.

A water manometer M_4 was connected to the inlet of the absorptiometer to indicate the pressure drop over the absorptiometer. This was of the order of 1 cm. of water and was therefore considered insignificant.

For calibration of the absorptiometer, air was passed to the saturator column (see Appendix 5(2) page 184) via valve V 10 with valve V 14 closed. From the saturator column the air/mercury stream flowed through valve V 9 to the rotameter R7. The air/mercury stream was then diluted with air via rotameter R4 and/or R5 and then passed to the absorptiometer. Calibration of the absorptiometer is fully described in Appendix 5 (2.) page 184).

Thermocouples (see Chapter III A (vi) page 57) and Appendix 1 (2) page 165) were located at:-

(a) The absorptiometer inlet.

(b) The exchanger inlet port.

(c) The exchanger outlet port.

(d) The interior of the tube bundle (2).

(e) The saturator outlet.

The thermocouple emfs were measured as follows. Each thermocouple was connected in turn (via a multipoint switch) to a thermocouple cold junction housed in liquid paraffin in a glass tube immersed in an ice/water mixture in an insulated Dewar flask. The resultant emf was measured using a Tinsley vernier potentiometer (type 4363E), a Pye Scalamp galvanometer (model 7890/S), a Weston standard cell (type SC1, No.7366) and a 2 volt Exide accumulator. A diagram of the thermocouple electrical circuit is given in Fig. 8(page 48).

(ii) The model exchanger.

A view of the assembled model exchanger is shown in Plate 3(page 49).

The model exchanger was similar to that used by Bergelin et al.(1) and Williams(2). Williams' model was slightly different from the Bergelin model as the latter's working drawings were not available to Williams, but were available for the present work. A table of the differences between the three models, which were very slight, is given in Appendix 7(page 197). A description of the model exchanger used in the present work is given below.

The model exchanger incorporated gasketted tube sheets and baffle plates, and extra wide ports for the entrance and exit of the shellside fluid. The gasketted baffle plates eliminated two of the major leakage paths through the exchanger, firstly the leakage between the baffle edge and the shell wall, and secondly that between the tubes and the tube holes in the baffles. To minimise the other leakage stream, which is between the tube bundle and the shell wall, the tubes were

THERMOCOUPLE CIRCUIT INCORPORATING
MULTIPOINT SWITCH TO SIX HOT JUNCTIONS

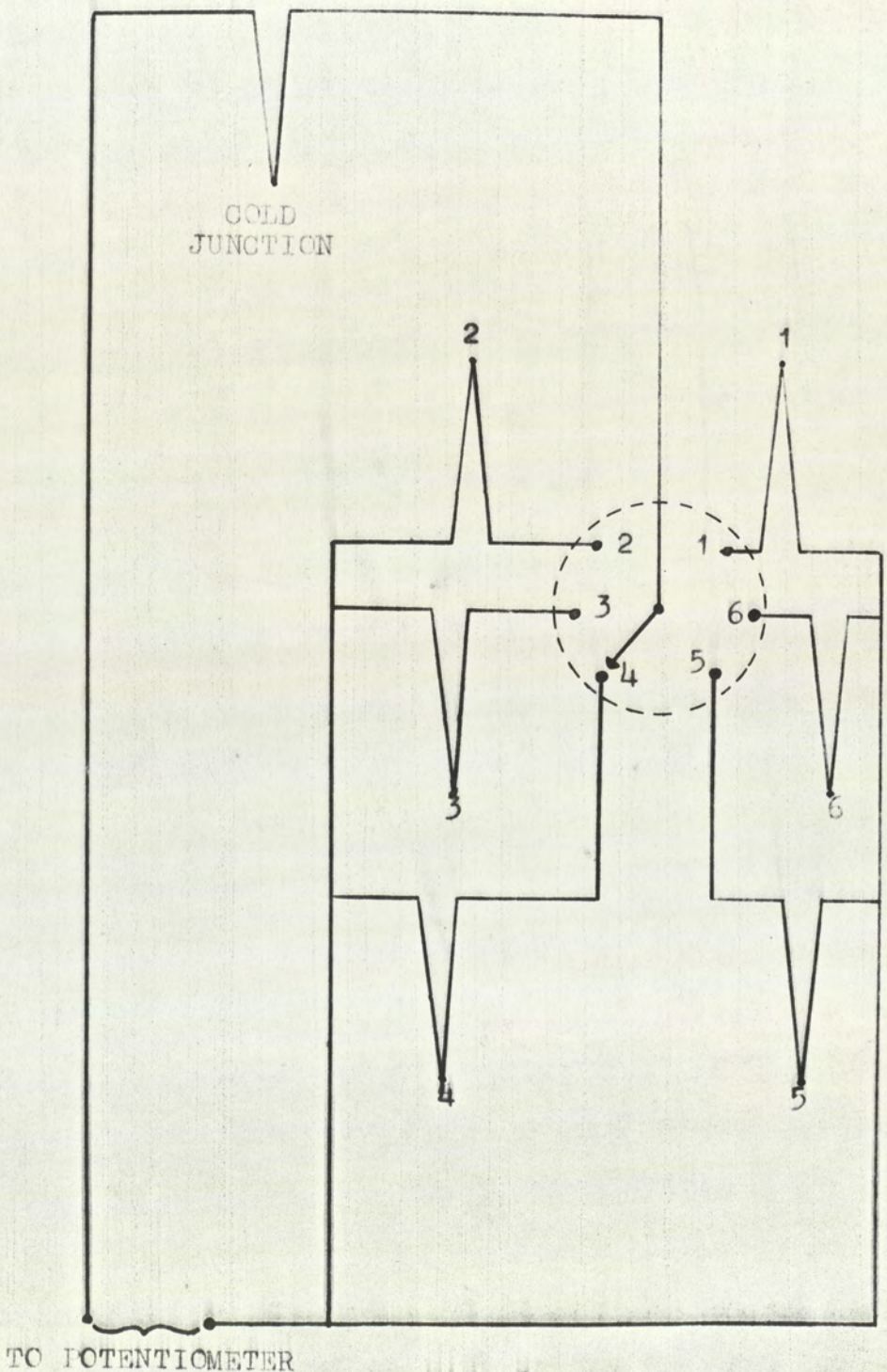

FIG. 8.

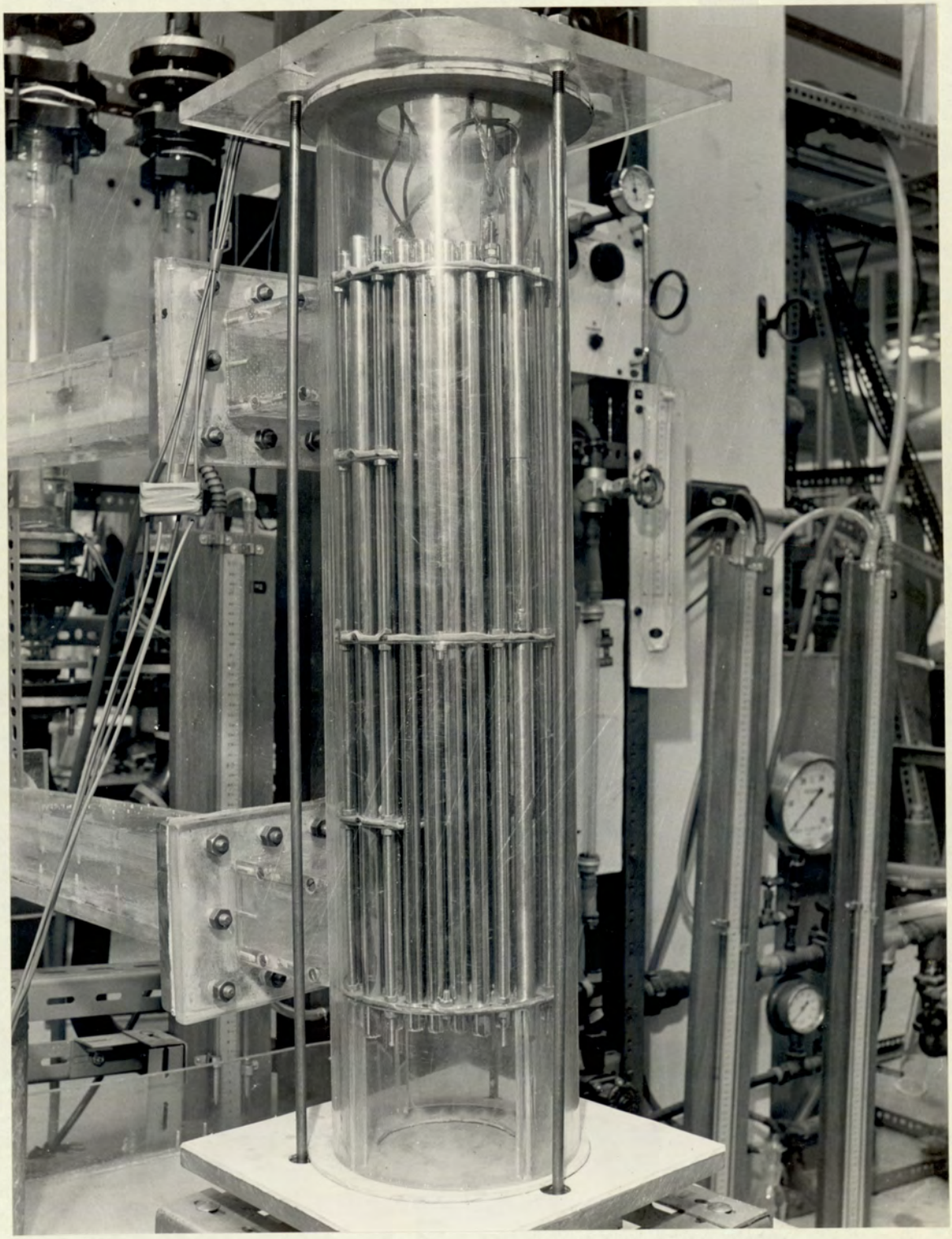

PLATE NO.3.

placed as close to the shell wall as possible and this narrow clearance together with the baffle spacer bars allowed only a small leakage round the bundle. The large rectangular ports kept to a minimum the entrance and exit effects of the fluid on the transfer coefficients.

It was proposed that the baffle gaskets should eventually be removed, firstly removing the gaskets between the baffles and the shell, and secondly those between the tubes and baffle holes. The result of removing these baffles would be to cause the flow pattern in the model exchanger to resemble more closely that in the commercial product. It is however worth mentioning that the silting up of a commercial exchanger may form "gaskets" which minimise the leakage paths.

In the present work the exchanger was used as in the work done by Williams, i.e. there was no tubeside fluid, and a tube in the tube bundle was replaced by a mercurised transfer probe (see Chapter III A (iii) page 53). In the present work air was used as the shellside fluid, whereas Williams used nitrogen.

(a) Tube bundle construction (see Fig. 4 page 36).

The tube bundle was comprised of eighty $\frac{3}{8}$" O.D. mild steel tubes 17" long, arranged on a staggered square pitch of 1·25 pitch to diameter ratio. The baffles and tube plates consisted of a sandwich of two $\frac{1}{16}$" mild steel plates and one $\frac{1}{16}$" silicone rubber gasket. The baffles were cut at $\frac{3}{16}$" less than the shell diameter ($5\frac{1}{4}$") and drilled with $\frac{1}{32}$" oversize holes for the tubes. The gaskets on the other hand were cut at $\frac{1}{16}$" over the shell diameter and punched at $\frac{1}{32}$" under the tube diameter so that when the tube bundle was inserted into the shell tight fits were obtained between the tubes and baffle holes,

and between the baffles and the shell.

The baffle spacing was maintained at 3·86" by the use of 4BA stainless steel screwed rods and nuts, and the spacing between the inner faces of the tube plates was set at 16".

Baffles were manufactured with cut downs of 18·4%, 31% and 43·7% of the diameter to allow the effect of baffle cut down on individual tube transfer coefficients to be studied.

All the mild steel tubes and plates were chromium plated, and stainless steel spacer rods, nuts and washers were used, as rust catalyses the oxidation of mercury. The gaskets were made from silicone rubber (see Chapter III A (iv) page 56) as it possessed exceptional pliability and did not absorb mercury onto its surface.

(b) Exchanger shell construction (see Fig.9 page 52).

The exchanger shell was constructed from a $5\frac{1}{4}$" inside diameter, 24" long, cast perspex tube having a wall thickness of $\frac{1}{4}$". Two rectangular ports, made from $\frac{1}{4}$" perspex sheet, having internal dimensions of 3" long by $1\frac{7}{8}$", were mounted in line on the shell. The distance between the port centres was $14\frac{1}{8}$" which allowed the inside faces of the tube plates to coincide exactly with the extreme edges of the ports.

The entrance and exit ports stood $2\frac{15}{16}$" above the shell surface at the centre line, and $3\frac{3}{4}$" above the shell surface at the lateral edges of the ports. Rectangular ducts, of $\frac{1}{2}$" perspex sheet, were dowelled and bolted to the port flanges and contracted from the port size to $1\frac{1}{2}$" square over a length of 18". Filler was used to blend

SCALE $\frac{1}{4}$" = 1"

BOLT HOLES OMITTED FOR CLARITY

SHELL MATERIAL $\frac{1}{4}$" PERSPEX

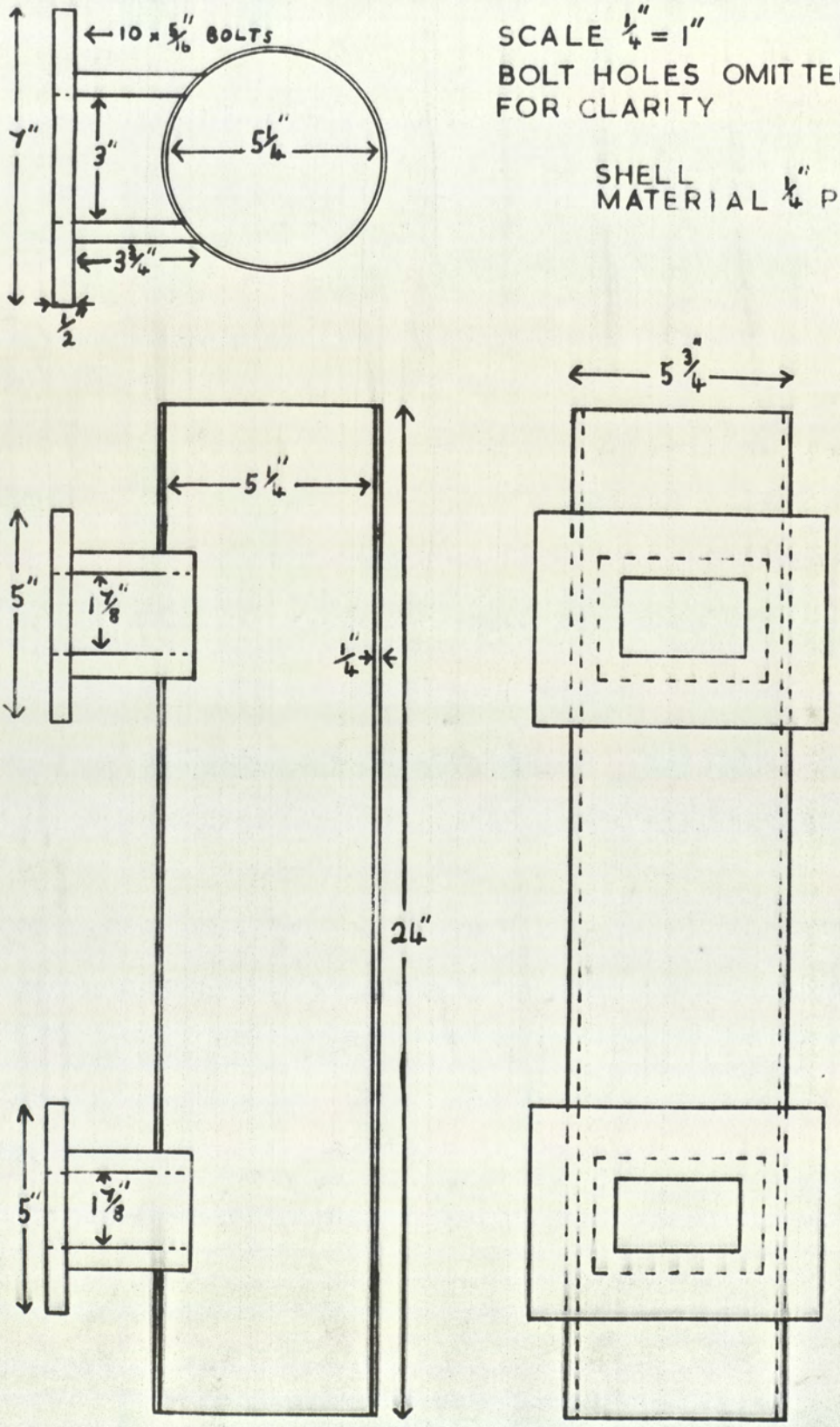

FIG. 9.

the square ends of these ducts into the $1\frac{1}{2}$" diameter pipework. These ducts allowed the fluid to expand gradually into, and contract gradually out of, the exchanger shell which minimised the entrance and exit effects of the fluid. The dowelled flanges and contoured filler prevented sudden changes of section in the duct. A disc and doughnut baffled mixer was incorporated in the exit duct to ensure that the air/mercury stream was homogeneous (but see Chapter IV page 99). A thermocouple was inserted in each of these ducts to measure the fluid stream temperatures.

A $\frac{1}{2}$" hole was drilled in the bottom of the shell wall through which a length of $\frac{3}{8}$" O.D. P.V.C. tube passed to carry the flushing mercury from the transfer probe drain to a collecting vessel outside the exchanger shell. This tube was sealed to the shell with plasticine when a run was in progress.

The exchanger ends were sealed with $\frac{1}{2}$" perspex plates, $\frac{1}{4}$" natural rubber gaskets and 4" Q.V.F. flanges acting as backing flanges. These endplates were secured with three external $\frac{1}{4}$" screwed rods and wingnuts. The top endplate had two $\frac{1}{8}$" O.D. stainless steel tubes cemented in for the flushing mercury to pass through. The probe thermocouple leads were also cemented into the top endplate, connection to the probes being by means of non-reversible two-pin plugs and sockets.

(iii) The transfer probe (see Fig 17 page 83 and Plate 4 page 54).

In order to carry out measurements of the individual tube transfer coefficients it was necessary to replace one tube in the

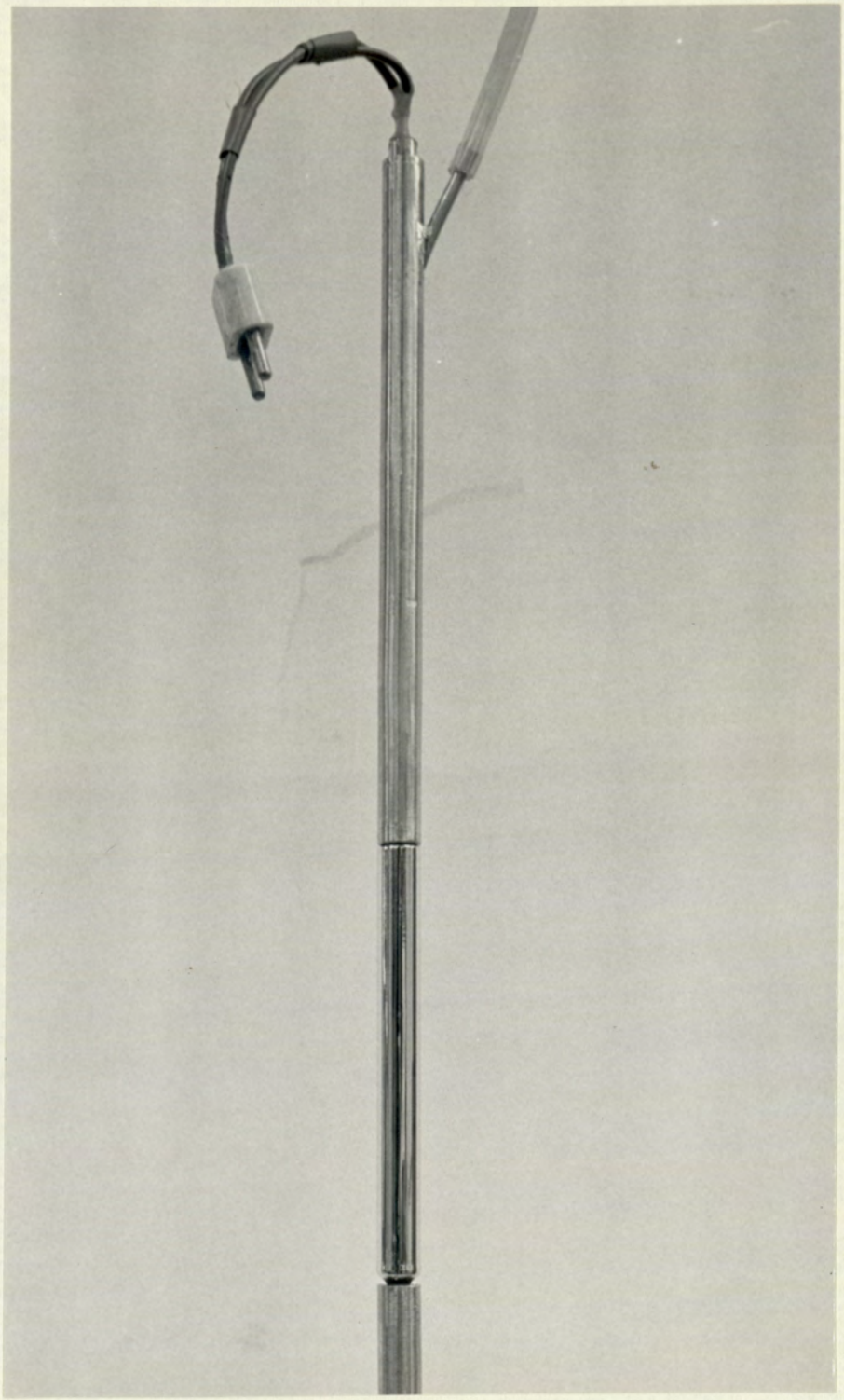

PLATE NO.4. THE TRANSFER PROBE, SHOWING THE MERCURY BULGE AT THE BOTTOM OF THE TRANSFER SURFACE.

bundle at a time with a mercurised transfer surface. Due to the number of different tube positions to be examined it was essential that this mercurised surface could be quickly inserted into, and withdrawn from the bundle. For this reason it was also necessary for the mercurised surface and its ancillaries to be as robust as possible. It was also very important that the temperature of the mercurised surface could be accurately determined, as the vapour pressure of mercury varies a great deal with temperature change. These factors dictated the design of the transfer probe which is described below.

The term transfer probe is used to describe a mercurised length of $\frac{3}{8}$" O.D. copper rod held between two lengths of stainless steel tube, which can replace any tube in the tube bundle. The mercurised surface was situated in the third baffle compartment from the inlet of the exchanger.

The top length of stainless steel tube consisted of two concentric tubes with a thermocouple passing down the inner tube and the thermocouple tip Araldited into the end of the threaded portion, i.e. projecting $\frac{3}{8}$" into the mercurised copper rod. Mercury was passed down the annulus formed between the inner and outer tubes into a weir formed in the top of the mercurised rod. The mercury then flowed down the mercurised surface renewing the surface and flushing the dirty mercury into the bottom stainless steel tube and out of the tube bundle. The thermocouple leads were connected to two-pin non-reversible plugs and sockets which connected to the plugs and leads passing out of the exchanger via the endplate(see Chapter III A (ii)6, page 51).

Full details of this transfer probe are given in Chapter III B of this dissertation which describes the development of the renewal in situ of mercury surfaces.

(iv) Gaskets.

Three criteria had to be borne in mind when choosing a material from which to make the tube bundle gaskets described in Chapter III A(ii)a, page 50. These criteria were:-

(a) The gasket surface should not be attacked by mercury or absorb mercury onto its surface.

(b) The material chosen should be pliable, and at the same time tear resistant, to facilitate constant replacement of tubes, and insertion of the bundle into the exchanger shell.

(c) The material chosen should have a low coefficient of friction, also to facilitate easy replacement of the tubes and insertion of the bundle into the shell.

These properties were difficult to find combined in one material and so a compromise had to be made.

Natural rubber absorbed mercury onto its surface and was therefore rejected.

All grades of Neoprene tried were unfortunately not pliable enough although ideal in the other respects.

Silicone rubbers were therefore investigated and the final one chosen seemed to provide the best combination of the above properties. Unfortunately none of the Silicone rubbers tested were as tear resistant as Neoprene rubber and so the gaskets had to be treated

carefully and replaced fairly frequently. The worst tearing occurred in the part of the gaskets which sealed the baffle edges to the exchanger shell. The final material selected was $\frac{1}{16}$" thick white silicone rubber of 40° Shore hardness manufactured by the Woodville Rubber Company of Ross-on-Wye.

Other gaskets in the apparatus, e.g. exchanger endplate gaskets, were made from $\frac{1}{8}$" thick natural rubber sheet supplied by the same Company.

(v) The Mercury Plating Bath.

The plating bath consisted of a 400 ml. conical flask, fitted with a mild steel anode down its side connected to the positive side of a 2 volt 5 amp battery charger. The copper rod to be plated was screwed onto the output shaft of a Kestner stirrer motor which had been threaded to suit. Electrical contact to the rod was made by means of a copper wiper on the stirrer motor's output shaft. Rotation of the rod prevented the hydrogen bubbles, liberated during the plating process, from adhering to the rod's surface and causing an uneven mercury surface to be deposited. The electrical circuit was completed with an ammeter and a rheostat. Full details of the plating solutions used and the exact plating procedure adopted for the copper rods and gauzes in the present work are given in Appendix 4 page 180 .

(vi) Thermocouples.

The thermocouples were constructed from NICHROME V (0·005" dia.) and ADVANCE (0·01" dia.) wires by capacitance discharge welding.

Due to the 2 : 1 diameter ratio of the wires difficulty was experienced in making a satisfactory weld bead and so several methods of fabrication were investigated. From these investigations it was found that capacitance welding gave the most reproducible and reliable joints.

The thermocouples were insulated with P.V.C. sleeving apart from in the transfer probes where twin bore ceramic tubes were employed.

Previous workers (2, 4) had found that these thermocouples were not attacked by mercury over long periods of time. This fact was confirmed in the present work.

Fabrication and calibration details, together with a calibration chart, are presented in Appendix 1(2), page 165.

(vii) The Absorptiometer.

A detailed description of the absorptiometer, which was a prototype HANOVIA mercury vapour detector, together with a circuit diagram, is given in Appendix 5(1), (page 183).

The electrical supply was fed from the 230 volt A.C. mains via a constant voltage transformer (C.V.T.) and a variac set to maintain the voltage at 200 as the cold discharge ultraviolet lamp was extremely sensitive to voltage change.

The ultraviolet lamp was also sensitive to ambient temperature and so a constant temperature was maintained in the instrument shield casing by the installation of a 250 watt infra red strip element as a heat source and a SUNVIC temperature probe controller and relay. The heating element was mounted on top of the internal chassis, well

away from the photocell and ultraviolet lamp which were mounted in separate containers under the chassis. Air was circulated round the case with a small centrifugal blower in a closed circuit.

Originally the absorptiometer had an ammeter with a range of 0 - 100 μA, graduated in 2 μA divisions, mounted on its front face. However, as it was necessary to keep the readings below 30 μA (by diluting the sample stream) because of the exponential nature of the calibration curve, the following modification was incorporated. The 0 - 100 μA range microammeter was replaced with a 0 - 50 μA microammeter with a series shunt of resistance equal to the internal resistance of the microammeter. This shunt was switched in circuit for setting the full scale deflection of the instrument and then switched out of circuit for calibration, thus giving a larger deflection of the microammeter needle for any given mercury concentration in the sample stream. This effective "doubling" of the scale facilitated more accurate measurements of mercury concentrations to be taken.

With air flowing through the absorptiometer at 15 litres/min the zero was set using a coarse control labelled "Adjust full light" and a fine control labelled "Balance". The full scale deflection of the microammeter, corresponding to extinction of the U.V. light, was set by switching the shunt in circuit, depressing the "Calibrate" button and adjusting the "Sensitivity" control. The shunt was then switched out of circuit.

A ROTOTHERM thermometer was mounted in the front of the casing

to provide a visual check that the meter temperature was constant at $32^{\circ}C \pm 1^{\circ}C$.

A four hour warm up period was allowed for the absorptiometer after it had been switched off for any reason. The absorptiometer was only normally switched off for external reasons, e.g. regeneration of the compressed air dryer.

****
****
**

B. Development of the technique for renewing a mercury surface in situ.

In the original mass transfer technique used by Maxwell and Storrow (4) a galvanically deposited mercury transfer surface was employed. As discussed in Chapter II this necessitated the plotting of ageing curves and the extrapolation of these back to zero time in order to compensate for the falling rate of transfer. Further to this, remercurisation of a surface did not give satisfactorily reproducible results which meant that the experimental technique was not precise enough to measure the variations in transfer rate across a tube bank. Williams (2) therefore adopted nitrogen as his working fluid and found that a short constant transfer rate was obtained before the onset of the falling rate. However, remercurisation of a surface still did not give reproducible results and so Williams turned his attention to the investigation of the mercurised surfaces. From this investigation resulted the use of an electroplating method for depositing the mercury film instead of the previously used galvanic deposition. At first Williams used a solution of mercuric nitrate for electroplating but this was not entirely satisfactory and so he adopted a complex ion solution found by Maugham (37) who was carrying out a survey of plating methods. The plating method finally developed in the present work is described in Appendix 4(page 180) and Chapter III A(v) (page 57). With this plating method and using nitrogen as the working fluid Williams reported constant transfer rate periods of up to an hour and complete reproducibility of transfer rates after the remercurisation of a surface.

It would seem that Williams did not investigate the use of air as the working fluid with his electro-deposited mercury surfaces yet from the foregoing it would seem that the constant rate transfer period was due rather more to the improved mercurisation technique than to the use of nitrogen as the working fluid.

The use of nitrogen as the working fluid resulted in a complicated experimental circuit (see Chapter III A, page 39) and it was therefore decided to investigate the possibility of using air as the working fluid in the present work. The use of air as the working fluid has two main disadvantages:-

(a) The air oxidises the mercurised surface resulting in a falling rate transfer period as the vapour pressure of mercuric oxide is very low compared with the vapour pressure of mercury.

(b) Ozone may be produced photochemically by the action of ultraviolet light upon air in the absorptiometer. The problem is that ozone has an absorption peak for ultraviolet light at 2537 Å which is extremely close to the absorption peak of mercury at 2534 Å.

The second of these two points will be dealt with first as it constituted only a minor problem in the present work. It was found that the formation of ozone could be reduced to an insignificant level by passing the gas stream through the absorptiometer at a rate of fifteen litres per minute in which case the residence time in the meter was too short for an appreciable amount of the oxygen in the gas stream to be converted to ozone. This was demonstrated by zeroing the absorptiometer with air passing through it (see Chapter III A(vii) page 58) and observing any zero shift.

It was found that with either no air flow or low air flow rates (circa five litres per minute) passing through the absorptiometer a zero shift occurred very quickly and ozone could be smelt at the absorptiometer outlet. When the air flow rate through the meter was maintained at fifteen litres per minute no zero shift was observed over several days.

Reverting to the problem of oxidation of the mercury surfaces, the first stage in the present experimental work was to determine whether a constant rate of transfer from the mercury surface could be obtained using air as the working fluid. If this had not been possible there would have been no justification for pursuing the development of the renewal in situ technique, and recourse to the method of Williams using nitrogen as the working fluid would have been unavoidable.

To determine whether or not a constant transfer rate could be obtained a transfer probe of the type used by Haggart (6) (See Fig. 14 page 71) was installed in a glass tube, by means of simplifix couplings, which had two side tubes on it so that air could be blown through the glass tube, over the mercurised surface, and then through the absorptiometer. A diagram of this apparatus is presented in Fig. 10 (page 64). Air was then blown through the tube at various flowrates via rotameter R1 (see circuit diagram given in Fig.7 (page 42)) and a sample was passed through the absorptiometer. The results of this experiment are presented in Figs. 11, 12, 13.

(see pages 65, 66, 67.)

The intention of the experiment had been to renew the mercury

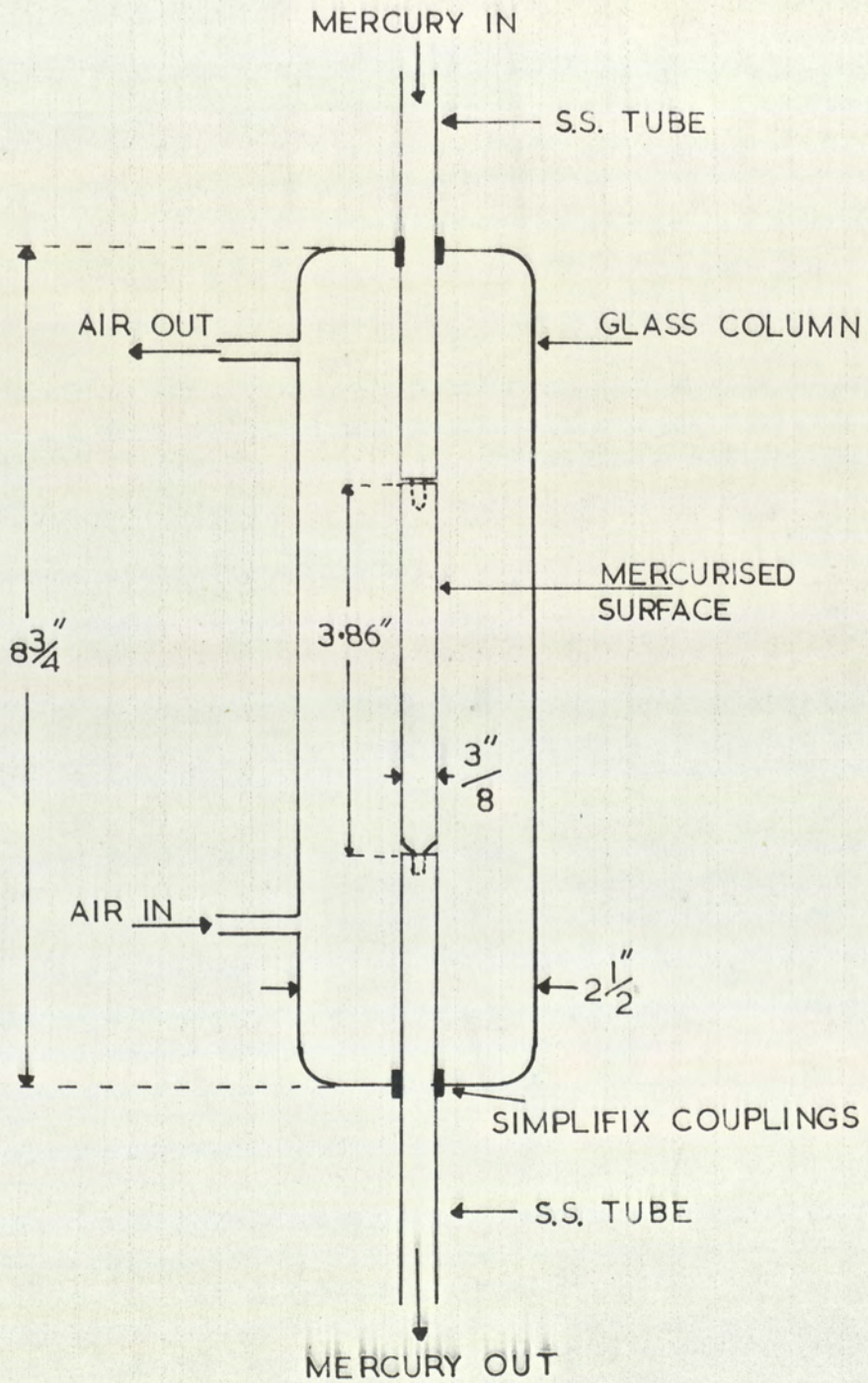
SCALE 1/2" = 1"
MERCURY IN
S.S. TUBE
AIR OUT
GLASS COLUMN
MERCURISED SURFACE
3·86"
8 3/4"
3/8"
AIR IN
2 1/2"
SIMPLIFIX COUPLINGS
S.S. TUBE
MERCURY OUT

FIG. 10.

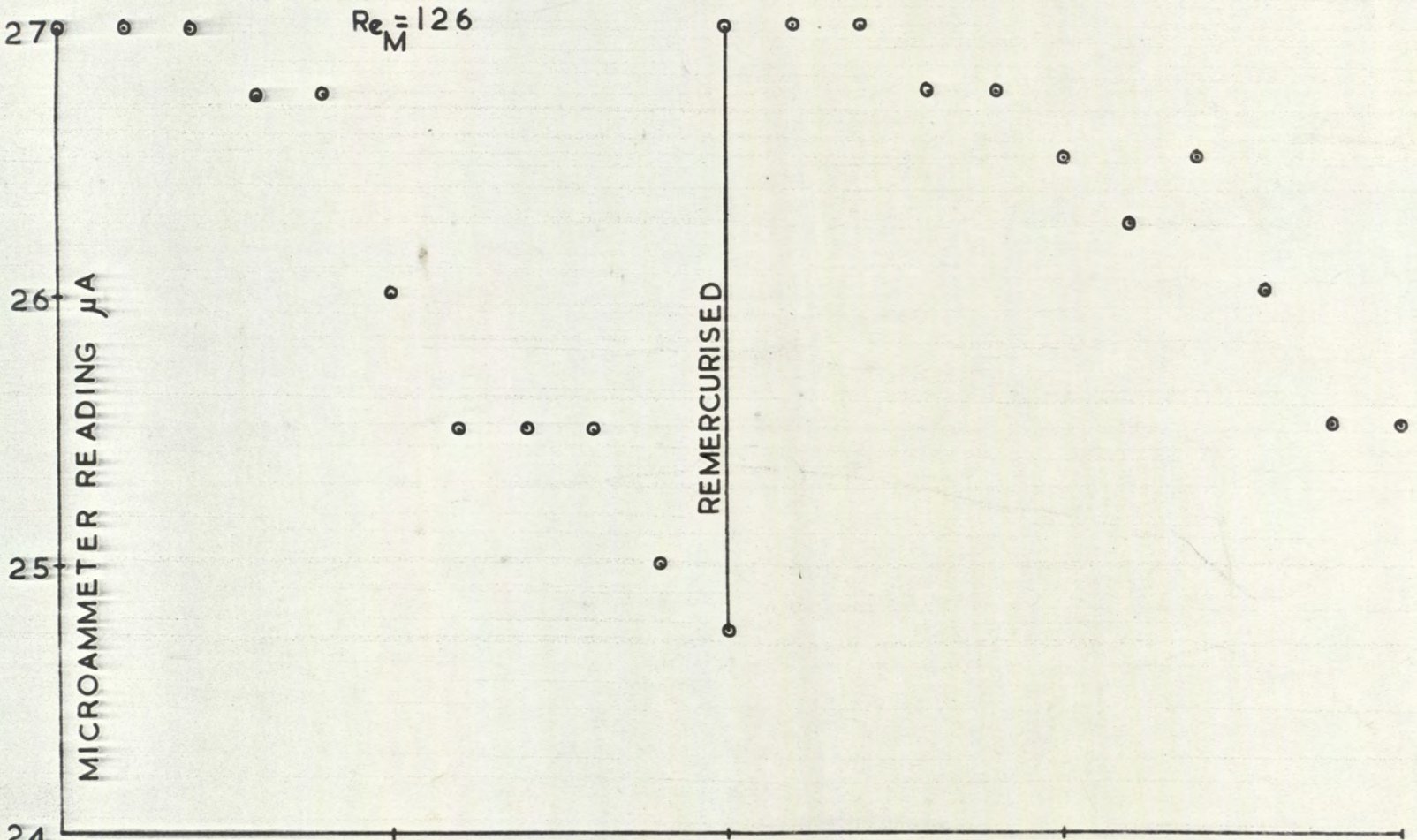
$Re_M = 126$
27
26
25
24
MICROAMMETER READING μA
REMERCURISED
0
5
10
15
20
MINS.

FIG. 11.

MICROAMMETER READING μA
23
22
21
0
5
10
15
20
MINS.
REMERCURISED
$Re_M = 500$

FIG. 12.

17
16
15
14
0
4
8
12
16
MICROAMMETER READING μA
MINS.
$R_M = 2100$
REMERCURISED

FIG. 13.

surface in situ but this was found to be unreliable and it was found to be better to replate and replace the rod. The plated rod was flushed with clean mercury, using a hypodermic syringe, and then immediately installed in the apparatus. The use of simplifix couplings, sealed with rubber O rings, to hold the transfer probe in the glass tube allowed the mercurised rod to be replaced in a matter of seconds. It can be seen from the results that a constant rate of transfer varying from one to three minutes was obtained before the onset of the falling rate period.

These experimental results indicated that it was a viable proposition to obtain individual tube mass transfer coefficients from mercurised surfaces using air as the working fluid provided that it took no longer than one or two minutes to obtain the required observations. This amount of time would be sufficient to obtain the results for one air velocity, but as the transfer factor must be obtained for a number of air flowrates for any given tube position, it was imperative to extend the constant rate period. It was proposed to produce this extended constant rate period by renewing the mercury surface in situ between each set of readings and thus prolonging the constant rate period indefinitely.

The remainder of this Chapter of the current work describes the development of a reliable method of renewing a mercury surface in situ.

The basic idea of renewing a mercury surface in situ is simple:- Clean mercury is fed via an inlet system to the vertically placed mercurised surface down which it flows flushing off the deteriorated and oxidised mercury, leaving a bright fresh mercury surface.

The flushed mercury then flows down a drainage system out of the apparatus. The experimental difficulties in carrying out this operation were found to be both varied and complex.

Haggart (6) had carried out some preliminary work on the renewal of mercury surfaces in situ. He demonstrated that the transfer rate from a mercurised surface freshly flooded with mercury was slightly higher than that from a mercurised surface produced by electroplating. He also found that no improvement in transfer rate was obtained by continuously flushing the surface with mercury, and this was confirmed in the present work as will be shown in Chapter IV.

Haggart was chiefly concerned with demonstrating a method rather than developing a technique. He did develop and use a renewal in situ system for a study of individual tube transfer coefficients in a rectangular tube bank using nitrogen as the working fluid. This too could be classified as demonstrating a method, as the tube pitch to diameter ratio of 2·66 was rather larger than usual which removed some of the technical difficulties encountered with the more usual pitch to diameter ratios (1·25 was used by Bergelin et al.(1), Williams (2) and in the present work). Furthermore a tube bank is experimentally less complex than a baffled shell and tube exchanger where individual tube coefficients in one baffle compartment are to be studied. For practical purposes a system may be ideal for studying coefficients in a tube bank but totally unsuited to studying coefficients in one compartment of a baffled cylindrical exchanger.

A programme was therefore initiated in the present work to develop a technique which could be used in the model exchanger

(described in Chapter III 3(ii). Haggart's original system (see Fig.14 page 71) was first carefully examined to find out whether it could be adapted for use in the model exchanger. Apart from other considerations the use of air as the working fluid in the present work made the mercury surface deterioration much more rapid and serious, due to oxidation, than that encountered by Haggart using nitrogen.

There were two major complications in the present system which entailed extensive modification to Haggart's system, and the final system developed in the present work was only similar to Haggart's system insofar as both systems were designed to renew a mercury surface in situ.

These complications were:-

(a) The temperature of the mercurised surface was required in order that the vapour pressure exerted by it could be calculated, and so a thermocouple (see Appendix 1(b), page 165) had to be incorporated in the inlet system. This necessitated the mercury inlet system being in the form of a coaxial tube with the thermocouple passing down the inner tube and the mercury flowing through the annulus formed between the inner and outer tubes. This mercury inlet system, incorporating a thermocouple was basically successful from its inception and most of the problems that were encountered with it were due to drainage problems and were solved when the high capacity drainage system was finally developed.

(b) Any spillage of mercury in the tube bundle would cause erroneous readings of the absorptiometer. Due to the small clearances between the tubes of the tube bundle (1·25 pitch to diameter

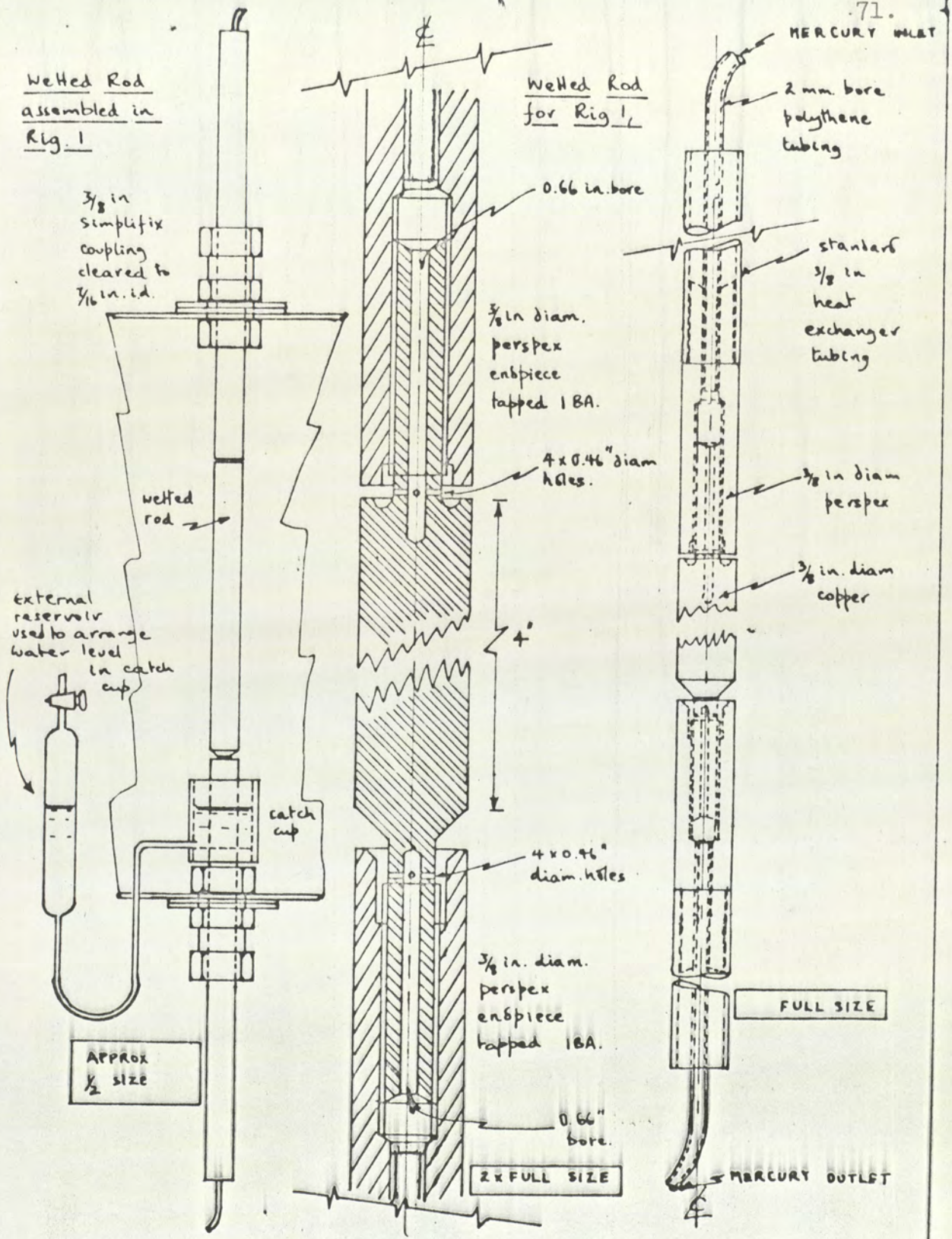

(HAGGART(6) FIG. 4.)

FIG. 14.

ratio) it was impossible to incorporate a catch cup to retain any mercury which did not flow down the drainage system. Apart from space considerations the incorporation of a catch cup in the tube bundle would have affected the shellside flow patterns which could not be tolerated. As well as there being no projections, such as catch cups, in the baffle compartment being studied, similarly no projections could be contemplated in the adjacent baffle compartments. This precluded the use of systems such as used by Haggart in his tube bank studies where the mercury surface was effectively extended at each end so as to be outside the tube bank.

As the work progressed it was found that the development of a really effective drainage system to catch 100% of the flushed mercury, and which did not project into the shellside flow, was to constitute the major proportion of the present experimental work.

The actual transfer surface consisted of a length (3·86") of electrolytic copper with an electroplated mercury surface. The ease of surface renewal of the rod was found to be directly related to the quality of the mercury plating. The method of electroplating used in the present work is described in Appendix 4,(page 180).
As described in Chapter III (page 39) the model tube bundle was mounted vertically so that the mercury surface could be renewed in situ. It is convenient therefore to refer to the top of the mercurised copper rod as the inlet, and the bottom as the drainage end respectively. The forms of the ends of the rods were developed in conjunction with the inlet and drainage mercury systems and will therefore be considered with those systems.

The whole assembly consisting of a mercury inlet system, a mercurised transfer surface and a mercury drainage system was termed a transfer probe.

(i) The mercury inlet system (see Fig.15, page 74).

The requirements of this system were firstly, by definition, to feed clean mercury to the mercurised transfer surface when it was desired to renew this surface, and secondly to measure the temperature of the transfer surface. It was decided, therefore, to use a coaxial tube with a thermocouple passing down the centre tube and into the mercurised copper rod and the flushing mercury passing down the annulus formed between the two tubes. The end of the inner tube was threaded $\frac{1}{4}$" BSF to screw into the mercurised copper rod and thus locate it and the thermocouple was insulated by twin bore ceramic tubes passed down the central $\frac{1}{8}$" diameter hole. The thermocouple tip was Araldited into the end of the tube so that it was flush with the end of the thread. The inner tube was machined from mild steel bar with a spigot at its lower end to locate it in the outer tube, which was stainless steel of $\frac{3}{8}$" outside diameter with a wall thickness of $\frac{1}{32}$". A short length of $\frac{1}{8}$" outside diameter $\frac{3}{32}$" bore stainless steel tube was welded onto this tube to serve as a mercury feed. This welding operation was not entirely satisfactory as the small sizes precluded the use of argon arc welding, and mercury attacked the more usual silver soldering alloys. However, a special high silver content rod was obtained (BS 1845 AG3) and no further trouble was experienced with mercury attacking the joint during the present work. (Araldite adhesive was tried for this joint but was

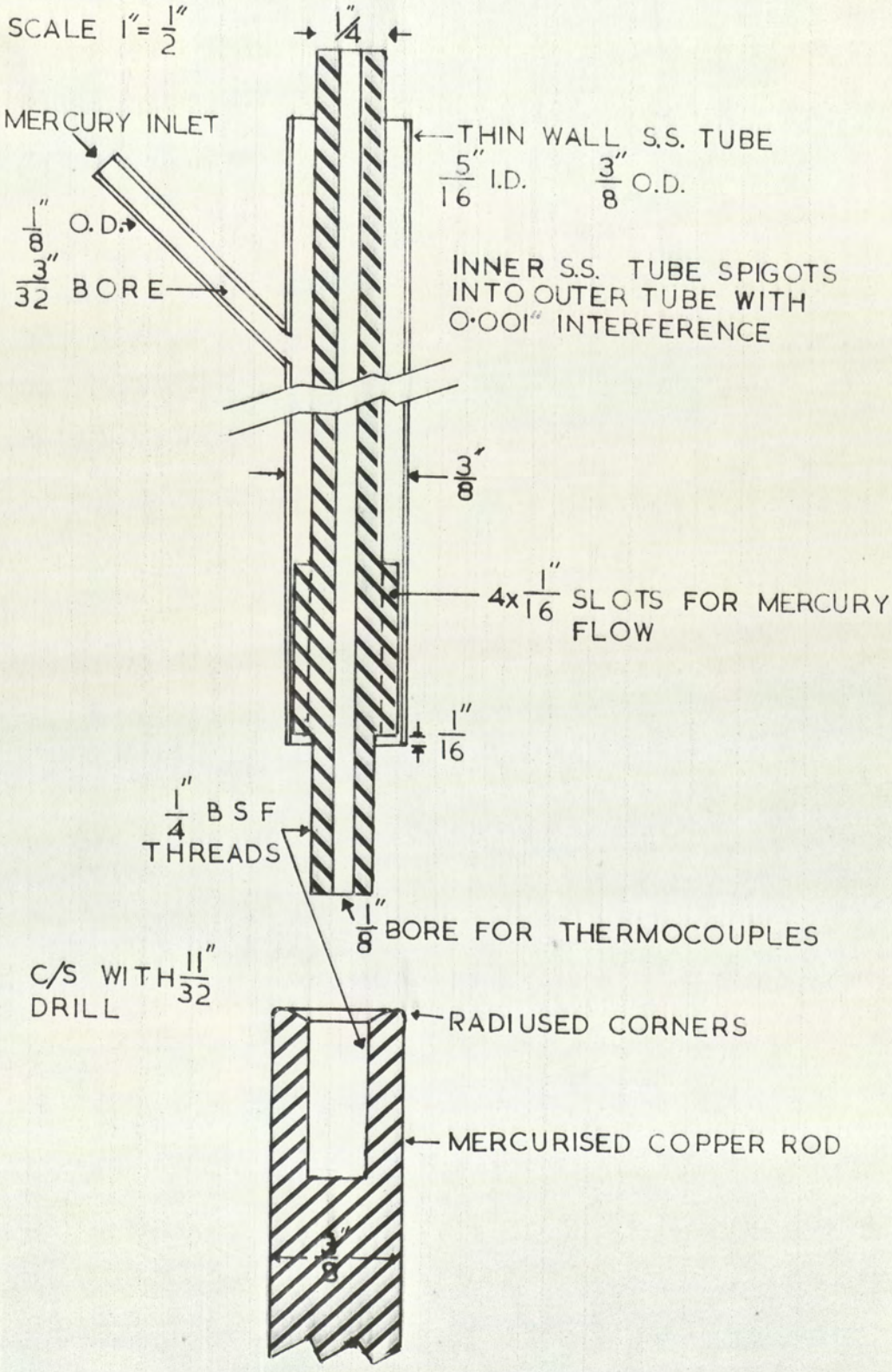
SCALE 1" = 1/2"
1/4"
MERCURY INLET
THIN WALL S.S. TUBE
5/16" I.D.
3/8" O.D.
1/8" O.D.
3/32" BORE
INNER S.S. TUBE SPIGOTS INTO OUTER TUBE WITH 0·001" INTERFERENCE
3/8"
4x 1/16" SLOTS FOR MERCURY FLOW
1/16"
1/4" BSF THREADS
1/8" BORE FOR THERMOCOUPLES
C/S WITH 11/32" DRILL
RADIUSED CORNERS
MERCURISED COPPER ROD
3/8"

FIG. 15.

found mechanically unreliable, possibly due to the difficulties of cleaning such small areas satisfactorily). If this system were used for future work it would be worthwhile to braze a gusset plate between the side arm and the main tube to increase the mechanical strength of the assembly.

As previously mentioned the inner tube was turned from mild steel bar and, as rust acts as a catalyst for the oxidation of mercury, chromium plated. Slots were milled in the locating spigot to allow the mercury to flow to the mercurised rod and so whenever it was desired to change the size or configuration of these slots it was necessary to rechrome the tube after modification. Apart from the fairly considerable delay incurred by the chroming process it was considered that the slots were never satisfactorily plated, and hence corrosion occurred. The use of stainless steel for this inner tube had previously been rejected because of the problem of availability, and its inherent machining problems, particularly the accurate drilling of small diameter holes. On account of the corrosion problem it was decided to fabricate the inner tubes from available stainless steel tube and bar stock. This was done by making the tube in two sections. The spigot section was turned from stainless steel bar and into this a length of stainless steel tube was fitted by freezing (with solid carbon dioxide). The dimensions of this composite inner tube were the same as those of the tube that it replaced. The use of stainless steel simplified modifications and removed the corrosion problem. However the problem with the mercury reflushing, which was thought to be due to corrosion, was not solved

by this change of material. The problem encountered was that the small amount of mercury which remained in the inlet system after flushing very quickly oxidised and deteriorated. The resulting effect was that the deteriorated mercury transfer surface to be flushed was often rather cleaner than the stream of flushing mercury which carried with it the dirty mercury left in the inlet system from the previous flushing operation. Although this problem was alleviated by regular cleaning of the inlet system (with dilute caustic soda and nitric acid) and modifications to the internal shape, e.g. streamlining the entry into the spigot slots to remove possible lodging places for the mercury, it was not finally solved until the high capacity mercury drainage system was developed when much higher flushing rates were possible. Controlling the mercury flow was also somewhat difficult as due to the high inertia of the mercury it tended to build up and then surge through the slots. Using larger slots and an external needle valve did not cure the surges and it seemed better to fill the annulus quickly with mercury and let this drain through the slots. The slot dimension was varied by degrees until it was sufficiently large to pass sufficient mercury to flush the transfer surface adequately without spillage occurring at the drainage end of the mercurised rod. When the final high capacity drainage system was introduced, and higher flushing rates were practicable, the slots were enlarged and although their width still controlled the flow surging did not occur. It can be seen from the above that for a reliable reflushing technique an adequate drainage system is of paramount importance.

The inlet end of the copper rod (see Fig. 15 page 74) was developed in conjunction with the mercury inlet system and it was found that the provision of a weir was the critical factor in ensuring even distribution of the flushing mercury. The final form taken was to countersink the copper rod slightly with an $\frac{11"}{32}$ drill and radius all the sharp corners as shown in the above Fig.15.

(ii) The mercury drainage system (see Fig.16, page 78).

At an early stage in the present work it was realised that production of an effective renewal in situ technique was mostly dependent on the drainage system. A great deal of the experimental study of the present work was therefore concerned with this problem and the final high capacity drainage system was only realised at the end of the present work.

As mentioned previously the small clearances of the tube bundle, apart from flow considerations, made it impossible to incorporate a catch cup, and as spilt mercury would invalidate the results it was imperative that all the flushing mercury passed down the drainage system.

As the mercury inlet system had to incorporate a thermocouple it was impossible to use Haggart's (6) basic design and so the system described above was developed. However as there were no such complications at the drainage end of the system it was decided to utilise Haggart's system if possible, and the first drainage system was essentially similar to that of Haggart. The modifications made and the different systems tried were not necessarily in the following

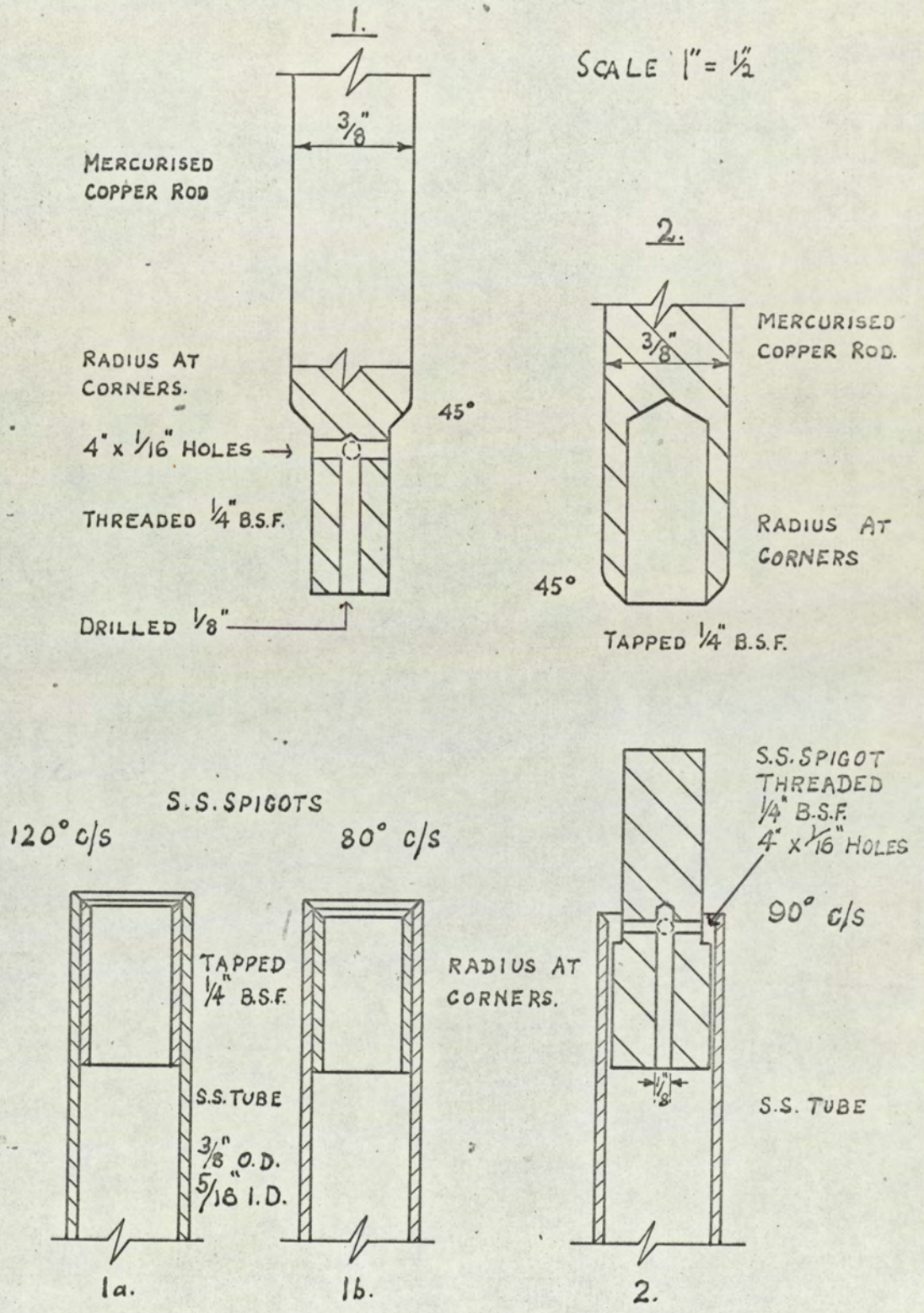
1.
SCALE 1" = ½"
3/8"
MERCURISED COPPER ROD
RADIUS AT CORNERS.
45°
4" x 1/16" HOLES
THREADED ¼" B.S.F.
DRILLED 1/8"
2.
3/8"
MERCURISED COPPER ROD.
RADIUS AT CORNERS
45°
TAPPED ¼" B.S.F.
S.S. SPIGOTS
120° c/s
80° c/s
TAPPED ¼" B.S.F.
S.S. TUBE
3/8" O.D.
5/16" I.D.
RADIUS AT CORNERS.
S.S. SPIGOT THREADED ¼" B.S.F.
4" x 1/16" HOLES
90° c/s
1/8"
S.S. TUBE
1a.
1b.
2.

FIG. 16

order, as modifications made to other components of the transfer probe affected the drainage.

The major problem seemed to be that the oxidised mercury, when flushed, tended to flake and the flakes blocked the radial drainage holes in the mercurised rod. This caused some spillage of mercury before the head of mercury forced the flakes through the holes. Increasing the hole diameter from 0·048" to 0·062" seemed to help the problem partially, but even so if only one hole blocked there would be spillage on that sector of the tube. Altering the taper angle of the mercurised rod and trying different radii also failed to make the system 100% reliable. The angle of countersink at the top of the drainage system (see Fig. 16 page 78) was also altered to give an increasing annulus area between itself and the taper on the rod, but no improvement was obtained after making the angle of countersink equal to the angle of taper. The bottom of the mercurised rod was threaded $\frac{1}{4}$"BSF and screwed into a spigot in the stainless steel catch tube. The spigot was pressed further into the tube, and the radial holes in the mercurised rod were relocated further down so as to have the mercury flowing into the well and then down the drain holes. It was thought that this had cured the spillage, but unfortunately the system was not completely reliable and so further development work was instigated.

Another system was devised (see Fig. 16 (2)page 78) in which the tapered end of the rod was tapped, and the spigot in the tube was redesigned to be longer and threaded so as to screw into the rod. The drainage holes in this case were drilled in the spigot.

The stainless steel spigot was quickly rejected as it did not wet with mercury. If mercury did go through the holes then, as the system did not wet, it tended to flow in pellets down the holes and this sucked the following mercury through the holes. The system resulted in either all or none of the mercury going through the drainage system. Another spigot was therefore made up without drainage holes in it, but with drain slots filed down the sides. The results were rather similar to the previous system so another spigot was constructed of mercury-plated copper. The results from this system were no better than those from the integral mercurised rod and drain holes and so the system was discontinued. The application of suction by a laboratory vacuum pump sometimes helped the drainage problem, but did not remove the spillage caused by one of the drain holes blocking. As results of this system were discouraging and on the whole not as good as those obtained with the modified Haggart's system it was decided to return to the latter system.

Although with modifications to radii and hole sizes this system became much more reliable extreme care was necessary with the rates of flushing. As it was impossible to increase the radial hole diameter above 0·062" and the axial hole diameter above 0·125" without seriously weakening the mercurised copper rod it was decided to investigate the possibility of using a copper plated mild steel rod. A mild steel rod was therefore constructed to the same dimensions as the copper rods, but with bigger drain holes in it, and this was then copper plated before being mercury plated. The small improvement obtained in drainage with the larger holes was

outweighed by the inherent mechanical weaknesses of the copper plating and so this approach was discontinued.

Continued development on the original system had resulted in reliable flushing of the mercury surface if the flushing mercury was fed to the inlet system via a size 18 hypodermic needle, and it was therefore decided to install the system in the model exchanger. Tubes 58 and 64 at the outside edge of the exchanger (see Fig. 4 page 36) were therefore replaced with a transfer probe, as being at the outside of the bundle the renewal of the mercury surface could be observed. Mercury was led to the inlet and from the drainage systems with P.V.C. tubing. As will be discussed in Chapter IV, although the mercurised rods appeared to be flushing the mass transfer factors were only about 5% of the expected values, i.e. the surface was oxidised. The situation was rather akin to that encountered with static films on wetted wall columns, and in this case the mercury was flowing down behind the transfer surface without renewing it. As the flushing rate was similar to that used by Haggart (30 ml/min.) using nitrogen it was thought that the deterioration of the mercury surface was rather more severe in this case due to oxidation.

It was obvious that further development was required, the main requisite being a higher capacity drainage system which would permit a higher flushing rate. This it was hoped would cure the stagnant film problem. Further experiments were conducted and minor modifications made to the drainage system without notable success. Application of suction was tried once more without achieving the required reliability of drainage. Finally when the possibility of

having to resort to the use of nitrogen as the working fluid was being considered, because it was thought that the absence of oxide on the mercury surface with this system would allow easier flushing, the high capacity drainage system was conceived and constructed. This system worked well from its inception and only small modifications were required to finalise its design.

It was realised that the mercury was having to make two ninety degree turns, one fairly gentle and the other very acute (from the radial to the axial holes in the mercurised rod). With the high inertia of mercury this was extremely difficult as once the mercury started to move it was extremely difficult to stop or to deviate it. Hence when a drainage hole blocked the mercury would not reroute itself but would instead continue in the same direction and spill. The inertia of the mercury was therefore employed to assist the flushing instead of hindering it as hitherto. New copper rods were made with ends similar to the original ends but without threads (see Fig. 17 page 83). The mercury flowed down the rod, and negotiated a gentle S bend and then flowed down into the drain tube. The mercurised rod was located by a shaft extending from a three legged spider spigot constructed of stainless steel, with the mercury entrance end of the legs streamlined to prevent mercury build up. The dimensions and angles were arrived at by experiment but as stated above the method worked well from inception and required very little modification.

With this system flushing rates as high as 90 ml./min. were possible (cf 30 ml./min. previously) and the problems referred to

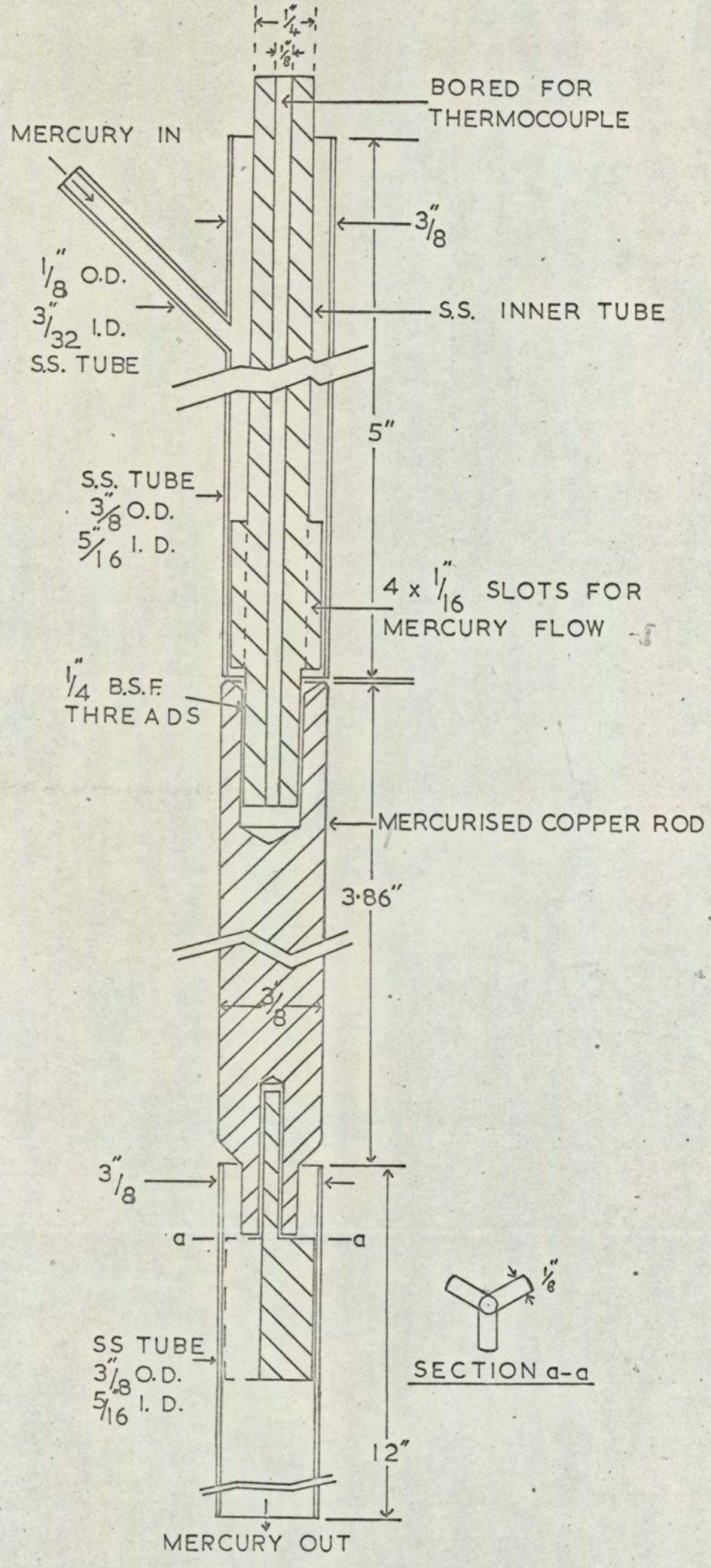

FIG. 17. — TRANSFER PROBE.

in the mercury inlet system were removed with the high flushing rate.

The renewal of the mercury surface was visually most striking, the dirty mercury film moving, as a sheath, down the transfer surface to be replaced by a fresh mirror-like surface. An oxide film developed over twelve hours was easily flushed away with this system, and for regular flushing i.e. between each flowrate, 5 ml. of mercury were adequate.

This transfer probe (Fig. 17) was therefore installed in the model exchanger, as previously, and the experimental results are discussed in Chapter IV of this dissertation.

A photograph of the final transfer probe is presanted in Plate 4 page 54.

C. Experimental Methods.

The experimental results were obtained by using the apparatus described in the previous sections of the current chapter, and in order that results should be reproducible from day to day a certain system of checks and order of operations were required. This section outlines these details and deals with the preliminaries to an experimental run, followed by mercurisation of the transfer surface and the insertion of the transfer surface into the exchanger bundle. The operations involved in the actual experimental run are then listed, followed by a description of the general maintenance programme of the apparatus.

(i) Preliminaries to an experimental run.

A check was made to ensure that all the services were working normally, electrical connections intact and manometer levels satisfactory. The absorptiometer was checked and adjusted, if necessary, as described in Appendix 5 page 183. The Dewar flask housing the thermocouple cold junction was filled with a mixture of crushed ice and distilled water, and the Scalamp galvanometer switched on. The accumulator was then standardised ready for the measurement of the thermocouple emfs.

(ii) Mercurisation of the transfer surfaces.

The rods to be mercury plated were buffed on a lathe with metal polish to produce a smooth shiny surface. They were dipped into hot Teepol solution, water rinsed, dipped into warm $\frac{N}{4}$ caustic soda solution, water rinsed, dipped into warn 4N sulphuric acid, water

rinsed, and finally fitted into the plating bath, (Chapter III A (v) page 57). All these operations were carried out using crucible tongs with P.V.C. sleeved ends. The rod was then electroplated using a current of 0·4 amps whilst being constantly rotated. The rod was then removed from the plating bath, taking care not to scratch the surface, rinsed in water and dried with ethanol. Surface films were then flushed off the rod with clean mercury using a hypodermic syringe. The rod was then inserted into a transfer probe assembly and a check made that the mercury surface could be satisfactorily renewed. If the surface "renewed" evenly the rod was stored under mercury until it was required. If it did not "renew" satisfactorily then the plating process was repeated. A new copper rod required plating at least five times before a well bonded mercury surface, which would renew satisfactorily, was established.

By storing the mercurised rods under mercury the surface of the rods was maintained indefinitely.

(iii) Insertion of the transfer probes into the tube bundle.

It was extremely important that the mercurised surfaces should not be touched by hand, or scratched, during assembly as this prevented perfect renewal of the surfaces. The mercurised rods were therefore always manipulated with P.V.C. sleeved tongs, or mild steel hooks in the holes at each end of the rods.

The mercurised rods were removed from storage and assembled into the transfer probe assembly, and a check was then made to ensure that the mercury surface could be satisfactorily renewed.

The mercurised section was then removed from the probe assembly and the inlet and drainage tubes were inserted into the bundle in the appropriate tube position. The mercurised rod was then manoeuvred sideways into the bundle, using mild steel hooks in the holes at each end, so that the spigot at the drainage end of the rod projected through the baffle. This spigot was then held with the tongs while the inlet tube was screwed onto the mercurised rod. The drainage tube was then inserted into the rod's spigot, the tongs withdrawn and a further check made to ensure that the mercurised surface could be renewed. The bundle was then inserted into the shell and the probe's thermocouple and mercury lines connected. Accurate positioning of the tube bundle in the shell was achieved by scribing guide lines on the tube bundle end plates and the exchanger shell.

(iv) The experimental run (see Fig. 7 page 42).

Having assembled the exchanger the various joints were tested for leakage by pressurizing with air and testing with Teepol solution. The mercurised surfaces were then renewed. The exchanger was brought on stream by opening valve V 1, and selecting the appropriate flowrate via rotameters R1 or R2. The range of flowrates investigated was from 25 - 2500 litres/minute i.e. $70 < Re_m < 7100$ and as far as possible identical flowrates were used for each tube position investigated.

For each flowrate a sample of the outlet gas from the exchanger was taken via valve V 14 and rotameters R3 and R6 into the absorptiometer. If the reading on the microammeter scale was

greater than 40 μA the sample stream was diluted by air via rotameters R4 or R5. A flow of 15 litres/min. of this stream was fed into the absorptiometer and the excess by-passed via valve V 7. To induce the sample stream to flow through the exchanger at low flowrates valve V 13 was partially closed as necessary.

After allowing the conditions to become steady, the following readings were noted:-

(a) Absorptiometer microammeter reading.

(b) Rotameter readings R1, R2, R3, R6 (and R4 or R5).

(c) Manometer readings M_1, M_2, M_3 and M_4.

(d) Exchanger thermocouple readings, i.e. gas inlet, gas outlet, transfer probes.

(e) Meter temperature.

(f) Ambient temperature and pressure.

Valve V 1 was then shut, and pure air was passed through the absorptiometer. If a zero shift had occurred the results were discarded and the run repeated.

The mercurised transfer surfaces were then renewed, and the above procedure repeated for another flowrate.

At the end of a series of runs at a given transfer probe position the bundle was removed from the exchanger shell ready for the next run. If the next run, at a different tube position, was not to be carried out immediately, the mercurised copper rods were stored under mercury until required.

(v). General Precautions and Maintenance.

The absorptiometer was only switched off if it needed repairing, and after repair a four hour warm up period was allowed. Normally air was kept flowing through the absorptiometer at 15 litres/min. to maintain a steady zero.

The Aerox filter was regularly cleaned by back flushing and the Birlec dryer was frequently regenerated.

Although a one hour warm up period was necessary for the Scalamp galvanometer to achieve stability it was not practicable to leave the galvanometer switched on constantly as the bulb life was very short.

The transfer surfaces were always stored under mercury to prevent deterioration of the mercurised surfaces.

****
****
**

CHAPTER IV

DISCUSSION OF EXPERIMENTAL RESULTS.

The major portion of the present experimental work was the development of a viable method of renewing a mercury surface in situ, as described in Chapter III B of the present work, (pages 61 - 84). Until this development work had been completed it was not possible to obtain any individual tube shellside mass transfer coefficients in the segmentally baffled shell and tube exchanger. It was therefore impossible to investigate comprehensively the effects of the various geometrical parameters, e.g. baffle cut down, baffle spacing, on the mass transfer coefficients and so the experimental runs carried out were designed to prove the present method of obtaining mass transfer coefficients by comparing these coefficients with those obtained by Williams (2).

To make this comparison it was proposed to carry out a series of experimental runs (Experimental methods were described in Chapter III C pages 85 - 89) so as to obtain results for the mass transfer factor j_{DM} versus the Reynolds number Re_M. These values of j_{DM} and Re_M could then be plotted and compared with the results obtained by Williams. Certain tubes, which it was thought by virtue of their position in the bundle, e.g. at the baffle edge, would best indicate the effectiveness of the present experimental methods, were selected for this purpose. These tubes were all at the bundle edge so that the mercury renewal could be visually checked. The numbers of these tubes (see Fig.4 page 36).

were 58 and 64 in the outlet baffle edge zone, 17 and 23 in the inlet baffle edge zone and 80. In all cases the 31% baffle cut down was employed.

For the first experimental run two transfer probes were installed in the mirror image tube positions 58 and 64 and the exchanger was brought on stream. A series of eleven values of the mass transfer factor j_{DM} were then obtained over the Reynolds number range from 68·5 to 6,800. These results are given in Table 6:1, Appendix 6 (page 188) and are represented graphically together with Williams' results for tubes 58 and 64 in Fig.18 (page 92). From inspection of the figure it will be seen that there is considerable variation between the results of Williams and the results obtained in the present work. This first experimental run was conducted with the early transfer probe drainage system (see Chapter III B page 61) and it was felt that the reason for the disparity of the results was due to inadequate renewal of the mercury transfer surface. From visual inspection it seemed that the flushing mercury stream was flowing down the mercurised rod behind the dirty mercury surface without flushing the dirty mercury away. This behaviour is analogous to that of static films in wetted wall columns. Because of this ineffective flushing of the mercury, further investigation of the renewal in situ technique was made and the high capacity drainage system was evolved as described in Chapter III B and shown in Fig.17 (page 83).

As will be discussed later in this section it would seem that unrepresentative sampling of the air/mercury stream, possibly caused

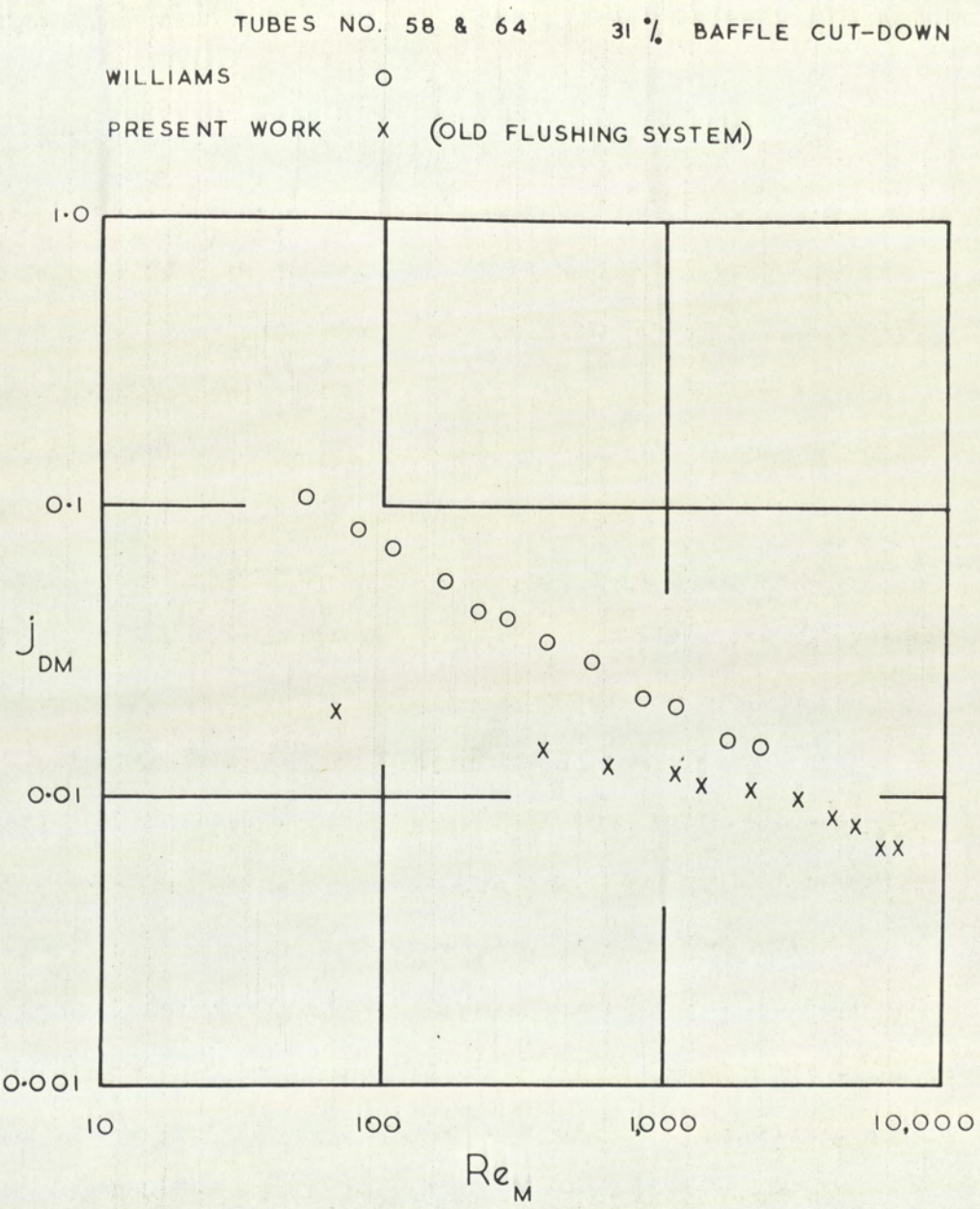
TUBES NO. 58 & 64
31 % BAFFLE CUT-DOWN
WILLIAMS O
PRESENT WORK X (OLD FLUSHING SYSTEM)
1·0
0·1
0·01
0·001
j_{DM}
10
100
1,000
10,000
Re_M

FIG. 18.

by incomplete mixing, was partially responsible for the divergence of the present results from those of Williams. But it is clear that most of the divergence was due to the flushing trouble, two experimental runs for the tube positions being stopped as visual observation showed that flushing was not occurring properly and closer observation showing that a static film was occurring. Of course when the renewal in situ technique was tried without air blowing through the exchanger it tended to be more reliable as oxidation of the mercury surface occurred much more slowly than was the case during an experimental run.

At this point in the work the high capacity drainage system (see Chapter III B page 61) was developed. A transfer probe incorporating the new drainage system was therefore installed in tube position 64 in the tube bundle and the exchanger was then brought on stream so that an air flow of 407 L/min., i.e. Re_M = 1122 was maintained over the mercurised surface. The following visual observations were made during this run.

At the beginning of the experimental run the transfer surface had a mirror finish. This mirror finish slowly disappeared to be replaced by a matt silver surface which first appeared at the top of the rod and then spread slowly down the rod surface. This effect was almost certainly due to the drainage of mercury from the rod, as the appearance of the matt surface coincided with the disappearance of the "bulge" at the base of the mercury surface (visible in Plate 4 page 54). This was about two minutes after the start of the experimental run. The mercury surface then began to deteriorate

and over the course of an hour a grey black film of oxidised mercury appeared on the surface of the rod. After sixty five minutes the mercurised surface was renewed in situ, and the same pattern of observations was noted. The run was repeated a third time and the mercurised rod was then left with the air passing through the exchanger for several hours, and then remained overnight in the tube bundle (safety regulations precluded leaving air blowing through the exchanger). After this period of time the surface of the rod was grey-black in colour and of flaky appearance. As will be described below, from the microammeter readings it would appear that at this stage the surface of the rod was virtually all oxidised mercury. Nevertheless the surface was renewed easily, and the surface was restored by this operation to its previous mirror finish. During this mercury surface renewal no mercury was spilt into the bundle and 15 ml. of mercury was sufficient to renew the surface. The surface renewal after 65 min. required only 5 ml. of mercury.

With the previous mercury drainage system it was not possible to reflush successfully a surface only one hour old, so it was felt that this reflushing after twelve hours proved that the high capacity drainage system was successful. For the sake of completeness the reflushing was repeated twice more after the mercurised surface had stood for twelve hours.

Having described the visual aspects of these experiments their quantitative nature will be assessed. The experimental results are tabulated in Table 6:2, Appendix 6 (Page 188) and the decay curve is plotted in Fig.19 (page 95).

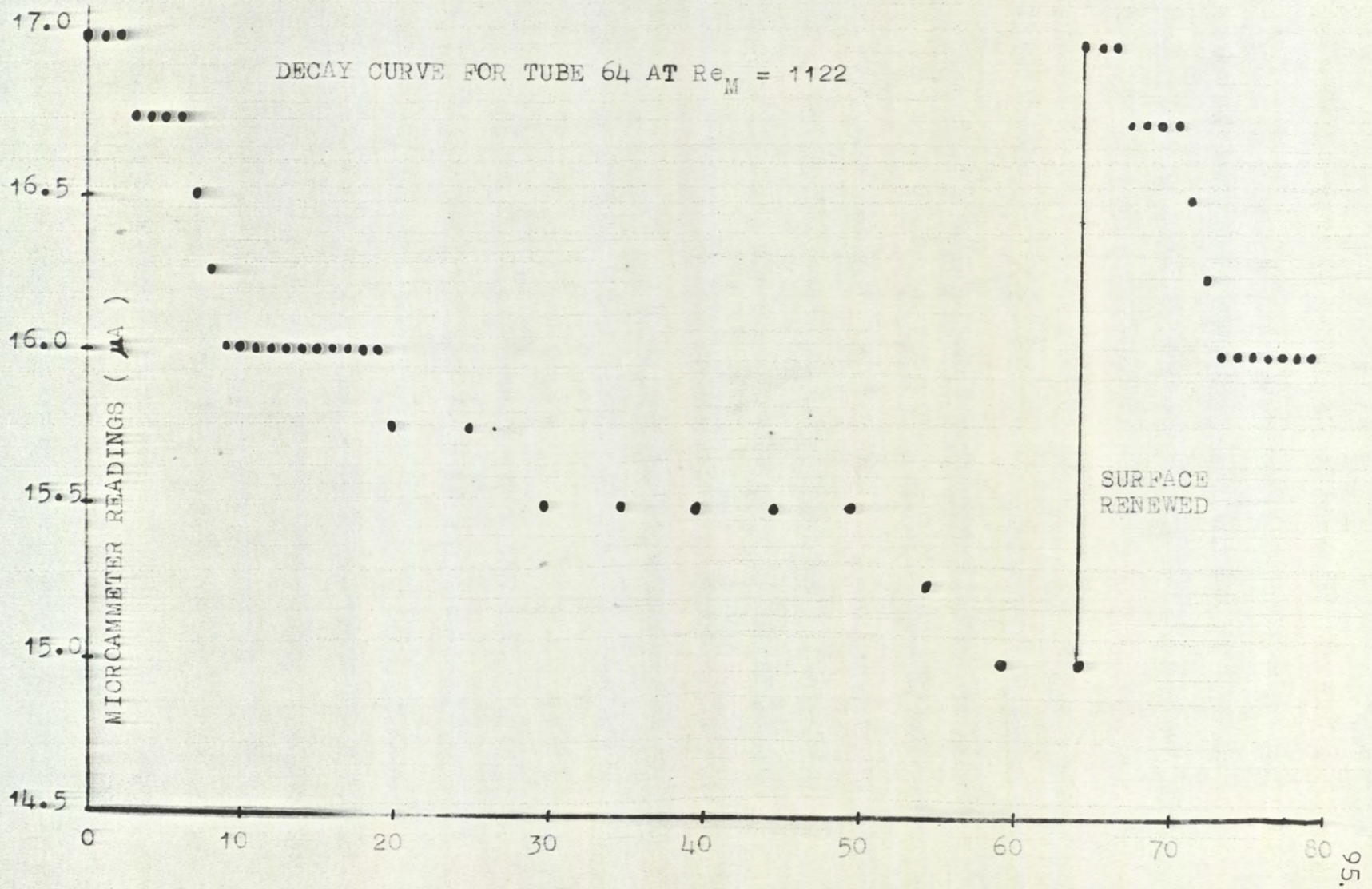
DECAY CURVE FOR TUBE 64 AT Re_M = 1122
MICROAMMETER READINGS (μA)
17.0
16.5
16.0
15.5
15.0
14.5
0
10
20
30
40
50
60
70
80
SURFACE RENEWED
TIME (mins)

FIG. 19.

From the decay curve it can be seen that at this air flowrate a constant transfer rate period is obtained for two minutes and the curve then falls gradually away. After sixty five minutes the microammeter reading had fallen by 11½% and the mercury surface was then renewed. The microammeter reading immediately returned to its initial position indicating that the mercury surface had been satisfactorily renewed. The above was repeated twice more with the same effect of returning the microammeter reading to its initial position.

At this point a continuous flow of mercury was maintained down the transfer probe to see if a higher microammeter reading was obtained. A higher reading was not obtained which confirmed the findings of Haggart (6), indicating that the mercury surface obtained by plating and renewing in situ exerted the full vapour pressure of liquid mercury.

The apparatus was then left overnight and after twelve hours the microammeter reading had fallen to 2·1 which was equivalent to a transfer factor of about 6% of the initial transfer factor, i.e. the surface of the rod was coated with oxidised mercury. However, after renewing the surface the microammeter reading returned to its initial position indicating that renewal of a mercury surface in situ could effectively prolong the constant transfer rate period indefinitely.

(At this stage it is worth mentioning the constant rate transfer periods obtained by Williams (2). Although as nitrogen was used there would be obviously no oxidation of the mercury surface, it is

possible that the use of horizontal mercurised rods increased the constant rate periods as drainage of mercury from the surface would be less severe than that encountered with vertical tubes.)

Having obtained a satisfactory method of renewing a mercury surface in situ experimental runs were continued on the aforementioned tube positions, i.e. 58, 64, 17 and 80, and the results from these experiments will now be discussed.

It was decided that in the case of the mirror image tubes 58 and 64 these tubes would be considered separately. This was done for two reasons, firstly to confirm that these tubes were indeed identical, i.e. there was no asymmetric flow through the present bundle, and secondly to cut down errors if the reflushing technique should prove troublesome. It was felt that with one tube if the surface did not renew satisfactorily then this fact would be obvious, but that with two tubes it would not be obvious if either or both surfaces were not renewing satisfactorily.

A transfer probe was therefore installed in tube position 64 and the exchanger was brought on stream. A series of values of the mass transfer factor j_{DM} were then obtained over the Reynolds number range from 55·5 to 6150. The results of this run are given in Table 6:3, Appendix 6 (page 190) and are represented graphically in Fig.20 (page 98) by the points marked X, together with Williams'(2) results.

It can be seen from Fig.20 in comparison with Fig.18 (page 92) that the deviation between Williams' results and the present results has been considerably reduced but not removed. The notable feature

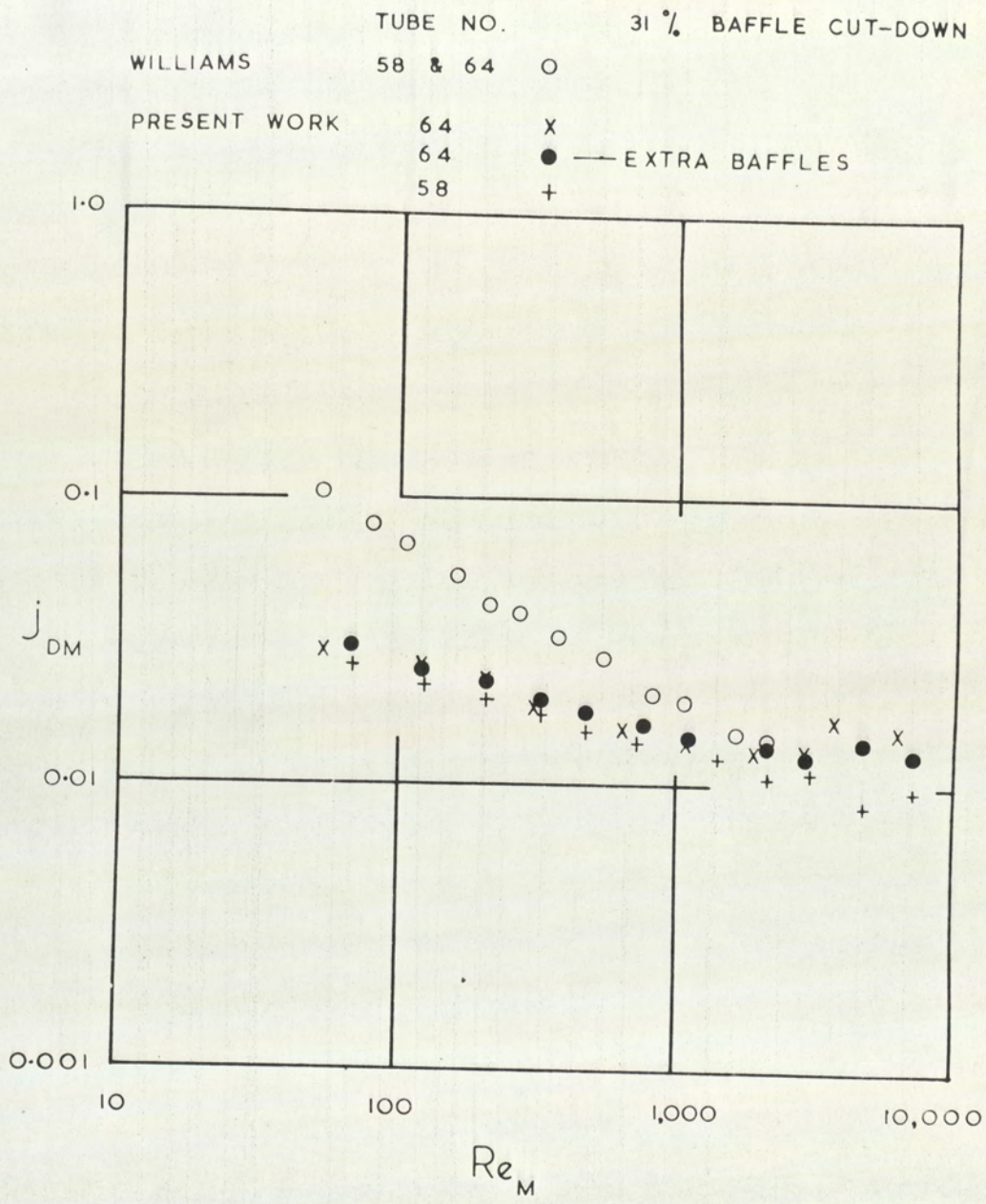
TUBE NO.
31 % BAFFLE CUT-DOWN
WILLIAMS
58 & 64 O
PRESENT WORK
64 X
64 ● —— EXTRA BAFFLES
58 +
1·0
0·1
0·01
0·001
j_{DM}
10
100
1,000
10,000
Re_M

FIG.20.

is that for Reynolds numbers of 10^3 and above the divergence disappears. It was thought that this indicated unrepresentative sampling of the air/mercury stream. The portion of the airflow which comes in contact with the mercurised surface acquires a very high concentration of mercury vapour and it is essential that this should be mixed with the remainder of the airflow so that a homogeneous air/mercury mixture is obtained before sampling takes place. An efficient mixing system is most needed at low flowrates since the higher the flowrate through the exchanger the greater the extent of mixing due to turbulence. In the above results the divergence from the results of Williams was most marked at low flowrates and it was thought that this was possibly due to poor mixing and so two more disc and doughnut baffles were installed in the exchanger exit ports. (If the divergence of results had occurred at the higher flowrates then this would have been attributed to oxidation of the mercury surface).

The experimental run was repeated with tube 64 and again with tube 58. The results for tube 64 are given in Table 6:4 Appendix 6 (page 190) and are represented on Fig.20 (page 98) by a •
The results for tube 58 are given in Table 6:5 (page 191) and are also represented in Fig.20 by a + .

From this graph it can be seen that installation of the extra baffles had not significantly affected the deviation between the results of Williams and the results of the present work. However it can be seen from the figure that the results obtained from tubes 58 and 64 are virtually identical and that they are therefore mirror image tubes.

The disparity in the results which appears at Reynolds numbers of 4,000 upwards may have been due to air surge in the compressed air line or some change in the flow patterns in the exchanger bundle. These changes in flow patterns through the bundle are due to changes in pressure drop occurring with velocity changes and thus flow redistribution occurs. Despite repeating the readings the deviation from the results of Williams still occurred, being more pronounced for tube 64 than for tube 58. As the readings were reproduced several times it is obvious that these deviations cannot be dismissed as scatter. From inspection of the figure it can be seen that the results for tube 64 at a Reynolds number of 6,000 is as far above an imaginary "mean" line through all the results as the result for tube 58 is below this mean. It is very possible therefore that a tube to baffle gasket was damaged so that air leaked through the tube hole and so more air flowed over tube 64 than 58, i.e. a flow redistribution occurred.

The installation of extra baffles affected no improvement in the divergence of results and so it was felt that for future work the adoption of an electrically driven propeller mixer should be investigated. Haggart(6) had installed a mixer of this type in his tube bank apparatus. It should also be possible to test the efficiency of the mixer by passing a mercury free stream of air and a mercury rich stream of air (from the saturator) through the mixer and then sampling the exit stream from the mixer. The theoretical concentration of mercury vapour in this stream could be obtained by a mass balance and thus it could be determined whether or not the mixer

was working. (Williams, with fewer baffles than in the present work, had no mixer problems. He did, however, have shorter expanders which would be expected to cause more turbulence and thus promote mixing.)

The experimental techniques were then repeated for tubes 17 and 23 in the inlet baffle edge zone and results of the mass transfer factor j_{DM} obtained over a range $69 < Re_M < 7500$. These results are given in Appendix 6 Tables 6:6 and 6:7 (pages 191 and 192) and are presented in graphical form in Fig.21 (page 102). The results for tube 17 are represented by $\times$ and for tube 23 by $\bullet$

As with the previous results the same pattern emerges of the deviation between the present results and those of Williams decreasing with increasing Reynolds number, and a discontinuity occurring at a Reynolds number of about 7,000. It should be pointed out that both these tubes and the tubes considered previously are at the bundle edge where it is most likely that flow redistribution due to bundle shell by-passing will occur. Repeating the experimental runs gave the same results which tends to add weight to the hypothesis of flow redistribution occurring at Reynolds numbers around 5 - 7000. Also from Fig. 21 it can be seen that the results for tubes 17 and 23 are virtually identical showing that these tubes are indeed mirror image tubes.

The final experimental run carried out was for tube position 80 and the results for j_{DM} versus Re_M are presented in Table 6:8 (Page 192) and are plotted in Fig.22 (page 103), together with the results of Williams. It can be seen that there is less

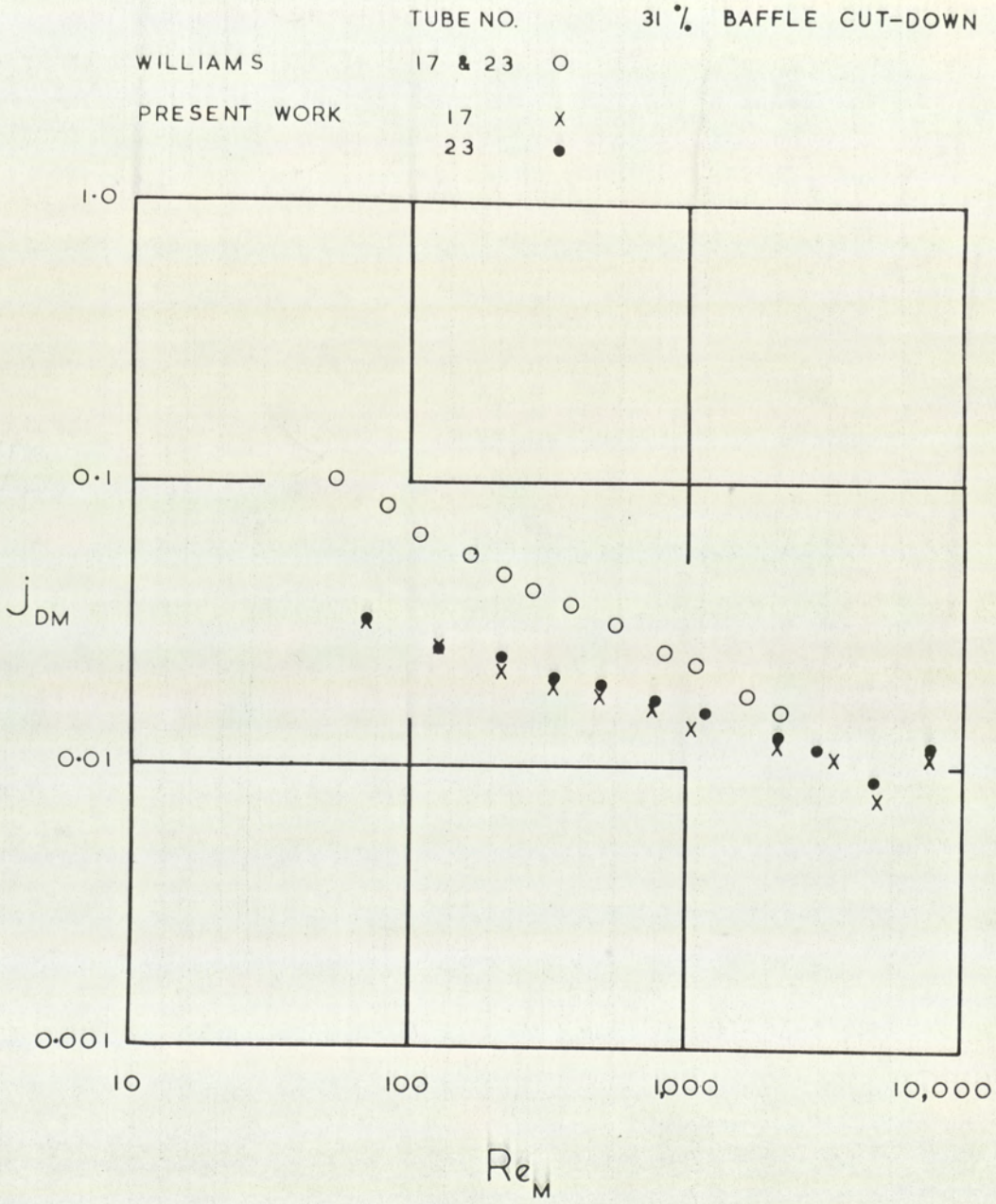
TUBE NO.
31 % BAFFLE CUT-DOWN
WILLIAMS
17 & 23
PRESENT WORK
17
23
1·0
0·1
0·01
0·001
j_{DM}
10
100
1,000
10,000
Re_M

FIG. 21.

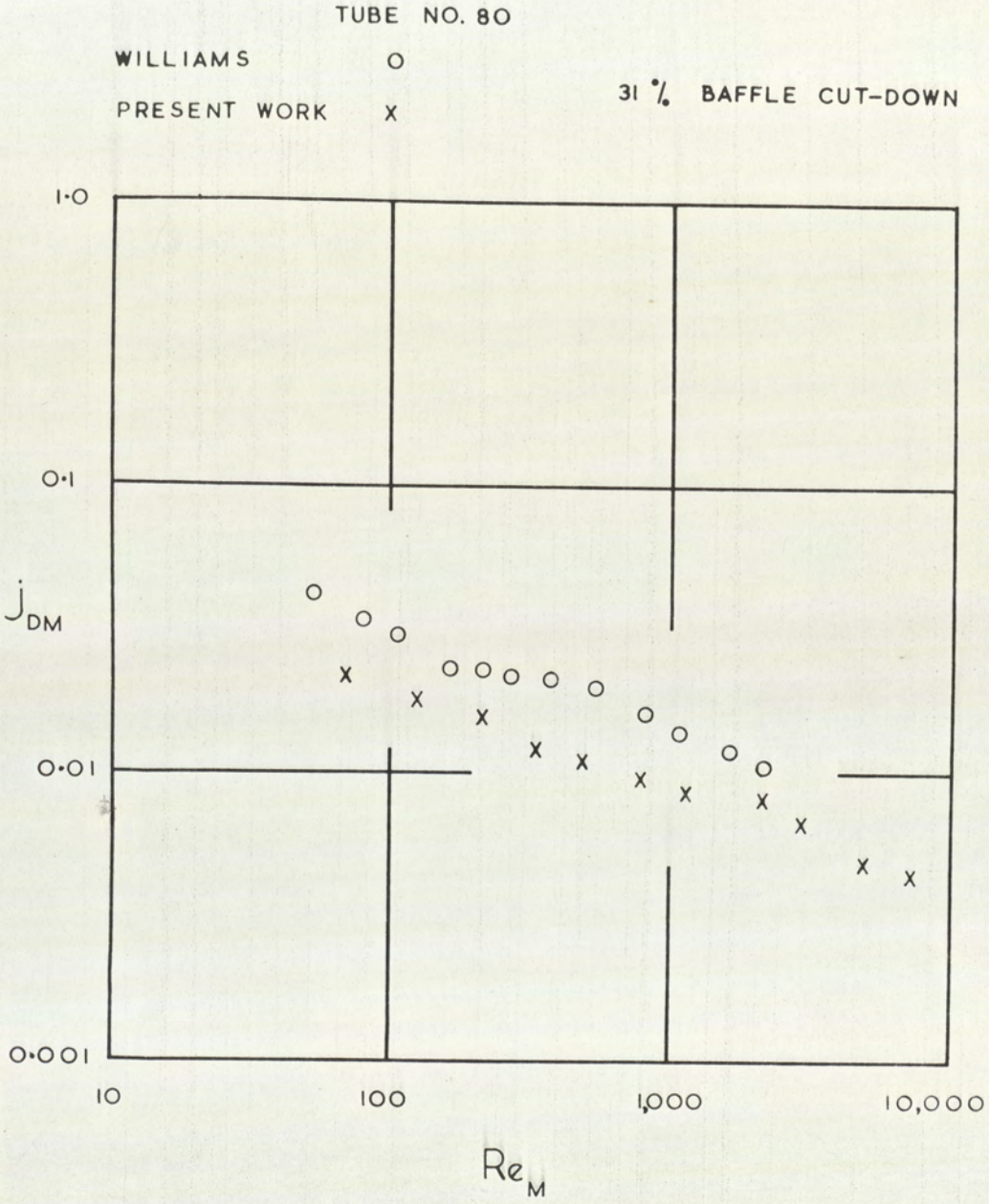
TUBE NO. 80
WILLIAMS O
PRESENT WORK X
31 % BAFFLE CUT-DOWN
1·0
0·1
0·01
0·001
j_{DM}
10
100
1,000
10,000
Re_M

FIG. 22.

divergence than with the other results and that although there are discontinuities in the results they are not as marked as with the other results. Also it can be seen that the results of Williams do not in this case fall on a straight line.

When considering the above results it can be seen that in each case a discontinuity occurs in the results at a Reynolds number of about 5,000. As the experimental runs were repeated several times it is very unlikely that experimental scatter can account for the discontinuities. Further, as Williams did not examine Reynolds numbers higher than 2,200 comparison with his results cannot be made. There is a possibility that this discontinuity may be due to a change in the flow around the tubes in the bundle.

The analogy to fluid flowing over a single cylinder will be considered. In this case the leading edge always has a laminar flow boundary layer but further around the cylinder this boundary layer may become turbulent and finally the flow breaks away resulting in a turbulent wake behind the cylinder. An increase in fluid velocity will cause the boundary layer to become turbulent at a point nearer the forward stagnation point and this results in an increase in skin friction. However, the turbulent boundary layer is much more stable than a laminar boundary layer and hence exists further around the cylinder and this has the effect of reducing the size of the turbulent wake and thus the form drag is reduced. The overall drag, which is the sum of the skin friction and the form drag, is thus reduced with a consequent lowering of the friction factor which may in turn affect the heat transfer characteristics of the system.

Giedt (33) carried out local measurement of heat transfer around a cylinder perpendicular to an air stream for various flowrates. At high Reynolds numbers a peak in the graph of (Nu) versus (Re) occurred at approximately 110° from the forward stagnation point. The peak size increased more rapidly than the rate of increase in Reynolds numbers. (Giedt then synthesised an average transfer coefficient from his local values and found good agreement between this average coefficient and the average coefficient experimentally determined by Hilpert (48)). It would seem that the peak obtained by Giedt was due to the change in the flow conditions of the air around the tube as the Reynolds number was increased.

It is possible that similar behaviour to the above was responsible for the steps in the j_{DM} versus Re_M graphs obtained in the present work. It would, however, be necessary to obtain results of j_{DM} for higher values of Re_M than those used in the present work, if possible extending the Reynolds number range up to about 15,000, to confirm or otherwise the above hypothesis.

During these experimental runs a close visual check was made during mercury surface renewal to see that the surface renewed satisfactorily and that no mercury spilt into the bundle. No evidence of the latter was seen but nevertheless a check was made to see what sort of decay curve arose from mercury droplets in the bundle and therefore what effect could be expected on the mass transfer factors obtained. In Williams work mercury droplets had occasionally been blown into the bundle at high flowrates and this limited the flowrates that could be used. Williams' experimental technique was to run at

the highest flowrate first and it was then felt that no more mercury would be blown around the bundle at the subsequent lower flowrates. Thenafter a series of readings Williams reassembled the bundle with dummy probes and repeated his experimental run and any reading obtained on the microammeter was then due to the spilt mercury. The microammeter readings obtained for the various flowrates in the dummy run were then subtracted from the readings obtained with the transfer probes in position.

There were two essential differences between the exchanger used by Williams and that used in the present work. Firstly the use of nitrogen as the working fluid meant that any mercury spilt in the bundle would not oxidise and so "lose" its vapour pressure. Secondly excess mercury could not drain away from the probes in Williams' apparatus and so would tend to hang under the horizontal probes and thus be blown into the bundle. In the present apparatus the mercury was oxidised very quickly as will be demonstrated below, and secondly the chance of mercury being blown around was lessened by the fact that any excess mercury would drain away. Nevertheless it was decided to carry out an experimental run in which the transfer probes were replaced by tubes, and $\frac{1}{2}$ ml. of mercury was dispersed in droplet form in the bundle and the bundle was then quickly reassembled, to keep to a minimum the oxidation before the run began and air was then blown through at a flowrate equivalent to a Reynolds number of 100. The experiment was repeated with Reynolds numbers of 1105 and 6150. The results are given in Appendix 6 Tables 6:9, 6:10, 6:11 (pages 193 and 194) and are represented graphically in

Fig. 23 (page 108). From the figure it can be seen that the mercury droplets placed in the bundle oxidised very quickly and thus had negligible effect on the experimental results. Obviously the higher the flowrate the more quickly the mercury oxidised so any error would have been more noticeable at lower flowrates, i.e. the error would have tended to decrease the divergence of the present results from those of Williams at low Reynolds numbers and to have increased the divergence at high Reynolds numbers.

From the foregoing it would seem that with a renewal in situ technique it is possible to use mercury transfer with air as the working fluid. This greatly simplifies the experimental apparatus compared with closed circuit systems employing nitrogen as the working fluid. However it would seem that more work needs to be done on mixing and sampling of air/mercury streams, before compatibility with the results of previous workers using mass transfer techniques is achieved.

****
****
**

DECAY CURVE FOR MERCURY DROPLETS IN BUNDLE

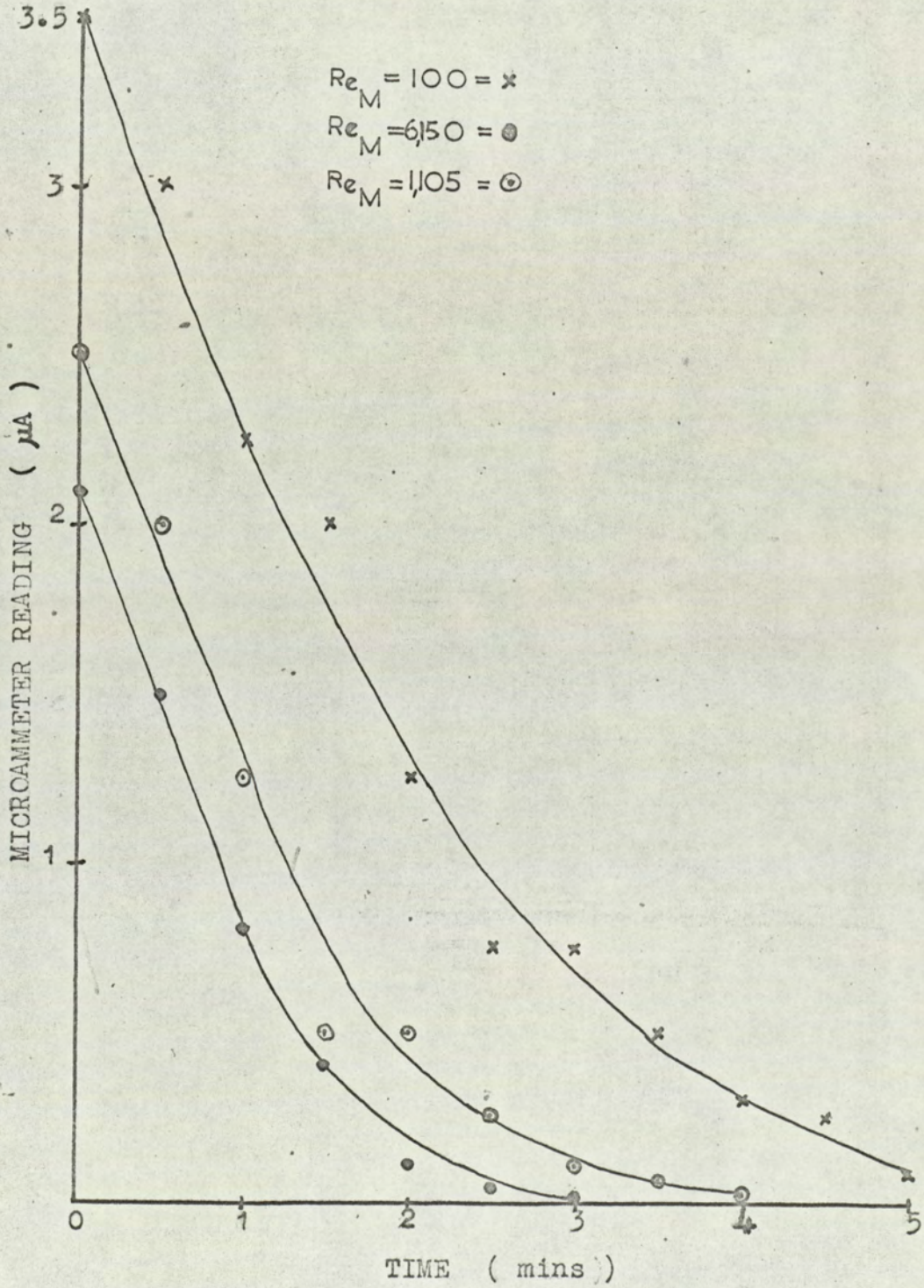

FIG. 23.

CHAPTER V.

A new analysis of the individual tube transfer coefficients obtained by Williams (2).

It was apparent at an early stage in the present work that a large amount of data for shellside transfer coefficients in baffled cylindrical shell and tube heat exchangers had been obtained by various workers, chiefly Bergelin et al. (1) and Williams (2). These data were presented in tabulated form and so it was not easy to see the effect of the various geometrical parameters on the transfer coefficients. In addition, as mentioned in Chapter II of the present work, Williams had presented contour maps of low and high transfer areas for various flowrates, and groups of tubes of similar transfer coefficients for various flowrates. However, while being a useful qualitative guide to the transfer characteristics of the bundle these contour maps did not take into account the regrouping of the tubes at different flowrates caused by the flow paths in the bundle changing with velocity. It was thus not easy to see the overall transfer pattern with this form of presentation.

It was therefore decided that in the present work a full analysis of the available data should be undertaken and that the results of this analysis should be presented in a form which allowed the overall transfer pattern to be assessed, i.e. the tube groupings should be independent of flowrate. It was thought that by this means the full effect of the various geometrical parameters might be further clarified and understood, and that those parameters requiring

further investigation could be identified.

The requirements of the new analysis were therefore that it should be quantitative in nature, and that the groups of tubes obtained should be independent of flowrate.

A plot of j_D against Re on log - log paper is not precisely linear. Nevertheless, so as to further this analysis, this plot was assumed to be linear in which case it would be represented by the expression:-

$$j_D = c\,(Re)^{-n} \qquad (1)$$

This is equivalent to the relationship:-

$$h \propto G^{1-n}$$

The first step in the present analysis was therefore to obtain the data in this form, and this was carried out by obtaining the regression lines for all the j_D against Re results. The slopes and constants (i.e. the intercepts on the j_D axis for Re = 1) of these lines were obtained by the method of least mean squares, using an Electronic Associates Ltd. PDS 1020 digital computer to carry out the arithmetic. The slopes and constants obtained are tabulated in Tables 8:1, 8:2 and 8:3 in Appendix 8 (pages 199-201) and details of the computer programme are given in Appendix 9 (page 221).

Having obtained the regression line slopes and constants a general examination of them was made.

(a) General comments on individual tube transfer coefficients.

A tube arrangement diagram as Fig. 4 (page 36) was drawn for each baffle cut down and the values of the regression lines slopes

and constants inserted into the appropriate tube position. The only conclusion to be made was that these values decreased from the outside to the centre of the bundle, and no other significant trends were observed. This approach was therefore discontinued.

(b) Identification of flow zones.

An inspection of the Reynolds number exponents was next made to see if there was any evidence of eddy and longitudinal flow as mentioned by previous workers (31, 32, 34).

By means of visual examination of the flow of glass beads in a model exchanger Gupta and Katz (31) had detected an eddy zone behind each baffle and a cross flow zone in front of the next baffle. Ambrose and Knudsen (32) and Gurushankariah and Knudsen (34) carried out an investigation of local transfer coefficients in a model exchanger using a heat sensing probe. The design of the probe allowed measurements to be made along the tube between the baffles and also at six points around the tube. The I.D. of the shell was 5·72" and the tube arrangements studied consisted of four tubes at $2\frac{3}{16}$" pitch and fourteen tubes at $1\frac{1}{4}$" pitch with 2, 4, 6 and 10 baffles. An eddy zone was detected for which the Nusselt number was slightly higher than that in the cross flow zone, but this was most marked in the case of large baffle spacings and the large tube spacings. It is of interest though that the difference between the transfer rates in the eddy and cross flow zones diminishes with decreases in baffle spacing and tube pitch and it is possible that with the very much smaller pitches used in the Delaware (1) and Williams (2) investigations that this difference may be insignificant. In any case

the results obtained from measurements of individual tube coefficients in the cross flow zone would be the average of the eddy and cross flow zones and so this method cannot be used to confirm or otherwise the existence of an eddy zone.

For true longitudinal flow to occur the value of the Reynolds number exponent would be -0•2 and the individual tube results of Williams were therefore examined to see if any evidence of this existed. For the three cut downs the tubes with the nearest exponent to this were 01 and 3234 for the 18•4% cut down, 01 and 80 for the 31% cutdown and 01 and 80 for the 43•7% cut down. The exponents in all these cases were between 0•342 and 0•394. It can be seen that in the case of these tubes the effect of baffle turnover will be to give a change in flow direction from cross flow through longitudinal flow to cross flow. (In the case of tube 3234 for the 18•4% baffle cut down, which has an exponent of 0•394, it would not seem possible for longitudinal flow to occur in this tube position and the low exponent probably arises by pure chance). However, as above, the individual tube result will be the average, and local measurements will have to be made to confirm the existence of true longitudinal flow. Nevertheless from the results of the above tubes it would seem that longitudinal flow does occur through part of the window zone.

Having examined the individual tube results of Williams (2) for eddy and longitudinal flow the next stage was to examine these results and those of Bergelin et al.(1). By inspection of the bundle average transfer coefficients obtained by Bergelin and the

synthesised bundle average obtained by Williams, discussed in Chapter II, it was found that:-

$$j_D = c\,(Re)^{-0.5}$$

and hence:-

$$h \propto G^{0.5}$$

Now if the exponent n is less than 0·5 then h must increase more rapidly than the average h, i.e. the local flow increases more rapidly than the average flow.

The order of the following parts of this Chapter should perhaps be mentioned here. It was felt that the final order adopted advanced the analysis in the most logical way, despite the fact that statistical techniques mentioned in the early parts of the Chapter are not fully explained until the latter parts of the Chapter.

The data of Williams and Bergelin et al. were in the form of tables of the mass and heat transfer factors respectively and Reynolds numbers. It was proposed to carry out several examinations and these are summarised below.

(i) Comparison of the corresponding rectangular tube bank transfer coefficients of Bergelin et al. and the individual tube transfer coefficients of Williams.

(ii) Comparison of the bundle average coefficients of Bergelin et al., the synthesised bundle average coefficients of Williams and the individual tube coefficients of Williams.

(iii) Tube grouping of the individual tube coefficients of Williams by histograms of regression line slopes.

(iv) Tube grouping by statistical analysis of the regression

lines (a) by slopes and (b) by slopes and constants.

In the statistical analyses IDENTICAL is used to describe tubes of transfer characteristics not significantly different at the levels of significance defined.

(i). Comparison of rectangular tube bank transfer coefficients and individual tube transfer coefficients.

As mentioned in Chapter II B of this work Bergelin et al.(1) have presented a correlation relating average tube bank transfer coefficients to bundle average coefficients for cylindrical exchangers. Statistical tests were therefore carried out to ascertain whether any agreement existed between the corresponding Bergelin tube bank data and the individual tube data of Williams (2).

No agreement was found to exist between the two sets of data.

It was thought that agreement might exist between the rectangular tube bank data and the average data obtained for the cross flow zone of a cylindrical exchanger. It was not possible to carry out any statistical tests, but a graphical investigation was made between the Bergelin rectangular tube bank data and the synthesised average cross flow data of Williams. This graph is presented in Fig.24 (page 115) and it can be seen that good agreement is obtained between the two sets of data at Reynolds number up to a 1,000 beyond which the deviation increases. A possible explanation for this is that at high flowrates the fluid will tend to flow straight from baffle edge to baffle edge i.e.there will be less window turn over effect, and hence there will be less flow normal to the bundle with a consequent deviation between the two sets of data.

WILLIAMS (2) SYNTHESISED CROSS FLOW ZONE AVERAGE

BCD { 43.7% ×
BCD { 31% ⊙
BCD { 18.4% ●

N.B. WHERE THESE RESULTS ARE THE SAME, ONLY THE 18.4% VALUE IS PLOTTED

DELAWARE (1) TUBE BANK DATA +

N.B. THESE RESULTS ARE FOR HEATING AND COOLING SO THERE ARE TWO j_{DM} VALUES FOR EACH Re VALUE

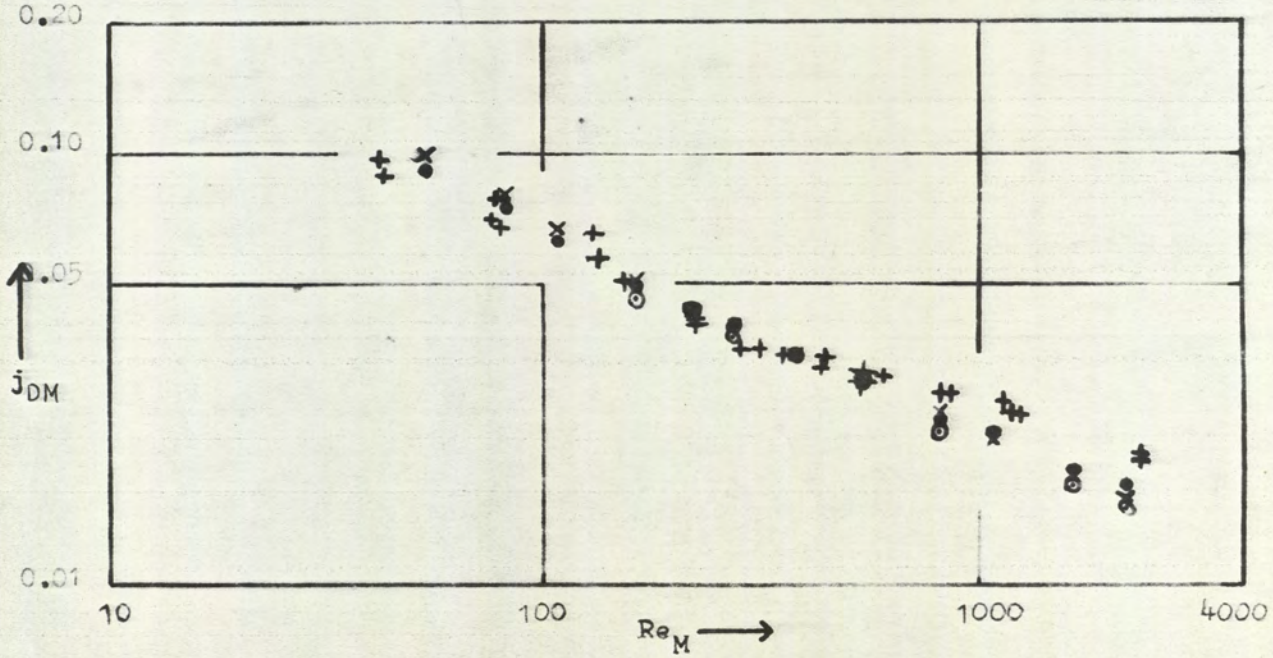

Fig.24.

(ii). Comparison of bundle average transfer coefficients and individual tube transfer coefficients.

Williams (2) had shown that the bundle average transfer coefficient predicted by the arithmetic average of his individual tube transfer coefficients was in agreement with the bundle average coefficients obtained by Bergelin et al.(1). It should perhaps be reiterated here that the Bergelin et al. investigation of transfer in a cylindrical exchanger only covered the case of the 43·7% baffle cut down at the baffle spacing used by Williams. It was therefore decided in the present work to ascertain whether any of the regression lines obtained from Williams individual tube coefficients were identical to the regression lines obtained from Bergelin et al.'s bundle average coefficient. (For the sake of completeness these tests were also carried out on the individual tube results for the 31% and 18·4% baffle cut downs, but proved negative.)

In the case of the 43·7% baffle cut down there was one agreement between the bundle average regression line of Bergelin and the individual regression lines of Williams. This was in the case of the mirror image tubes, positions 38 and 43 (see Fig.4 page 36). By statistical tests it was found that the levels of significant difference between the two regression lines was 0·95 for slope and 0·90 for constant. As will be shown later in this Chapter, this level of significance is on the borderline for slope, and although the intercepts are the same nevertheless a certain amount of doubt remains as to whether the regression lines are the same or not.

It was thought that it would be interesting to ascertain whether

any similar agreement existed for the other baffle cut down cases, between the individual tube coefficients and synthesised bundle averages of Williams. This investigation was undertaken graphically as the synthesised bundle average results were calculated, and not direct experimental values, and so a statistical analysis could not be used.

The previously mentioned case of the individual tube results of Williams (positions 38 and 43) found statistically to agree reasonably with the Bergelin bundle average for the 43·7% cut down was therefore plotted as a reference graph. The synthesised bundle average of Williams was then added to this graph (Fig. 25 page 118). As can be seen from the figure good agreement is obtained between the three sets of results.

In the case of the 31% baffle cut down tubes 38 and 43 are part of a larger group, as will be demonstrated later in this Chapter, and so the average of the individual tube coefficients of this group is plotted with the synthesised bundle average (Fig. 26 page 119). The agreement in this case would appear to be rather better than the agreement obtained in the case of the 43·7% baffle cut down.

Fig. 27 (page 120) shows the relationship between the individual tubes 38 and 43 and the synthesised bundle average for the case of the 18·4% baffle cut down. As in the case of the 31% baffle cut down tubes 38 and 43 are part of a larger group and the average value for this group is plotted. Once again a good agreement is obtained between the two sets of data.

It would therefore seem possible that an indication of the bundle

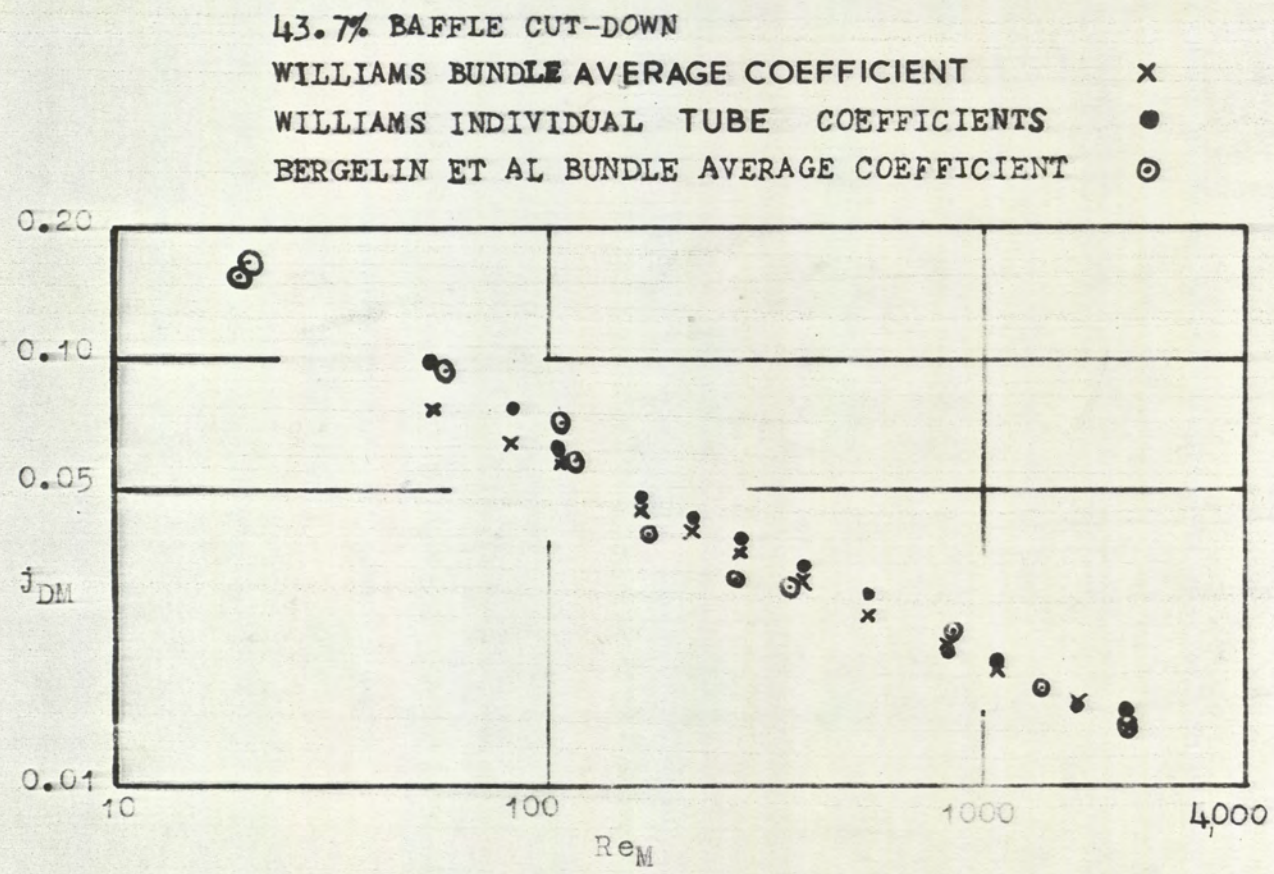
43.7% BAFFLE CUT-DOWN
WILLIAMS BUNDLE AVERAGE COEFFICIENT
WILLIAMS INDIVIDUAL TUBE COEFFICIENTS
BERGELIN ET AL BUNDLE AVERAGE COEFFICIENT
0.20
0.10
0.05
0.01
j_{DM}
10
100
1000
4,000
Re_M

FIG. 25.

31% BAFFLE CUT-DOWN

WILLIAMS BUNDLE AVERAGE COEFFICIENT ×

WILLIAMS INDIVIDUAL TUBE 3843 COEFFICIENT ●

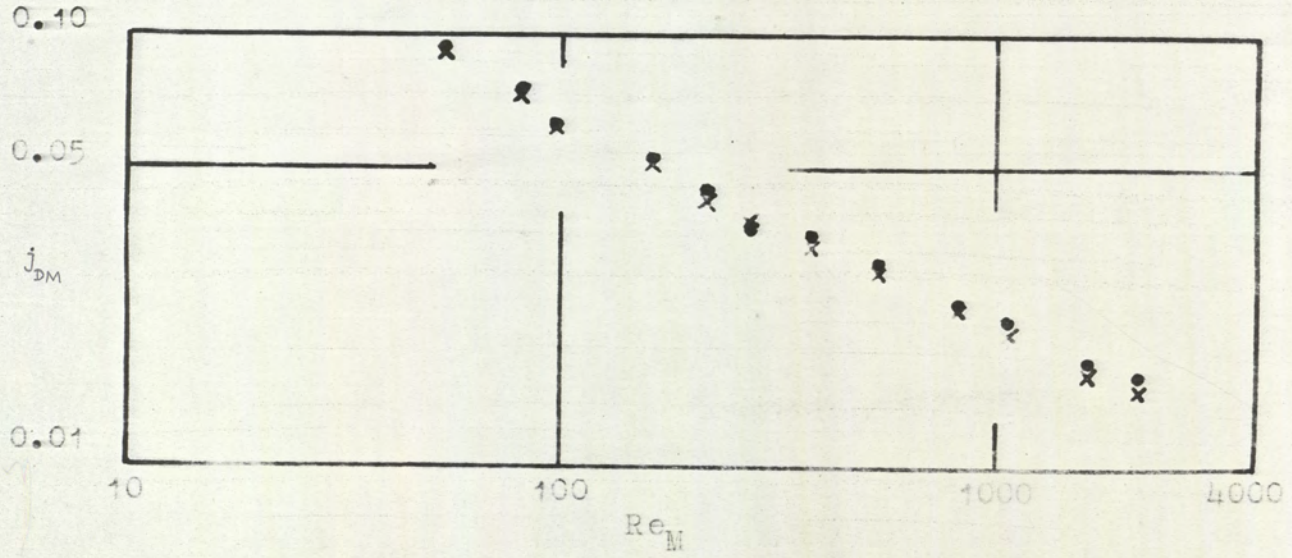

FIG. 26.

18.4% BAFFLE CUT-DOWN

WILLIAMS BUNDLE AVERAGE COEFFICIENT ×

WILLIAMS INDIVIDUAL TUBE 3843 COEFFICIENT ●

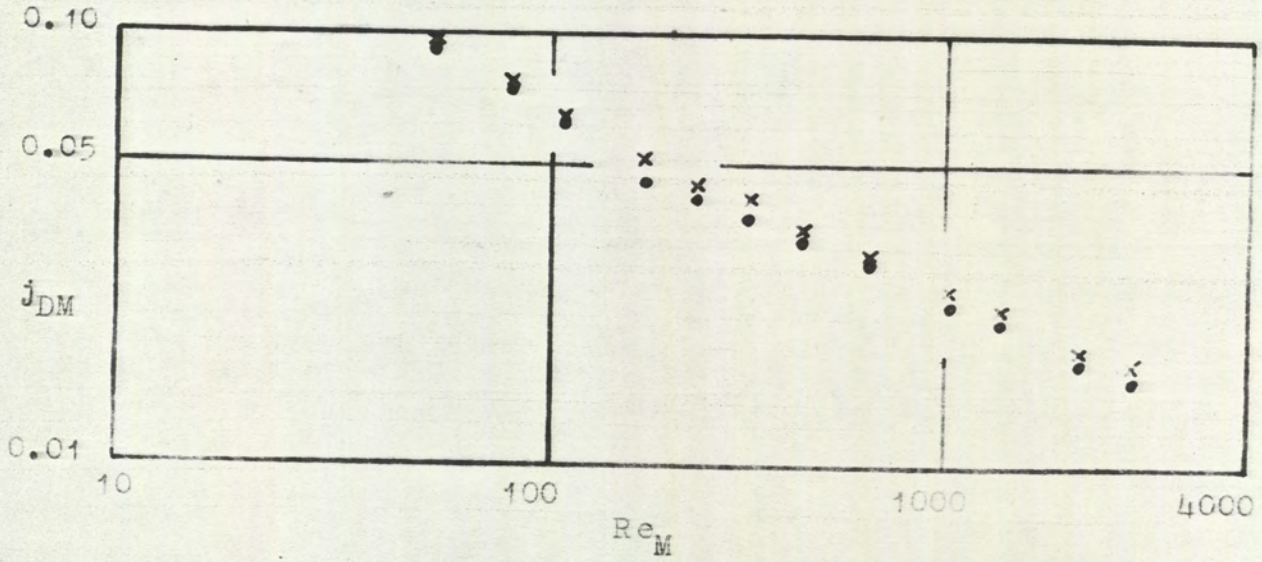

FIG. 27

average transfer coefficient for the exchanger considered in this work may be obtained from the values of the individual tube transfer coefficients of tubes 38 and 43, or their group average. These two tubes are located (see Fig. 4 page 36) in the centre row of tubes, one in from the bundle edge.

(iii).Tube grouping by histograms of regression line slopes.

A histogram for the 31% baffle cut down was constructed (see Fig. 28 page 122) with the cuts being made at regression line slopes of $< 0{\cdot}35$, $< 0{\cdot}40$, $< 0{\cdot}45$ etc. thus obtaining groups of tubes of similar slope i.e. the tubes in any one group have an equal proportional increase in transfer with flowrate, and there is no redistribution of flow pattern with variations in flowrate. A second histogram (see Fig. 29 page 123) was then constructed with the cuts being made at regression line slopes of $< 0{\cdot}375$, $< 0{\cdot}425$, $< 0{\cdot}475$ etc. From the figure it can be seen that different groups are obtained in the second case, but with the creation of new borderline cases rather than the elimination of borderline cases. Many histograms could be constructed using different cuts but it is extremely difficult to decide how to deal with the borderline cases and it is also difficult to be unambiguous about choosing the cuts. However, apart from this arbitrary choice of cuts this method of representing the data has another serious disadvantage. Although the groups of tubes presented in this way are independent of flowrate (cf. the contour maps of Williams) nevertheless no indication is given as to whether or not the transfer coefficients of the constituent tubes of any groups are equal.

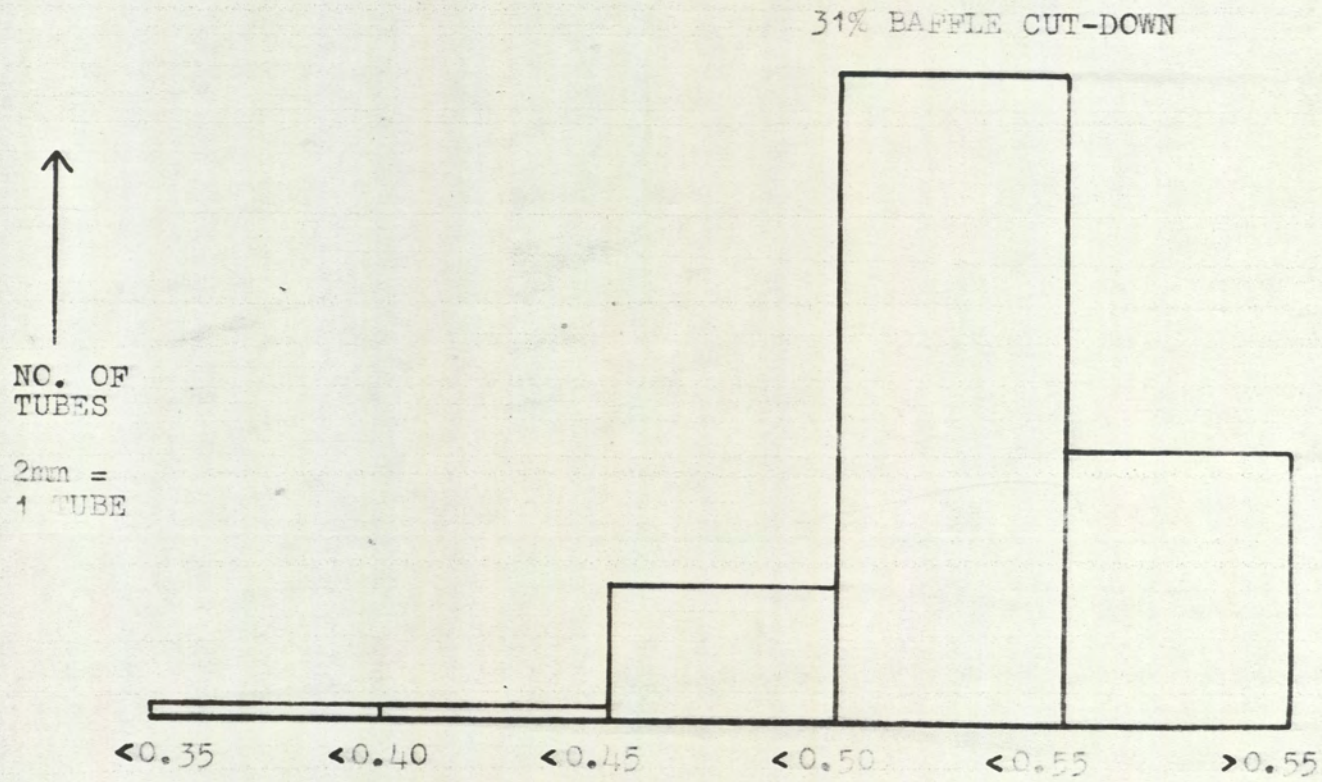

SLOPES OF REGRESSION LINES

FIG. 28.

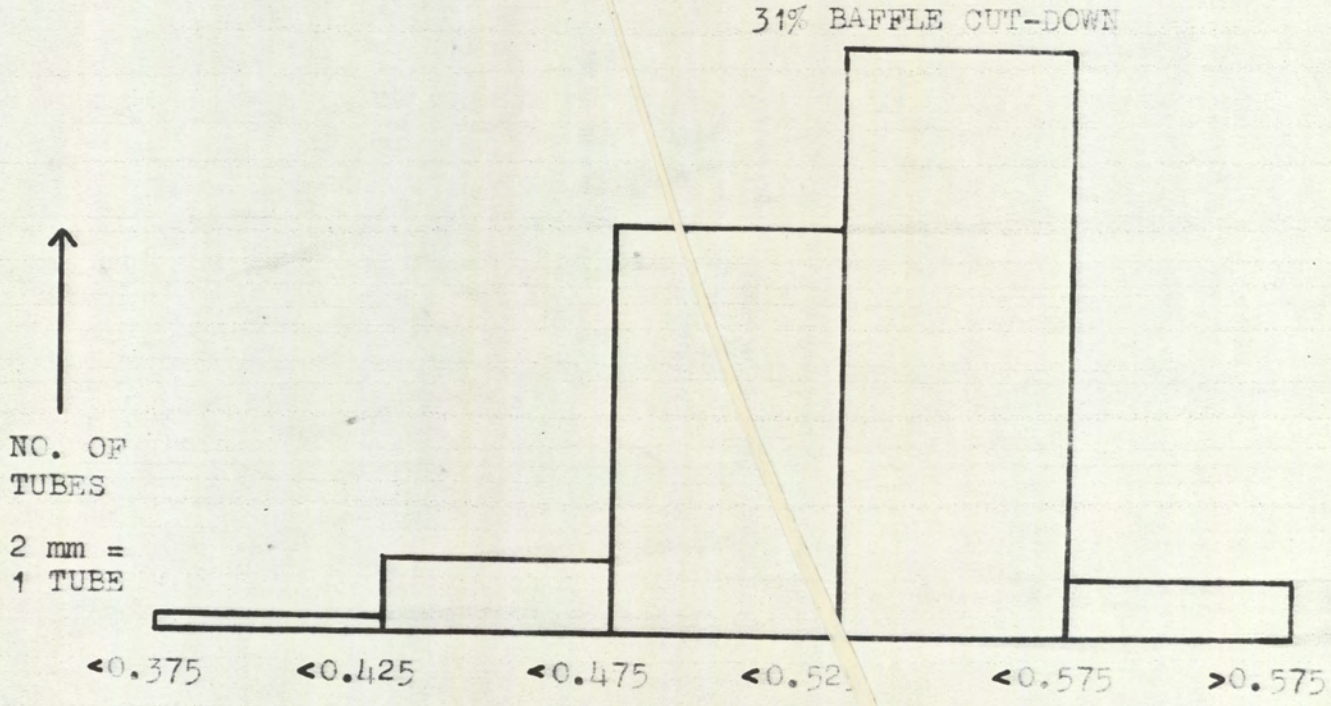
31% BAFFLE CUT-DOWN
NO. OF TUBES
2 mm = 1 TUBE
<0.375
<0.425
<0.475
<0.52
<0.575
>0.575
SLOPES OF REGRESSION LINES

FIG. 29.

To indicate this a technique must be employed which compares the regression line constants as well as the regression line slopes. In this way groups of tubes of identical regression lines are obtained, whereas in the above histogram method families of tubes with parallel regression lines may be obtained.

(iv). Tube grouping by statistical analysis of the regression line slopes and constants.

In view of the mass of data to be investigated in the present work it was decided that a statistical method of analysis should be employed, utilising the null hypothesis. The null hypothesis assumes that the regression lines are identical and the statistical method seeks to establish the truth or otherwise of the hypothesis. The method involves comparing the regression line slopes by means of the "t" test for two lines, or the "F" test for more than two lines, so as to obtain groups of lines of identical slope, and then to test the constants of these regression lines in the same way. Thus groups of identical regression lines were identified. These "t" and "F" tests are standard statistical methodology as described by Brownlee (38), and details of these tests are given in Appendix 9 (page 221) together with details of the programmes for the PDS 1020 computer which carried out the arithmetic. The tests involved obtaining various arithmetical summations and differences until finally a "t" or "F" value was calculated at a certain number of degrees of freedom, depending on the number of points being considered. These values of "t" or "F" were then compared with tables of the fractional points of the "t" and "F"

distributions as given by Brownlee. If a certain "t"value was between two "t" values in the table then it was said to be significant at the lower of the two tabulated values. The "F" values were treated in the same way. In the present work a level of significance of 0·975 i.e. the calculated "t" or "F" value being larger than the tabulated "t" or "F" values at 0·975, was taken to indicate that the null-hypothesis was void and that the regression lines being tested were different. This concept of significance may be clarified as follows, the illustration being applicable to the "F" test as well as the "t" test, although in fact the "F" test is used when more than two regression lines are being examined.

If, for example, two regression lines, each of twelve experimentally determined points, are considered then the "t" test determines whether or not the total number of points, i.e. twenty four, may in fact be represented by one line. If this is the case then the two lines considered are identical. However in any experimentally determined data a certain amount of scatter of the points from their regression line is inevitable. The problem to be examined in the case of the above twenty four points is therefore whether the scatter arises by chance, or is due to the existence of two distinct lines. The statistically determined level of significance indicates whether the scatter of the points is due to chance or not. If the calculated "t" value is significant at the 0·90 level then there is a one in ten chance that the difference arises by chance and it is taken that the lines are the same. If the "t" value is significant at the 0·975 level then there is only a one in forty chance that the

difference in the statistics being tested arises by chance, and it is extremely unlikely that the lines are the same. This leaves a borderline case of the "t" value being significant at the 0·95 level (one in twenty) and in this case more investigation is needed. In the present work however there were no examples of both the slope and constant "t" values being significant at the 0·95 level, the case being that if the slope "t" value was borderline the constant "t" value would not be, and vice versa, and so any doubt was removed.

(a) Tube grouping by statistical analysis of the regression line slopes.

As stated earlier in the present Chapter it was felt that the final order adopted presented the analysis in the most logical progression. For this reason tube grouping by slope is considered next.

It became obvious from the statistical analysis of slopes and constants that there were relatively few identical tubes in the tube bundle. Furthermore it was seen that groups of tubes of identical slope (cf. histogram groupings by arbitrary cuts) would clarify the flow patterns in the exchanger bundle and indicate very clearly the relation between baffle cut down and flow patterns, and hence it should be possible to decide which of the three baffle cut downs studied gave the most even heat transfer, which in turn indicated which cut down gave the most even flow distribution.

Ideally the flow through a baffled cylindrical tube bundle should be of a sinusoidal form with the nodes of the sine curve

symmetrical to the baffles. In this case the tubes in the outlet window zone of one baffle zone form the inlet window zone of the next baffle zone. If therefore an examination is made of Williams (2) individual tube results for the inlet and outlet window zones, by comparing tubes of equivalent position in each zone, then it will be seen whether or not the flow pattern through the bundle is symmetrical or not. (Fig. 30 page 128, illustrates how the flow may be symmetrical or not).

Secondly if the cross flow zone of a baffled cylindrical tube bundle is indeed similar to a rectangular tube bundle, as demonstrated in the first section of the current Chapter, then it might be expected that a large group of tubes in the cross flow zone would have identical slope.

Accordingly the regression line slopes were examined by means of the "t" and "F" tests. Whereas in the case of grouping of regression lines by slopes and constants doubtful slope values of "t" or "F" were clarified by reference to the constant "t" or "F" values this was not the case when grouping by slope only. Therefore a lower value of significance was taken to indicate that the slopes were not the same, this level of significance being 0·90. Any deviation from this rule will be fully discussed in the following dissertation.

The first stage was to test the slopes of all equivalent tubes e.g. 11 and 65, 8 and 73, in the inlet and outlet window zones and then to test rows of equivalent tubes e.g. the inlet and outlet baffle edge rows to see whether any agreement existed. Obviously numerous

SYMMETRICAL FLOW ——————

ASYMMETRICAL FLOW - - - - -

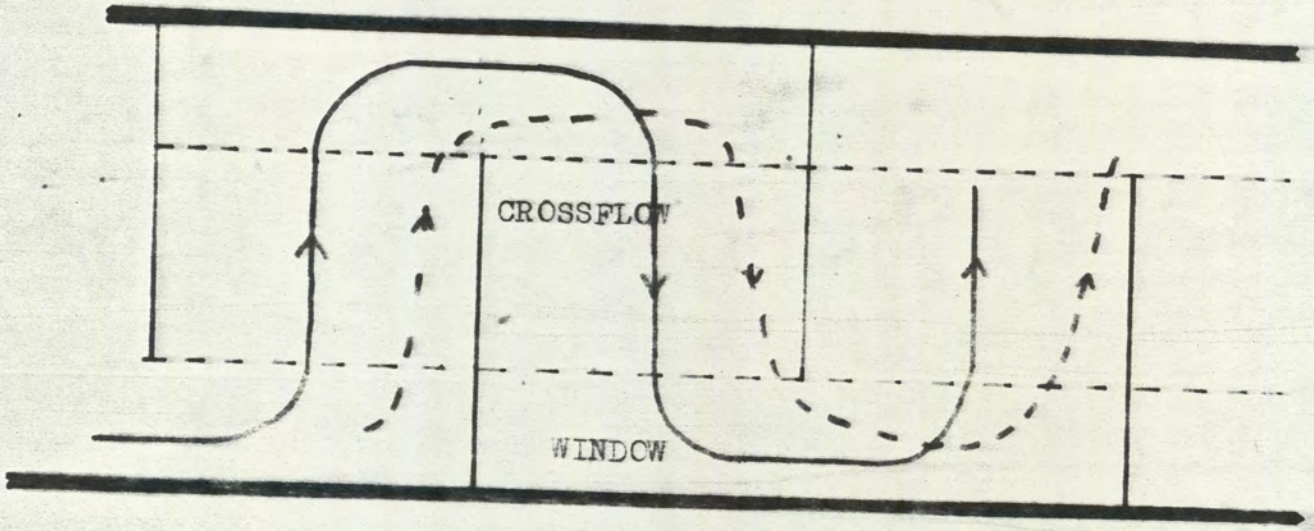

FLOW SYMMETRICAL AND ASYMMETRICAL TO THE BAFFLES

FIG. 30.

permutations of tubes existed but reference to the tube arrangement diagram (Fig. 4 page 36) avoided the more obvious anomalies.

Not surprisingly the cross flow zone was much more difficult to examine and a technique was arrived at which was to be of great help when testing not only the cross flow zones but also when later examining the bundles for identical tubes, i.e. tubes of identical slopes and constants. This technique was quite simple and consisted of plotting a graph of slope versus constant for each regression line for each baffle cut down; those tubes which grouped together on the graphs were then tested. These three plots are presented in Figs. 31, 32 and 33, (pages 130, 131, 132). It is extremely interesting to note that the plots obtained are approximately linear. Without these plots the selection of tubes to test for grouping would have been exceedingly difficult, and involved a considerable amount of trial and error grouping.

The grouping of tubes of identical slope are presented in the following diagrams:-

Fig.34 (page 134) for the 18.4% baffle cut down case.

Fig.35 (page 136) for the 31% baffle cut down case.

Fig.36 (page 139) for the 43.7% baffle cut down case.

The numerical values for the "t" and "F" tests for these groups of tubes are presented in Appendix 8 Tables 8:5 to 8:17 (pages 206 - 214).

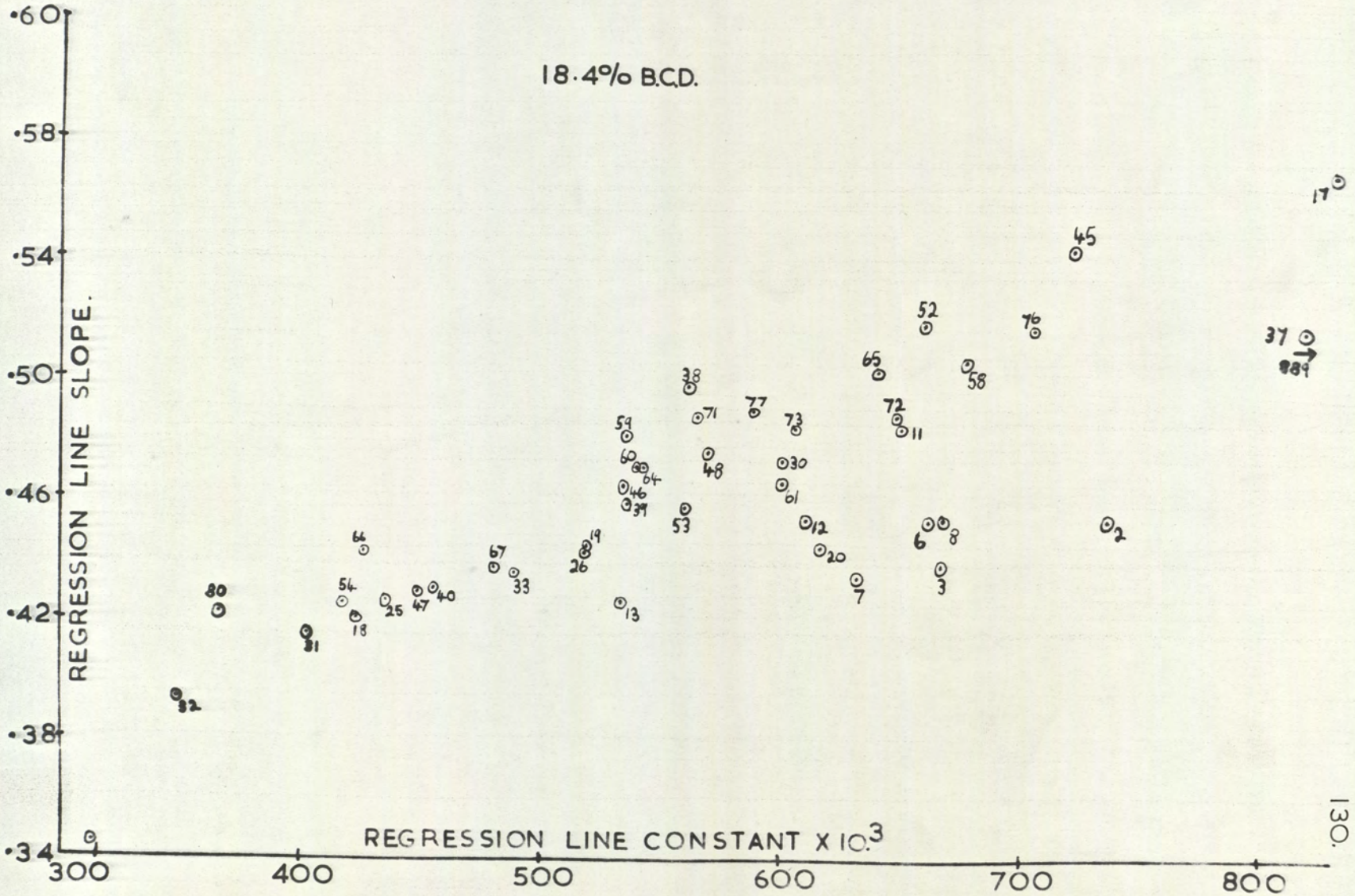
18·4% B.C.D.
REGRESSION LINE SLOPE.
·60
·58
·54
·50
·46
·42
·38
·34
REGRESSION LINE CONSTANT X 10.3
300
400
500
600
700
800

FIG. 31.

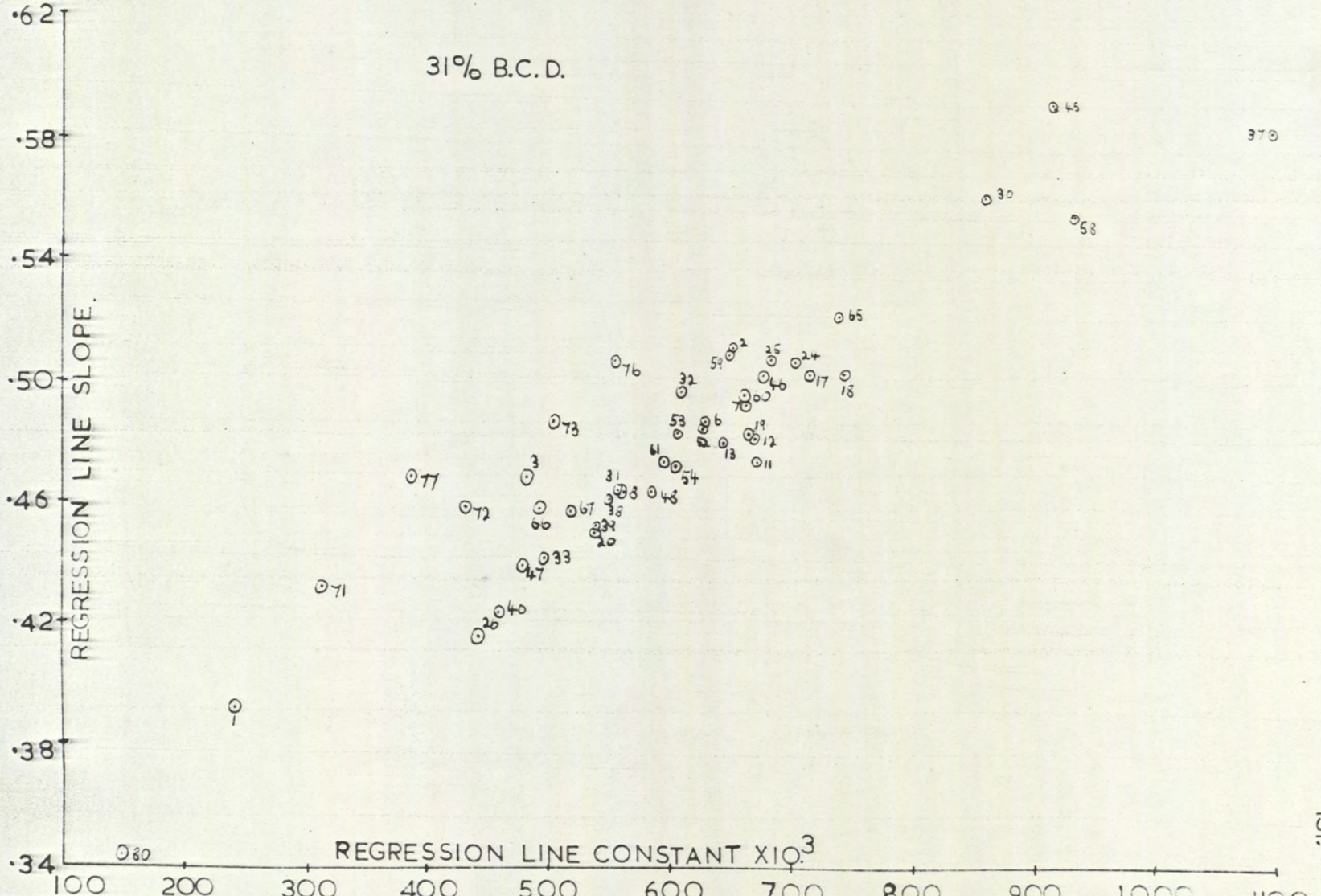
31% B.C.D.
REGRESSION LINE SLOPE.
·62
·58
·54
·50
·46
·42
·38
·34
REGRESSION LINE CONSTANT X10.3
100
200
300
400
500
600
700
800
900
1,000
1,100

FIG. 32.

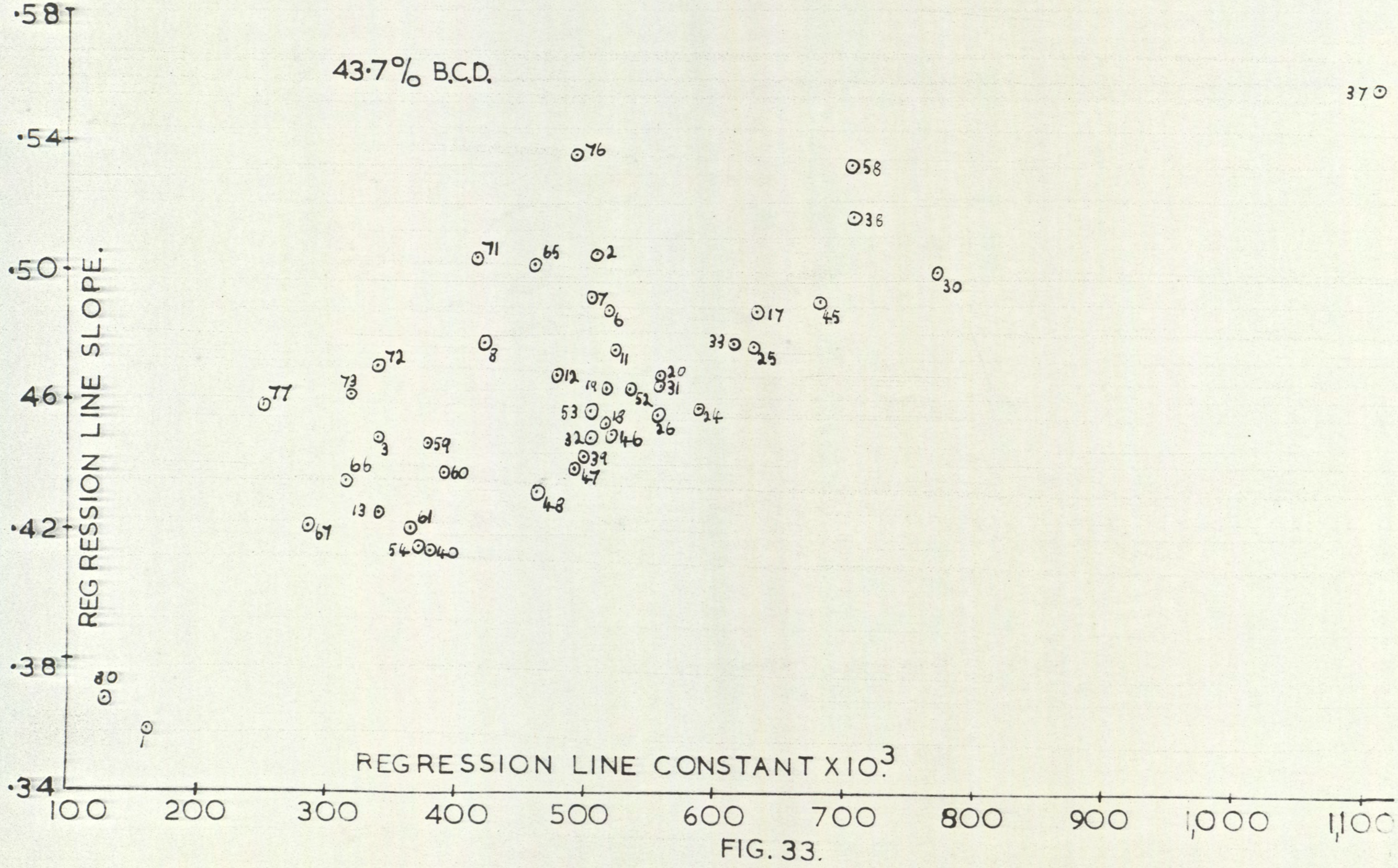
43·7% B.C.D.
·58
·54
·50
·46
·42
·38
REG RESSION LINE SLOPE.
REGRESSION LINE CONSTANT X10.3
100
200
300
400
500
600
700
800
900
1,000
1,100

FIG. 33.

The 18·4% baffle cut down case (see Fig.34 page 134 .)

In this case four groups of tubes are obtained, three in the cross flow zone and one in the window zones. The main feature is that group 1 consists of the rows of tubes which constitute the outlet and inlet baffle edge zones. This indicates that for the baffle edge the flow pattern through the bundle is symmetrical and that the outlet baffle edge zone of one baffle compartment has the same transfer as the inlet baffle edge zone of the next baffle compartment, which is what would be expected. The fact that the rest of the inlet and outlet window zones differ shows that the flow through the exchanger is not completely symmetrical about the baffles. By looking at the values of the regression line slopes (Table 8:1) this asymmetry of flow is underlined as the remainder of the tubes in the inlet window zone have n < group n whereas the tubes in the outlet window zone have n > group n.

The cross flow zone is divided into three groups, groups 2, 3 and 4. Group 2 has a value of n > 0·5 i.e. the local flow through this group does not increase as quickly as the average flow through the bundle. This may be explained as at low flowrates the fluidstream will tend to by-pass the bundle and flow through this group of tubes whereas at higher flowrates proportionately more fluid flows through the main body of the cross flow zone.

Groups 3 and 4 show the flow patterns through the remainder of the cross flow zone, with the local flow through group 3 increasing slightly more quickly than the flow through group 4, i.e. a further example of the fluid by-passing the centre of the bundle as

18·4% B.C.D. SLOPE GROUPS

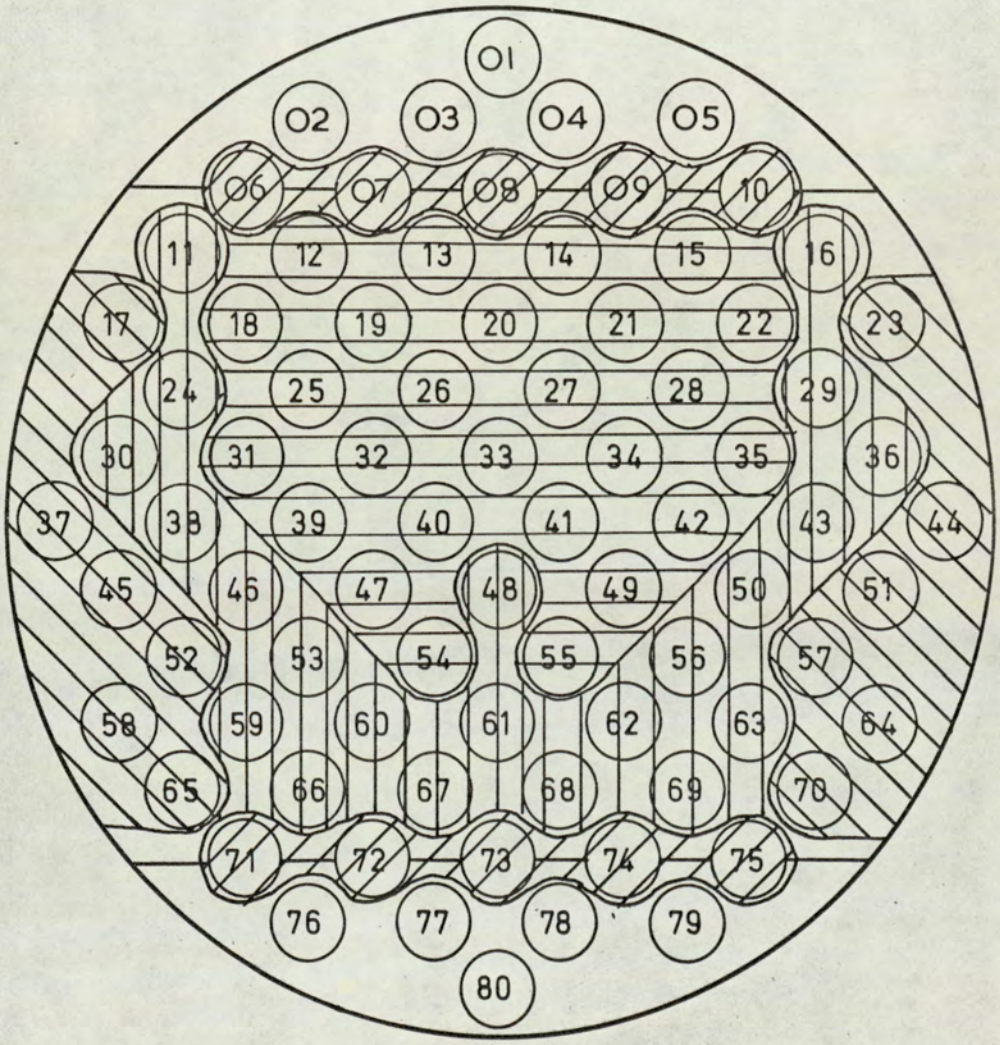

GROUP		SLOPE
1	///	0·466
2	\\\	0·524
3	≡	0·431
4	|||	0·466

FIG. 34.

illustrated by group 2 but not as pronounced as in that case. It is noteworthy that the average slope of group 4 is identical to that of the baffle edge zone 1, showing that the flow through the trailing edge of the cross flow zone is identical to that of the outlet baffle edge zone. However the change in slope from group 1 to group 3 indicates that there is an acute change of flow between the row of tubes in the inlet baffle edge zone and the next row of tubes which is in the cross flow zone.

For this cut down then the overall picture is that the fluid flow is asymmetrical with respect to the baffles, and that a large amount of redistribution of fluid flow occurs in the cross flow zone.

The 31% baffle cut down case (see Fig.33 page 132).

In this case five groups of tubes are obtained, four of which are in the cross flow zone.

The most striking feature of this baffle cut down is that the entire inlet and outlet window zones, with the exception of tubes 01 and 80, form an identical slope group, indicating that for this baffle cut down the fluid flow is symmetrical to the baffles and that the outlet window zone for one baffle compartment is indeed the inlet window zone for the next baffle compartment. It should be stated that taking a level of significance of 0·90 to indicate that a group of tubes is not of identical slope excludes tubes 1723 from this group. However as will be shown later in this section this pair of tubes constitutes part of a group of identical tubes, all of which are included in the inlet window zone, and it was therefore felt that

31% B.C.D. SLOPE GROUPS

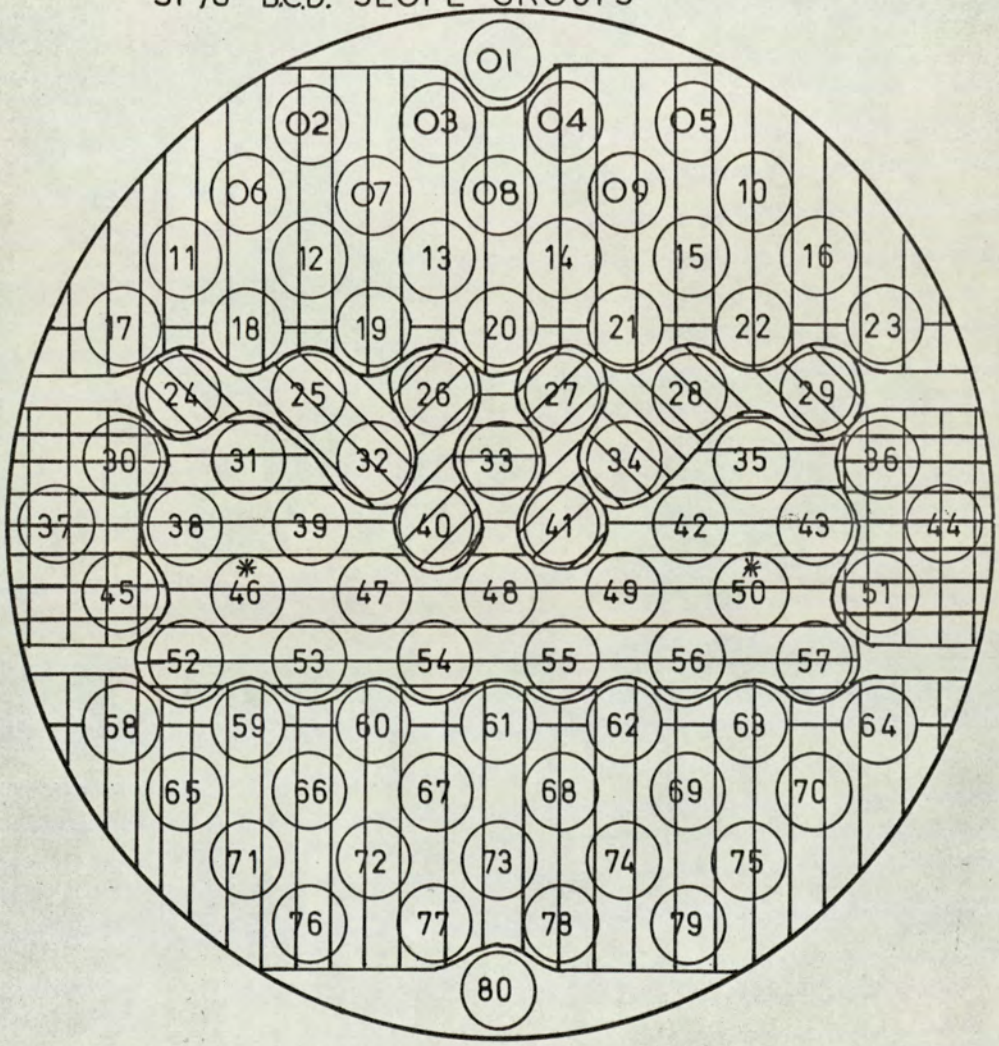

GROUP		SLOPE
1	III	0·483
2	##	0·577
3	≡	0·463
	+*	0·467 (SEE TEXT)
4	\\\	0·502
5	///	0·577

FIG. 35.

inclusion of tubes 1723 in this large group of tubes of identical slope was justified.

The remaining four groups of tubes are all in the cross flow zone. Group 2 consists of three tubes at the edge of the bundle with a value of $n = 0.577$, indicating, as in the case of the 18.4% baffle cut down, a large amount of fluid flow by-passing the bundle at low flowrates.

Group 3 constitutes the major part of the cross flow zone and it is interesting that apart from the aforementioned group 2 at the edge of the bundle a fairly large "block" of "true cross flow zone" exists and the other minor groups are probably due purely to entrance effects after the 180° turn made by the fluid passing through the baffle window. As in the case of 1723 in group 1 tubes 4650 were excluded if a level of significance of 0.90 was taken to indicate that a group of tubes was not of identical slope, nevertheless it was included with this group for the same reason as 1723 was included with group 1.

Groups 4 and 5 would seem to be interrelated in that they are next to each other and group 4 has n greater than the n value for the large cross flow group 3, while group 5 has n less than the value for the large group. This would seem to indicate that these groups perform some sort of fluid straightening action at the entrance to the cross flow zone.

For this cut down then it would seem that the fluid flow is symmetrical with respect to the baffles and that there is no redistribution of flow with velocity change in the window zone.

It would further seem that there is a reasonable cross flow zone apart from entrance effects, and the effect due to the fluid by-passing the tube bundle at low Reynolds numbers.

The 43.7% baffle cut down case (see Fig.36 page 139).

In this case four groups of tubes are obtained, all of which are in the window zones, but in fact two of the "groups" are just pairs of tubes in the inlet and outlet window zones.

Considering the pairs of tubes, groups 1 and 2 , it can be seen that group 1 consists of tubes 1314 in the inlet window zone and tubes 6768 in the outlet window zone, and that group 2 consists of tubes 3036 and 4551 in the inlet and outlet baffle edge zones respectively. Group 1 is probably due purely to a flow rearrangement between groups 3 and 4. The fact that there is not a row of identical tubes in the centre of the bundle indicates that there is no cross flow zone as such with this baffle cut down. The fact that group 4 has a lower slope value than group 1 shows that more of the air is passing down the centre of the bundle. However as the slope of group 2 is 0·496, i.e. the average slope, it would seem that there is not much bundle by-passing occurring.

Groups 3 and 4 together form the major part of the window zones and although they show that a certain degree of symmetry exists with respect to the fluid flow and the baffles, they highlight the fact that with this cut down very much poorer flow distribution is achieved than in the case of the 31% baffle cut down.

43·7% B.C.D. SLOPE GROUPS

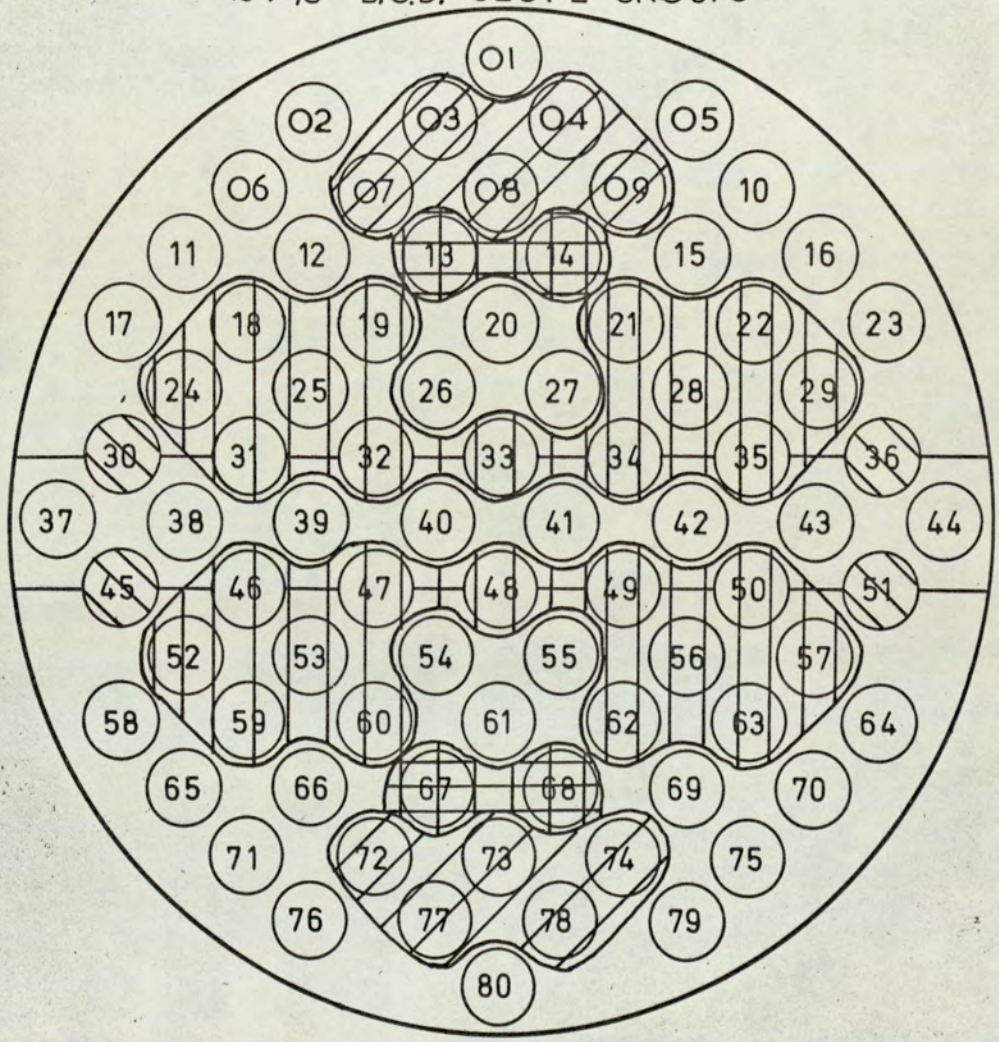

GROUP		SLOPE
1	###	0·424
2	\\\	0·496
3	///	0·469
4	|||	0·454

FIG. 36.

(a). Conclusions from tube grouping by statistical analysis of regression line slopes.

Looking at the three figures it can be seen that the 31% baffle cut down gives a very much better flow distribution than the other cut downs considered here.

The 18·4% cut down gives a flow pattern through the bundle which would appear to be asymmetric to the baffle, and several large groups of tubes in the cross flow zone which shows evidence of a lot of flow redistributions and also a large bundle by-pass flow.

The 31% cut down gives an obviously symmetric flow through the bundle with respect to the baffles. Furthermore although there are a certain amount of entrance effects and flow redistribution in the cross flow zone there would appear to be only a small by-pass flow.

Finally the 43·7% cut down appears to give the worst flow distribution and this of course increases the chances of certain tubes forming hotspots, as will be seen by reference to Table 8:3 in Appendix 8 (page 203) where it is obvious that the values of the regression line slopes show the greatest scatter of the three cut downs considered here.

It can be seen then that the 31% baffle cut down gives the best shellside flow distribution for this particular design of segmentally baffled cylindrical shell and tube heat exchanger.

To complete this section of the analysis the average intercepts of the tube groups were calculated and are given as follows:-

Group	Baffle cut down.		
	18•4%	31%	43•7%
1	0•630	0•604	0•314
2	0•736	0•953	0•725
3	0•483	0•560 + * 0•571	0•365
4	0•550	0•697	0•516
5	--	0•450	--

From this table only general comments may be made. For the three baffle cut downs studied the groups at the bundle edge have the highest transfer coefficient, followed by the baffle edge groups and finally the cross flow groups. For the 18•4% baffle cut down the trailing cross flow group has the higher coefficient. In the 31% baffle cut down case the average of groups 4 and 5 is approximately equal to group 3, i.e. the whole of the cross flow zone is approximately equal, emphasising that the 31% baffle cut down gives the best fluid distribution of the three cut downs studied. While the above general comments about transfer coefficients are true for the 43•7% case the above table serves merely to confirm the poor fluid distribution occasioned by this cut down.

The last section of this Chapter will examine the groups of identical tubes for the three baffle cut downs.

(b) Tube grouping by statistical analysis of regression line slopes and constants.

Groups of tubes obtained by this technique are groups of tubes of identical transfer characteristics, i.e. not only are the groups independent of fluid flowrates but also the transfer coefficients of the constituent tubes of any group are equal.

As mentioned in the discussion of tube grouping by slope a mass of data required analysis, and selection of tubes to test for grouping was rationalised by utilising the tube arrangement diagram (Fig. 4 page 36) and the graphs of regression line slopes versus regression line constants (Figs. 31, 32, 33 see pages 130, 131, 132.)

It will be appreciated that after carrying out a large number of tests, a certain experience was gained in group allocation, but even so there were many permutations to be investigated before the final tube groupings were obtained.

These final groups are presented in the following diagrams:-

Fig. 37 (page 144) for the 18•4% baffle cut down.

Fig. 38 (page 146) for the 31% baffle cut down.

Fig. 39 (page 149) for the 43•7% baffle cut down.

The numerical values for the "t" and "F" tests for these groups of tubes are presented in Appendix 8 Tables 8:18 to 8:27 (pages 215 - 220).

The 18•4% baffle cut down case (see Fig.37 page 144).

In this instance three groups are obtained, all of which are in the cross flow zone, there being one large group and two small groups:-

1822, 2528, 3135, 3234, 4041, 4749, 5455.

For this group $n = 0.42$ and $c = 0.419$. So by substitution in equation 1 (page 110) we obtain the expression:-

$$j_{DM} = 0.419\ (Re_M)^{-0.42}$$

As mentioned earlier in the present section (see page 113) if the value of n is less than 0•5 then the local flow is increasing more rapidly than the average flow.

The next group comprises tubes: 1921, 2627.

For this group $n = 0.43$ and $c = 0.518$ and therefore we obtain

$$j_{DM} = 0.518\ (Re_M)^{-0.43}$$

It can be seen that the local flow for this group is also increasing more rapidly than the average flow.

The final group comprises tubes: 3843, 3942, 4650, and for this group $n = 0.47$ and $c = 0.544$.

Thus $$j_{DM} = 0.544\ (Re_M)^{-0.47}$$

Again, the local flow is increasing more rapidly than the average flow. Williams (2) demonstrated that the average cross flow zone data could be represented by the expression:-

$$j_{DM} = 0.5\ (Re_M)^{-0.5} + 0.0037 \quad \text{for} \quad 200 < Re < 2000.$$

18·4% IDENTICAL GROUPS

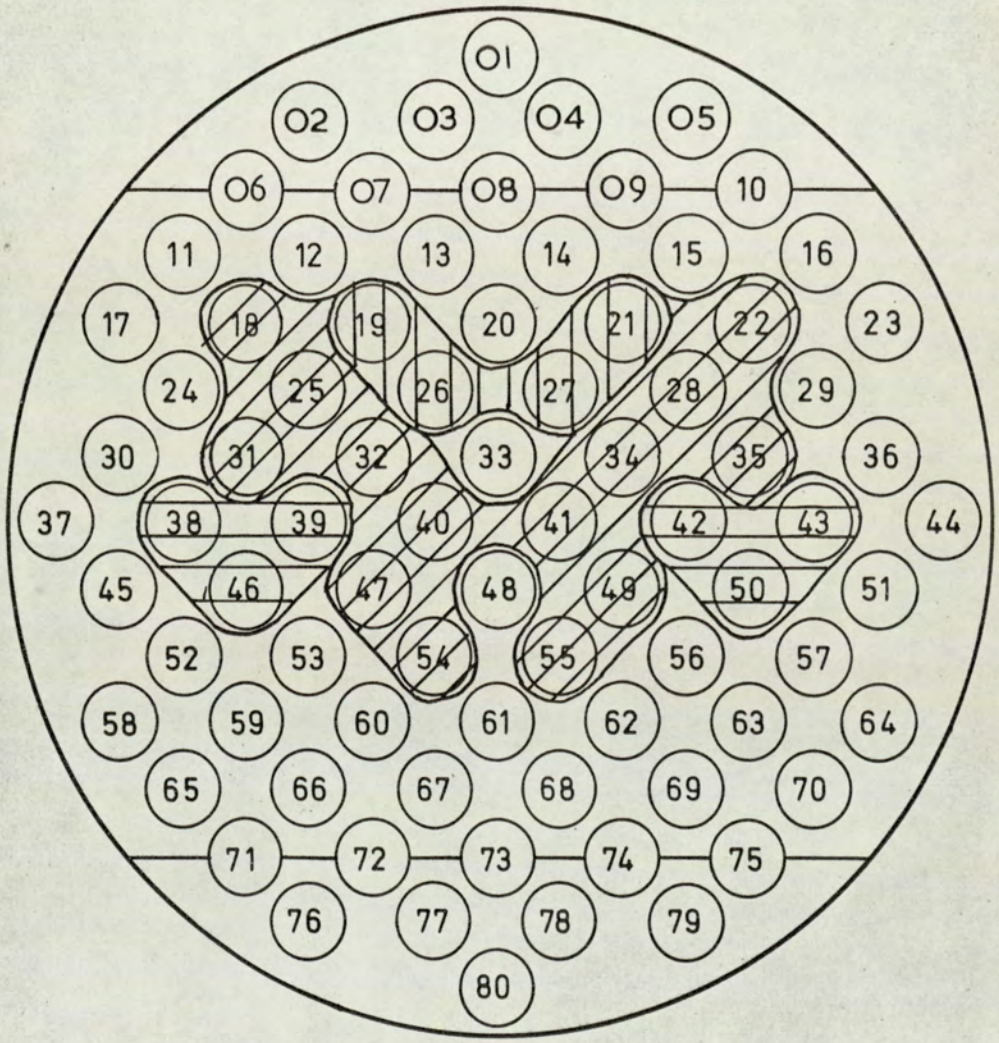

GROUP		SLOPE	CONSTANT
1	III	0·433	0·519
2	///	0·420	0·419
3	≡	0·466	0·544

FIG. 37.

This phenomenon of the local flow increasing more rapidly than the average flow increases may be clarified as follows. At low flowrates the fluid stream will tend to by-pass between the tube bundle and the shell wall, whereas at higher flowrates more of the fluid will be forced through the bundle. Hence the fluid flow through the centre of the bundle increases more rapidly than the average fluid flow increases.

The 31% baffle cut down case (see Fig.38 page 146).

For this cut down five groups of tubes are obtained:-

A very large group containing the centre column of tubes, most of the tubes in the trailing part of the cross flow zone and the centre of the outlet baffle edge zone. The tubes concerned are:-
08, 20, 3135, 33, 3843, 3942, 4650, 4749, 48, 5257, 5356,5455, 6062, 61.
For this group $n = 0{\cdot}47$ and $c = 0{\cdot}576$.

$$\therefore \quad j_{DM} = 0{\cdot}576\ (Re)_M^{-0{\cdot}47}$$

Although it may still be said that the flow through this group increases more rapidly than the average flow, it can be seen that this group constitutes the major portion of the cross flow zone. As will be discussed later in this section this would seem to be a function of the baffle cut down.

Another group is comprised of the inlet baffle edge and the adjacent row of tubes in the inlet window zone:-
1215, 1314, 1723, 1822, 1921; for this group $n = 0{\cdot}49$ and $c = 0{\cdot}685$

$$\therefore \quad j_{DM} = 0{\cdot}685\ (Re)_M^{-0{\cdot}49}$$

31% B.C.D. IDENTICAL GROUPS

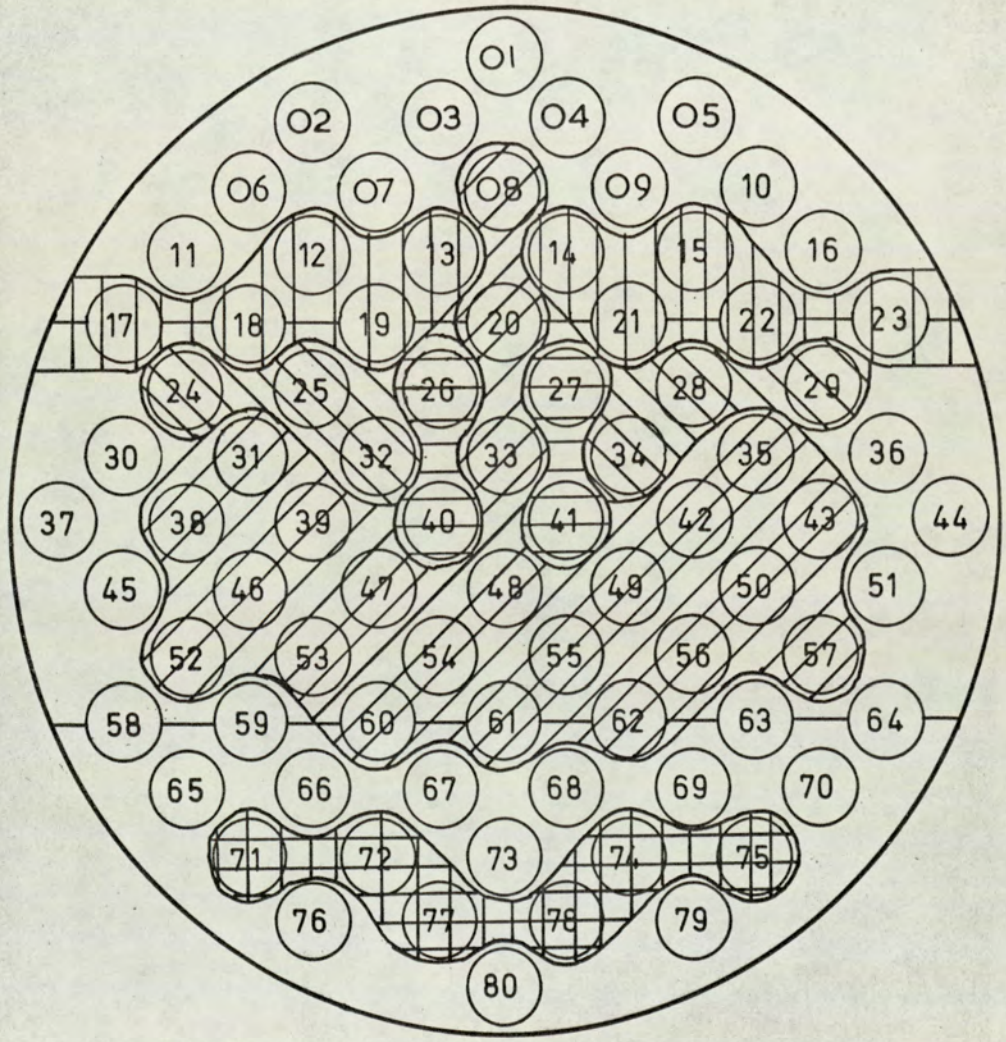

GROUP		SLOPE	CONSTANT
1	///	0·468	0·576
2	|||	0·488	0·685
3	\\\	0·502	0·663
4	≡	0·419	0·450
5	#	0·453	0·377

FIG. 38.

In the case of this group the local fluid flow increase is almost identical to the average flow increase as all the tubes are included in two rows.

There are two small groups between the previously mentioned inlet window zone group and cross flow zone group.

2627, 4041 for which $n = 0.42$ and $c = 0.450$

$$\therefore \quad j_{DM} = 0.450\ (Re_M)^{-0.42}$$

and 2429, 2528, 3234 for which $n = 0.50$ and $c = 0.664$

$$\therefore \quad j_{DM} = 0.664\ (Re_M)^{-0.50}$$

The first of these two groups has an n value less than the large cross flow group, i.e. the flow through this group is increasing more rapidly than the average flow, and this could well be due to a wake effect from the centre row of tubes which lead into the large cross flow group combined with the group in the inlet window zone and inlet baffle edge zone.

The second of the groups is the only group found for any of the cut downs studied which had the same n value as the cross flow zone average found by Williams, i.e. $n = 0.50$. This is a higher n value than either the inlet window zone, small cross flow zone group, or large cross flow zone groups that it lies between. This group shows just how complex the flow paths are, and as its local flow increases more slowly than the flow through the groups surrounding it, and bearing in mind its position in the bundle, it is probably due to a large extent to the effect of the bundle to shell by-pass flow.

The final group for this baffle cut down is in the outlet window zone:- 7175, 7274, 7778, for which $n = 0{\cdot}45$ and $c = 0{\cdot}377$

$$\therefore \quad j_{DM} = 0{\cdot}377\ (Re)_M^{-0{\cdot}45}$$

The local flow through this group increases more rapidly than the average flow through the bundle. This is probably due to flow stratification and bundle by-passing at low Reynolds numbers.

The 43·7% baffle cut down case (see Fig. 39 page 149).

For this baffle cut down there are two groups of identical tubes.

The first group consists of most of the cross flow zone, the inlet and outlet baffle edge zones and the trailing part of the inlet window zone:-

2528, 2627, 3135, 3234, 33, 3942, 4650, 4749, 48

for which $n = 0{\cdot}45$ and $c = 0{\cdot}538$

$$\therefore \quad j_{DM} = 0{\cdot}538\ (Re)_M^{-0{\cdot}45}$$

The fact that the local flow through this group increases more rapidly than the average flow through the bundle is partially due to the bundle by-pass flowstream, as well as the fact that the baffles in this cut down case, as demonstrated by the tube groupings obtained by slope comparison alone, do not distribute the flow at all evenly. The reasons for the two tubes 4041, which are of course mirror image tubes, not forming part of this group although situated in the middle of it, are not clear. This anomaly is possibly due to a wake effect from tubes 2627 and 33 compounded with the previously mentioned poor fluid distribution obtained with this baffle cut down, or may be just

43·7% B.C.D. IDENTICAL GROUPS

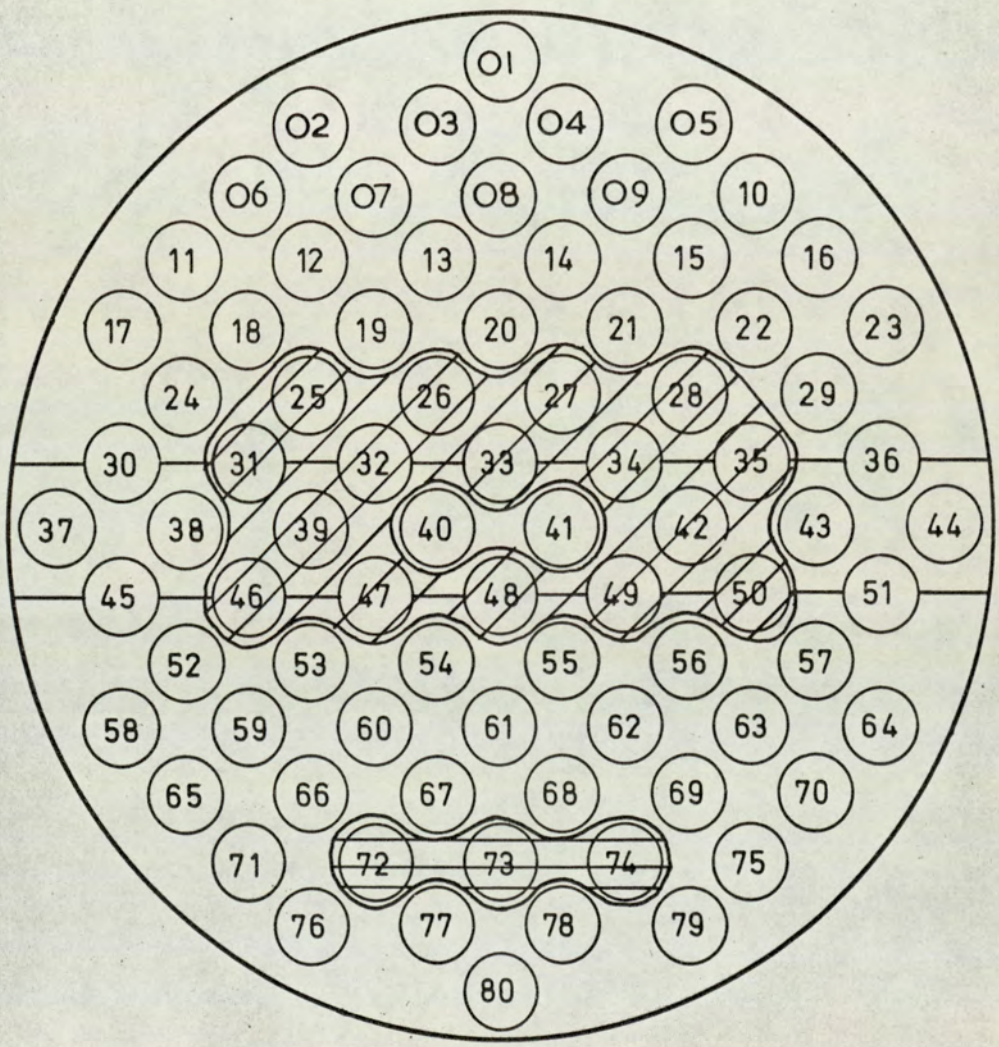

GROUP	SLOPE	CONSTANT
1 ≡	0·466	0·330
2 ///	0·454	0·538

FIG. 39.

fortuitous.

The other group obtained for this baffle cut down is in the outlet window zone:- 7274, 73 for which $n = 0{\cdot}47$ and $c = 0{\cdot}331$

$$\therefore \quad j_{D_M} = 0{\cdot}331\ (Re)_M^{-0{\cdot}47}$$

This group is in the same position as the slightly larger group obtained with the 31% baffle cut down, and also appears in the group obtained by slope grouping in the previously discussed 43·7% baffle cut down slope group (see Fig.36, page 139.)

The existence of this group is probably due to shell to bundle by-passing at low flowrates and also to the fact that with this cut down the flow will tend to by-pass some of the tubes in the bundle, situated at a distance from the baffle, at low flowrates.

Conclusions from tube grouping by statistical analysis of regression line slopes and constants.

This method of grouping of identical tubes serves to confirm further the conclusions obtained from tube grouping by regression line slopes.

It can be seen from the Reynolds number exponents of the groups that with one exception (the inlet baffle edge group obtained with the 31% baffle cut down) the local flow through the groups is increasing more rapidly than the average flow through the bundle. Further, with the exception of the above mentioned group, none of the groups of identical tubes contain tubes at the bundle edge and this would seem to show that at low Reynolds number a large proportion of the flow tends to by-pass the bundle.

From examination of the tube groupings obtained it can be seen that, of the three baffle cut downs studied, the 31% baffle cut down gives the most even fluid distribution and hence the most even transfer characteristics, and with a large group of identical tubes in the cross flow zone it would seem that the least amount of by-passing is obtained with this cut down. Also of the cross flow groups obtained for the three baffle cut downs the cross flow group in the 31% baffle cut down case has a Reynolds number exponent (0.47) nearest to the average exponent of 0.50. This would seem to lend further weight to the fact that the least bundle by-passing occurs with the 31% baffle cut down.

When heat exchangers are being used to deal with heat sensitive fluids it is obviously extremely important to avoid hotspots. From the tube groupings, and from the data given in Tables 8:1, 8:2, 8:3, see pages (199, 201, 203) it can be seen that the 43.7% baffle cut down is the most likely to give hotspots.

It would seem therefore that for an exchanger of the design studied in this case that a baffle cut down of about 31% would seem to give the best results, and that when other baffle cut downs are employed some form of fluid redistribution should be incorporated. Where a tube is a known hotspot it would be easily possible to block that tube, but of course the tube should not be removed or the shellside flow pattern would be upset.

****
****
**

CONCLUSIONS.

A satisfactory method of renewing a mercury coated transfer surface in situ has been developed. The use of this technique permits a constant rate transfer period to be maintained indefinitely when air is used as the working fluid. This in turn means that a simple once through experimental rig can be utilised whereas if nitrogen is to be used then a complicated closed circuit must be employed to conserve the nitrogen.

From the experimental runs carried out with the model exchanger it would seem that with more development work on the mixing and sampling of air/mercury streams, the experimental methods developed and utilised in the present work should give results compatible with those obtained by Williams (2) using a mercury/nitrogen system.

From analysis of the results of Bergelin et al.(1) and Williams (2) it seems that the cross flow zone of a segmentally baffled cylindrical shell and tube exchanger behaves as a rectangular tube bank.

For an exchanger of the type considered in this analysis it would seem that an indication of the bundle average transfer coefficient may be obtained from the individual tube transfer coefficient of the tubes 38 and 43.

By means of a statistical analysis of the regression lines obtained from the individual tube transfer coefficients of Williams it has been possible to construct groups of tubes of identical slope for each baffle cut down. From these groupings it has been shown

that the 31% baffle cut down gives the most even fluid flow distribution and hence the most even transfer. The 43.7% baffle cut down gives the worst flow distribution and the greatest chance of local hotspots.

The statistical analysis was then extended to give groups of tubes of identical regression line slopes and constants for the three baffle cut downs. From these groupings it is confirmed that the 31% baffle cut down gives the most even flow distribution of the three baffle cut downs studied, with the least evidence of bundle to shell by-passing. This study also confirmed that the 43.7% gave the worst flow distribution and the greatest likelihood of hotspots. Although the 18.4% baffle cut down did not give such bad distribution as the 43.7% cut down nevertheless it would seem that when baffle cut downs other than 31% are employed for this design of exchanger some form of flow redistributor should be incorporated. Further, where tubes can be predicted as hotspots they should be sealed off on the tubeside when heat sensitive materials are being processed.

****
****
**

RECOMMENDATIONS FOR FUTURE WORK.

If the present experimental method is to be used in future work it is obvious that the first stage of that work must be to improve the mixing of the air/mercury stream, particularly at low Reynolds numbers, as incomplete mixing leads to inaccurate results.

Three lines are then suggested for future work:-

(a) The use of mercurised transfer surfaces equal in length to half the baffle spacing. This would clarify the position regarding the symmetry of flow about the baffles. It would also be possible to study the effect of baffle spacing on the transfer coefficients.

(b) A study of the baffle compartments at the inlet and exit ports of the exchanger. This would determine the effect on the transfer coefficients of flow deviations caused by the inlet and exit ports.

(c) To repeat the investigations so far carried out with firstly baffle to tube hole and secondly baffle to shell by-passing so that the effects of leakage on the exchanger performance could be determined.

****
****
**

A P P E N D I C E S

****
****
****
*

APPENDICES

APPENDICES. Continued .....

****
****
**

APPENDIX 1.

CALIBRATION DATA.

(1) ROTAMETERS.

The following rotameters were used in the experimental circuit described in Chapter III A (i).

Rotameter No.	Range.	Fluid	Type.
R1	100 - 1000 Litres/min.	Air	Metric 47A
R2	200 - 2000 Litres/min.	"	Metric 65A
R3	2 - 20 Litres/min.	"	Metric 10A
R4	2 - 20 Litres/min.	"	Metric 10A
R5	5 - 50 Litres/min.	"	Metric 14A
R6	2 - 20 Litres/min.	"	Metric 10A
R7	0 - 1 Litres/min.	"	----

Rotameter R7 was calibrated by the manufacturer.

Calibration curves for the other six rotameters are given (pages 161-164). These calibration curves were obtained using data supplied by the Rotameter Manufacturing Company Ltd. in their publication RP.3000, entitled "Calibration Data for Metric Series Rotameters". This method which is described below was found to agree with the following experimental methods:-

(a) For Rotameters R3, R4, R5 and R6:-

These four rotameters were experimentally calibrated using a water displacement method, and a Parkinson Cowan wet gas meter.

(b) For Rotameters R1 and R2:-

These two rotameters were experimentally calibrated using a manufacturer calibrated Kent venturi meter.

Rotameter Calibration using "Calibration Data for Metric Series Rotameters" (39).

Rotameter calibration by this method was carried out utilising a PDS.1020 digital computer and part of a computer programme developed by J. B. Akers (40).

COMPUTER PROGRAMME 1

CALCULATION OF AIR FLOW RATES FROM ROTAMETER MEASUREMENTS.

PR.5401 INTERPRETER.
RETAIN 1+

1	INP	19	C9-	37	D9-	55	C21-
2	CI-	20	L2-	38	C4-	56	INP
3	INP	21	S9-	39	L2-	57	TYPE
4	C2-	22	C17-	40	M9-	58	M21-
5	INP	23	L8-	41	D1-	59	M7-
6	C10-	24	D6-	42	D17-	60	D5-
7	INP	25	LOG	43	SQRT	61	M6-
8	C11-	26	M12-	44	C20-	62	D8-
9	INP	27	EXP	45	M10-	63	M22-
10	C7-	28	C15-	46	M4-	64	D24-
11	INP	29	L8-	47	LOG	65	M23-
12	A6-	30	A13-	48	D19-	66	M18-
13	C8-	31	C16-	49	A18-	67	D26-
14	L3-	32	L6-	50	C/R	68	D26-
15	M7-	33	A13-	51	TYPE	69	D25-
16	D5-	34	D16-	52	L11-	70	TYPE
17	M6-	35	M15-	53	D20-	71	JMP9
18	D8-	36	M14	54	TYPE	72	RETAIN

Before the programme is commenced, constants are required in the following scratchpad locations:-

Scratchpad location	3	5	6	12	13	14	18
Constant	$1{\cdot}293 \times 10^{-3}$	76·0	273·1	1·5	114·0	$1{\cdot}709 \times 10^{-4}$	4

The rotameter and flow constants ω , α , K_1 and K_2 were fed into the computer at input steps 1, 3, 5 and 7. For each result the upstream conditions were then fed in as pressure (cm.Hg) at input step 9 and temperature ($^{\circ}C$) at input step 11. Using these data the computer calculated and printed out values of I and F_T. From the appropriate rotameter chart of I against scale reading a value of F was obtained and fed into the computer at input step 56. The volumetric flow rate of the rotameter was then calculated and printed out at computer step 57. [The programme continues to calculate and then prints out the mass flow rate, as required by Akers.]

The flow rate was then corrected to a free volume flow rate by the relationship:-

$$Q_2 = Q_1 \sqrt{\frac{p_1}{p_2}}$$

where:- Q_1 = calculated flow rate at pressure p_1

Q_1 = flow rate in free volumes.

p_2 = atmospheric pressure.

No justification could be found for using a more complex relationship.

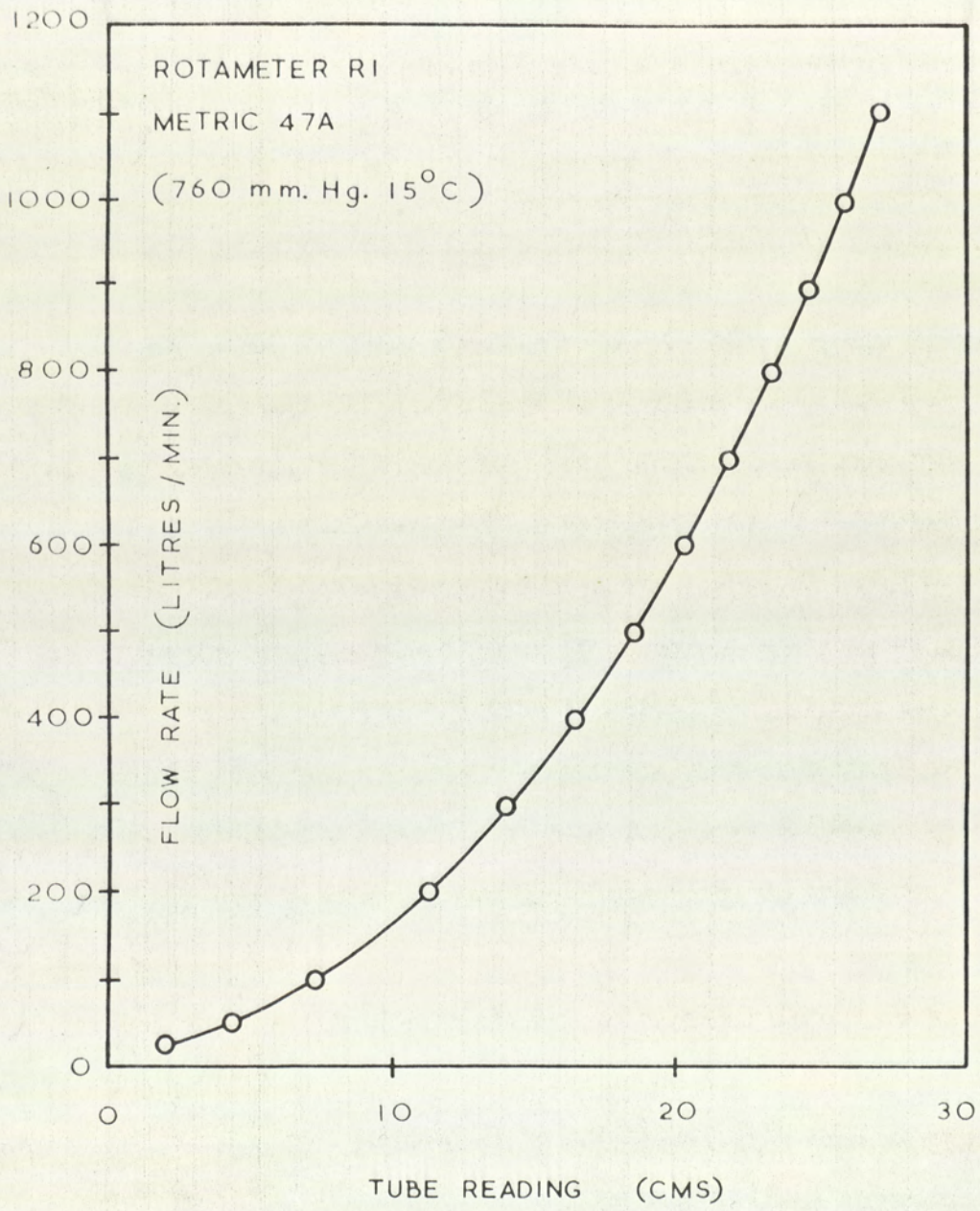
ROTAMETER R1
METRIC 47A
(760 mm. Hg. 15°C)
FLOW RATE (LITRES / MIN.)
1200
1000
800
600
400
200
0
0
10
20
30
TUBE READING (CMS)

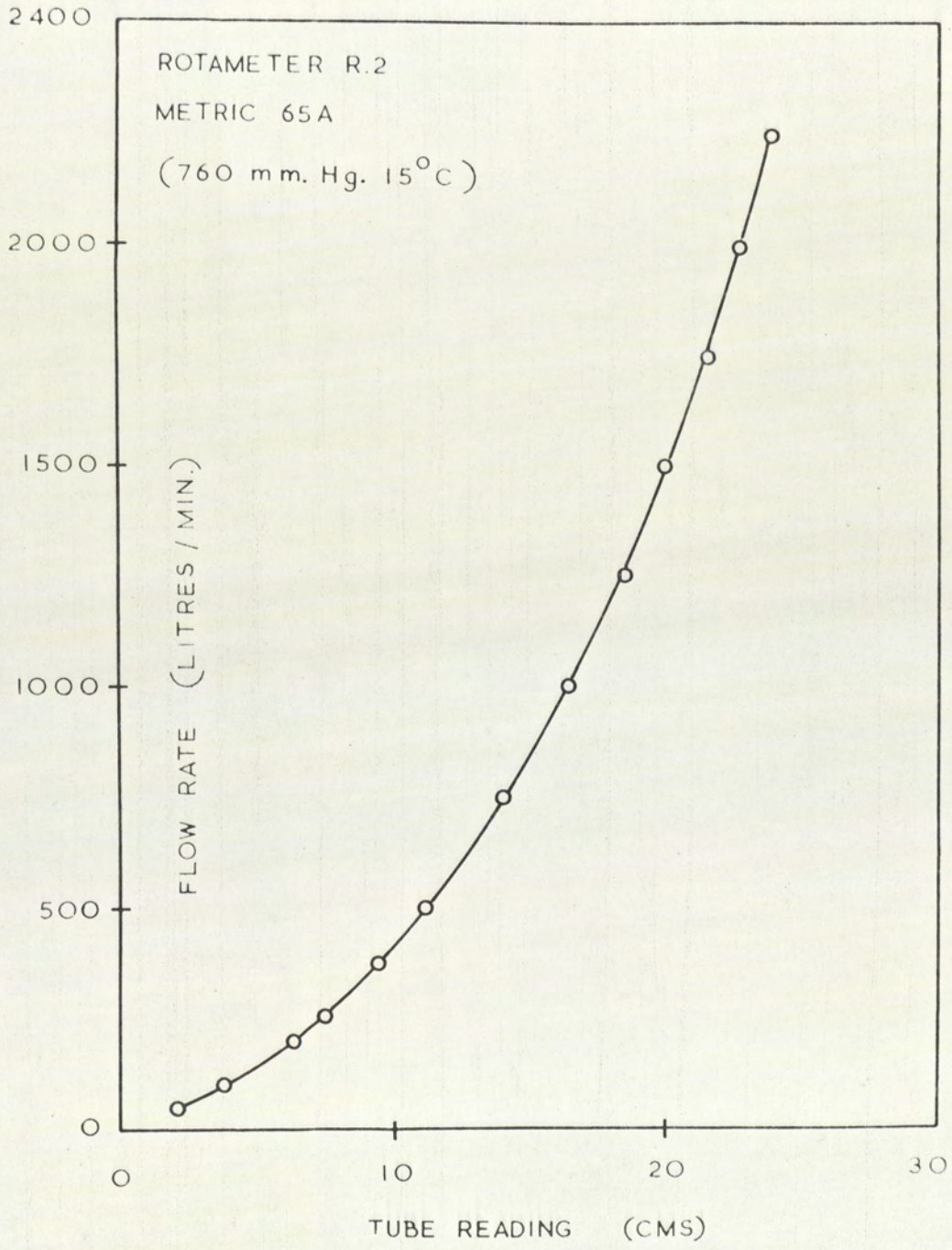
ROTAMETER R.2
METRIC 65A
(760 mm. Hg. 15°C)
2400
2000
1500
1000
500
0
FLOW RATE (LITRES / MIN.)
0
10
20
30
TUBE READING (CMS)

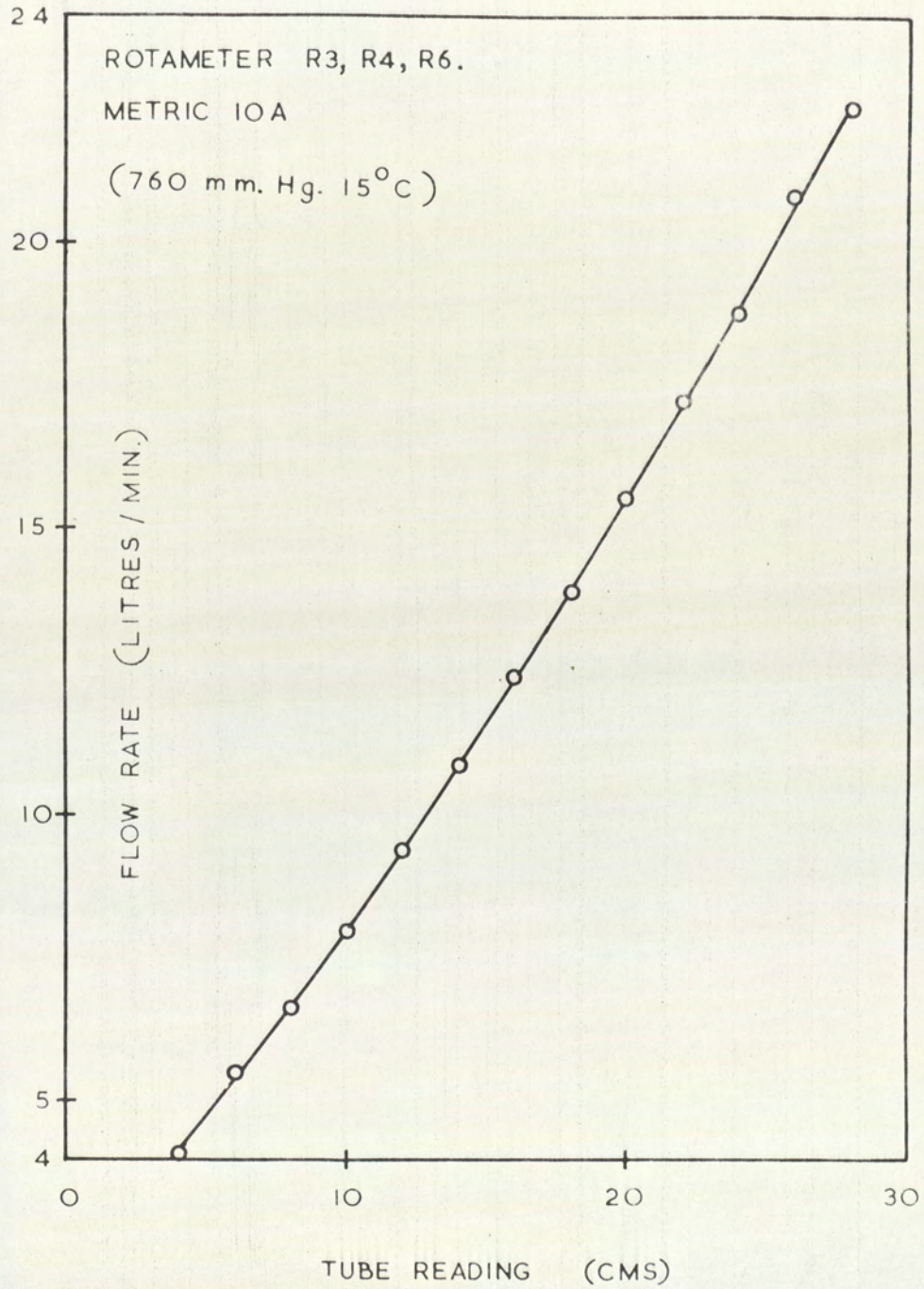
ROTAMETER R3, R4, R6.
METRIC 10A
(760 mm. Hg. 15°C)
FLOW RATE (LITRES / MIN.)
24
20
15
10
5
4
0
10
20
30
TUBE READING (CMS)

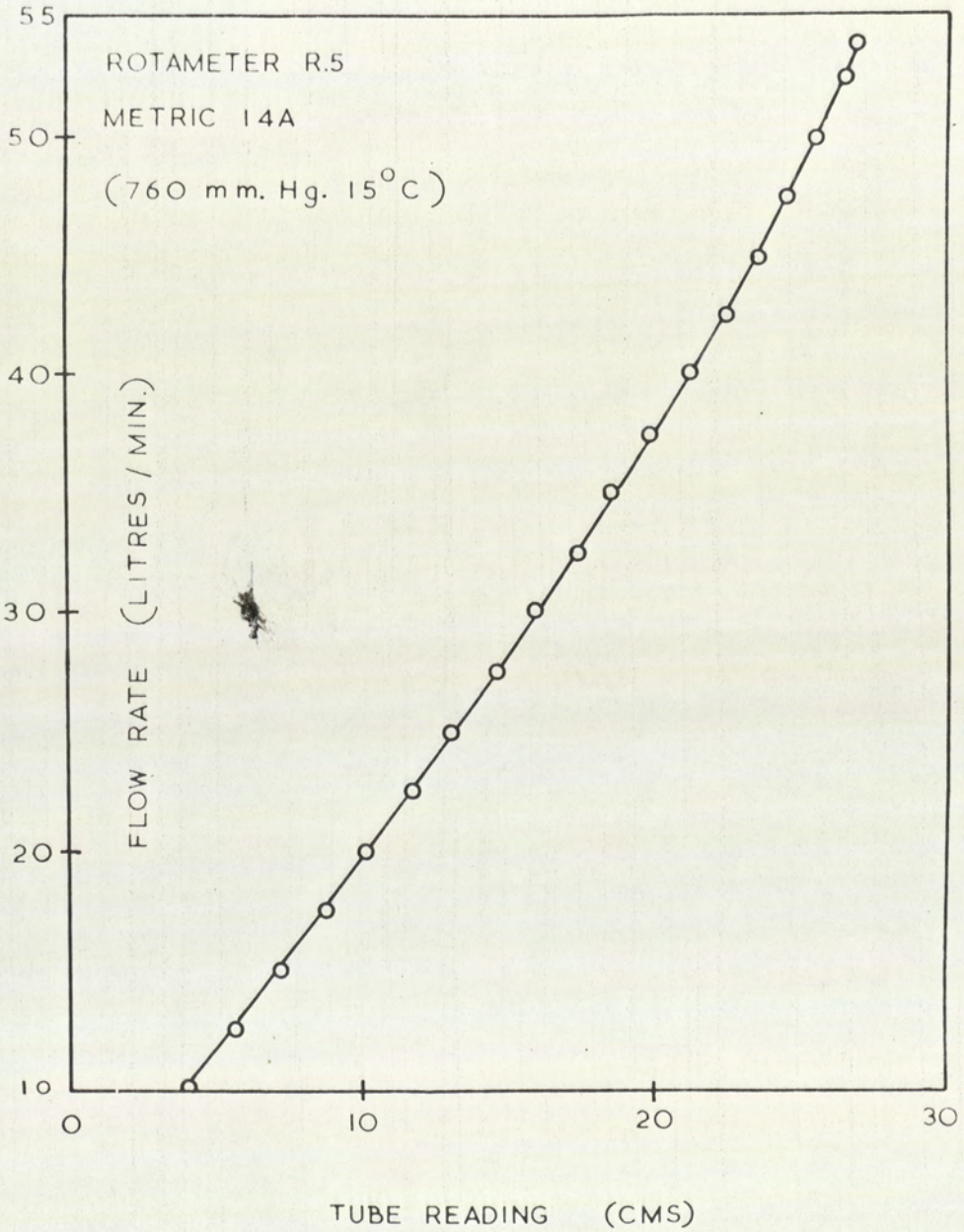
ROTAMETER R.5
METRIC 14A
(760 mm. Hg. 15°C)
FLOW RATE (LITRES / MIN.)
55
50
40
30
20
10
0
10
20
30
TUBE READING (CMS)

1. (2) Thermocouples.

The thermocouples were made by capacitance discharge welding of NICHROME V (0·005" diameter) and ADVANCE (0·01" diameter).

The actual settings of the welding machine are given to facilitate future construction of these thermocouples:-

Capacitance Discharge Welder made by SPEMBLEY LTD.
(Chatham, Kent).

Type WP3 Serial No. 005.

Settings:- D.C. volts = 52
Left hand capacitance at 2
Right hand capacitance at 0·5

If the joint is mechanically strong, i.e. does not easily pull apart, then a successful thermocouple results.

The thermocouples were then aged by alternately heating and cooling them several times, before being calibrated at the two fixed points:-

Melting point of ice 0°C.
Melting point of pure sodium sulphate heptahydrate 32·48°C.

The intermediate points were checked using a grade A 0·1°C/division mercury in glass thermometer.

The graph of EMF against Temperature was found to be linear over this range, and all the thermocouples were found to be in agreement to within ± 2 μ V. The thermocouple sensitivity

was found to be 43·9 μ V per ^{o}C.

A calibration curve is shown on page 167.

Thermocouple positions:-

TC1	....	Absorptiometer inlet.
TC2	....	Inlet port of exchanger.
TC3	....	Outlet port of exchanger.
TC4 and TC5		Transfer probes.
TC6	....	Saturator outlet.

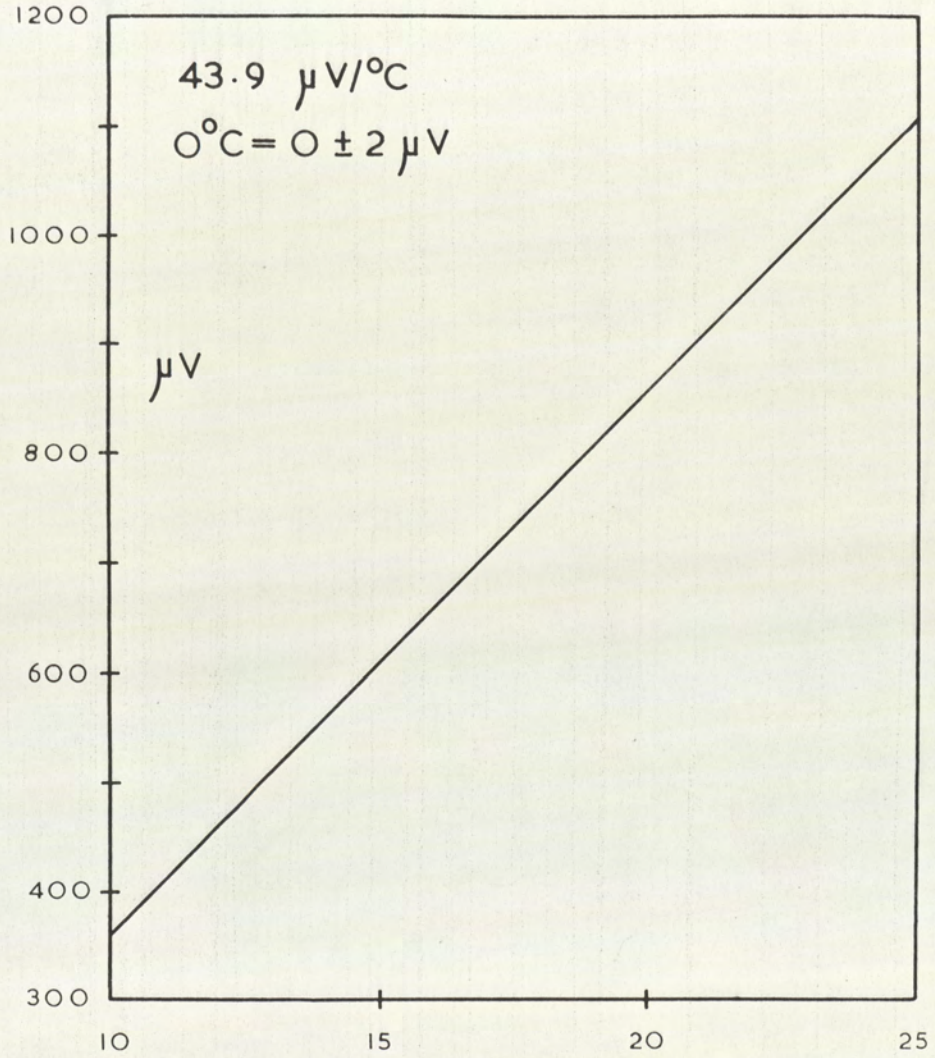

THERMOCOUPLE CALIBRATION CURVE

1.

(3) Absorptiometer.

The calibration technique for the absorptiometer is described in Appendix 5 (2). The calibration curve on page 169 was obtained at a thermostat temperature of 32°C ± 1°C. Air was used as the carrier gas, and the mercury / air stream was fed to the absorptiometer at 15 litres/min. It was found that the calibration curve could be reproduced without variation over several runs.

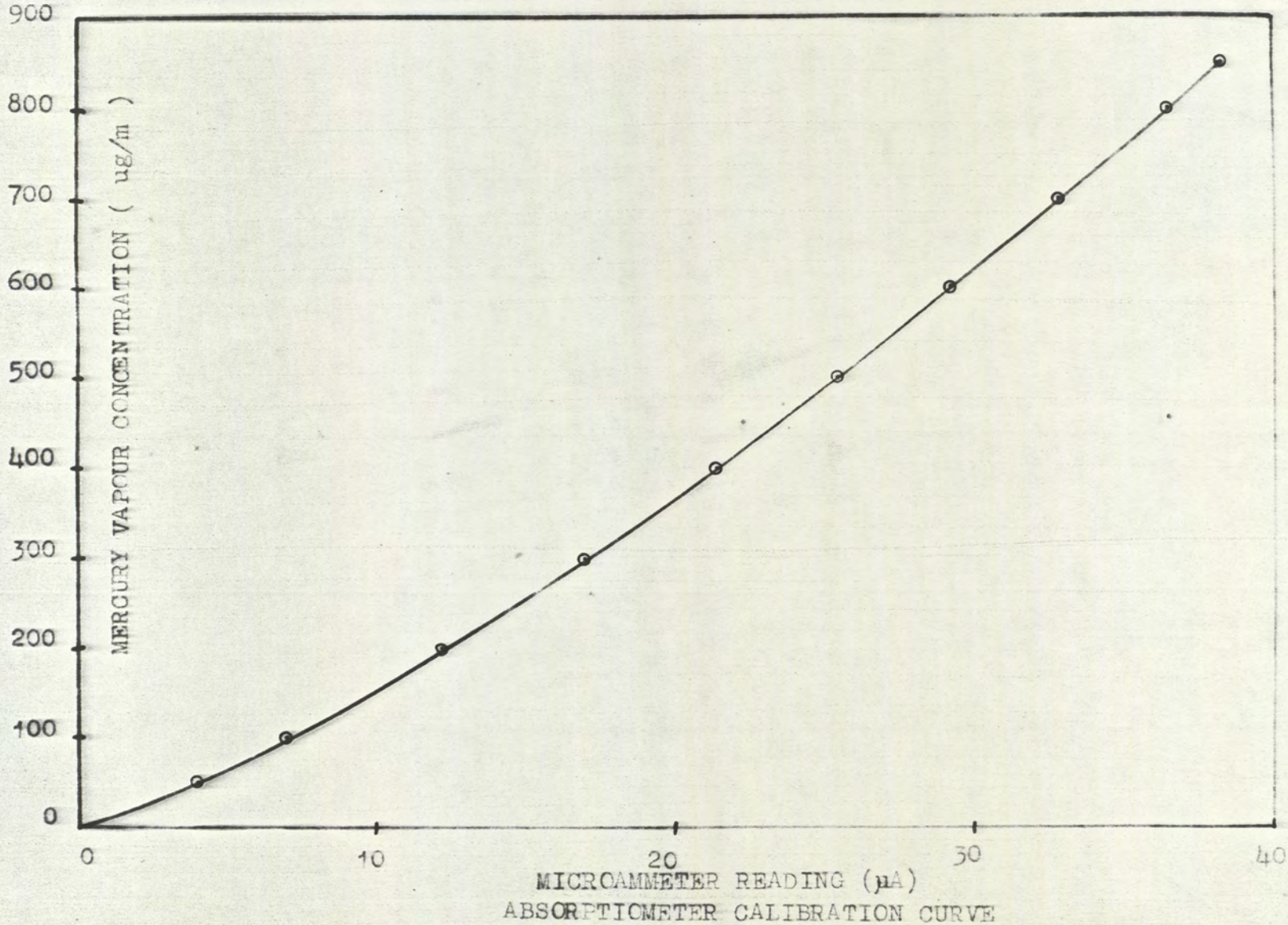

ABSORPTIOMETER CALIBRATION CURVE

APPENDIX 2.

PHYSICAL PROPERTIES.

(1) Saturation concentration of Mercury vapour.

Values of the saturated vapour pressure of mercury were calculated according to the work of Ernsberger and Pitman (41).

They recommended the equation:-

$$\log p^* = 11{\cdot}0372 - \frac{3204}{T}$$ where p^* is in microns Hg. T is in $^{\circ}A$.

and found a deviation of $\pm$ 0.8% between calculated and observed vapour pressures, over a temperature range of 12 - 50°C.

Assuming the ideal gas laws to hold, the saturation vapour pressures were converted to concentrations:-

$$c^* = \frac{nM}{V} = \frac{M\,p^*}{RT}$$

$$c^* = \frac{200{\cdot}61\ p^*\ \times\ 10^{-3}}{62{\cdot}361\ T} \text{ gms/litre}$$

$$c^* = \frac{200{\cdot}61\ p^*\ \times\ 10^{6}}{62{\cdot}361\ T} \ \mu g/m^3.$$

A table of c^* and T is given in table 2:1.

TABLE 2 : 1

T°C	p* microns Hg	c* µg/m^3
10	0•5243	5957•9
11	0•5747	6507•4
12	0•6295	7103•0
13	0•6891	7748•4
14	0•7539	8447•1
15	0•8242	9203•3
16	0•9006	10021
17	0•9834	10905
18	1•073	11860
19	1•170	12891
20	1•276	14003
21	1•390	15203
22	1•513	16496
23	1•647	17888
24	1•791	19388
25	1•946	21002

^{2} (2). DIFFUSION COEFFICIENT

The diffusion coefficient was calculated by the method of Hirschfelder, Curtiss and Bird (42) using the appropriate tables as given by Reid and Sherwood (43).

$$D_{12}\,P = \frac{0.001858\ T^{3/2}}{\sigma_{12}^2\ \Omega_D} \left[\frac{M_1 + M_2}{M_1\,M_2}\right]^{\frac{1}{2}}$$

For mercury $M_1 = 200.61$ and for air $M_2 = 28.97$

$$\therefore \left[\frac{M_1 + M_2}{M_1 M_2}\right]^{\frac{1}{2}} = 0.1988$$

$\sigma_{12} = \frac{1}{2}(\sigma_1 + \sigma_2)$ and $\sigma_{Hg} = 2.898$ and $\sigma_{air} = 3.617$

$$\therefore \quad \sigma_{12} = 3.2575.$$

$$\sigma_{12}^2 = 10.611$$

$$\therefore \quad D_{12}P = \frac{0.001858 \times 0.1988}{10.611\ \Omega_D}\ T^{3/2} = 0.00003481\ \frac{T^{3/2}}{\Omega_D}$$

Now for mercury $\frac{\varepsilon_1}{k} = 851$ and for air $\frac{\varepsilon_2}{k} = 97$

and $$\frac{kT}{\varepsilon_{12}} = \frac{kT}{\sqrt{\varepsilon_1\ \varepsilon_2}} = 0.00348\ T.$$

A table of $\sim_D$ against $\frac{k\,T}{\varepsilon_{12}}$ is given in Reid and Sherwood.

From the appropriate part of the table a graph of $\sim_D$ against $\frac{k\,T}{\varepsilon_{12}}$ was plotted (see Fig. 2:1 (page 174)) and they were used to construct Table 2 : 2 of diffusion coefficients against temperature , which is presented below:-

TABLE 2 : 2

$T^{\circ}C$	$T^{\circ}K$	$T^{3/2}$	$\frac{KT}{\varepsilon_{12}}$	$\sim_D$	$D_{12}P$ $cm^2/sec.$
10	283•1	4763	0•985	1•45	0•11434
11	284•1	4789	0•989	1•447	0•11521
12	285•1	4814	0•992	1•445	0•11597
13	286•1	4839	0•995	1•4425	0•11677
14	287•1	4865	0•999	1•44	0•11760
15	288•1	4890	1•0026	1•4375	0•11841
16	289•1	4915	1•006	1•435	0•11925
17	290•1	4941	1•009	1•433	0•12003
18	291•1	4967	1•013	1•43	0•12091
19	292•1	4992	1•017	1•4275	0•12173
20	293•1	5018	1•020	1•4255	0•12254
21	294•1	5044	1•023	1•4235	0•12335
22	295•1	5069	1•027	1•421	0•12417
23	296•1	5095	1•030	1•419	0•12499
24	297•1	5121	1•034	1•416	0•12589
25	298•1	5147	1•037	1•4145	0•12666

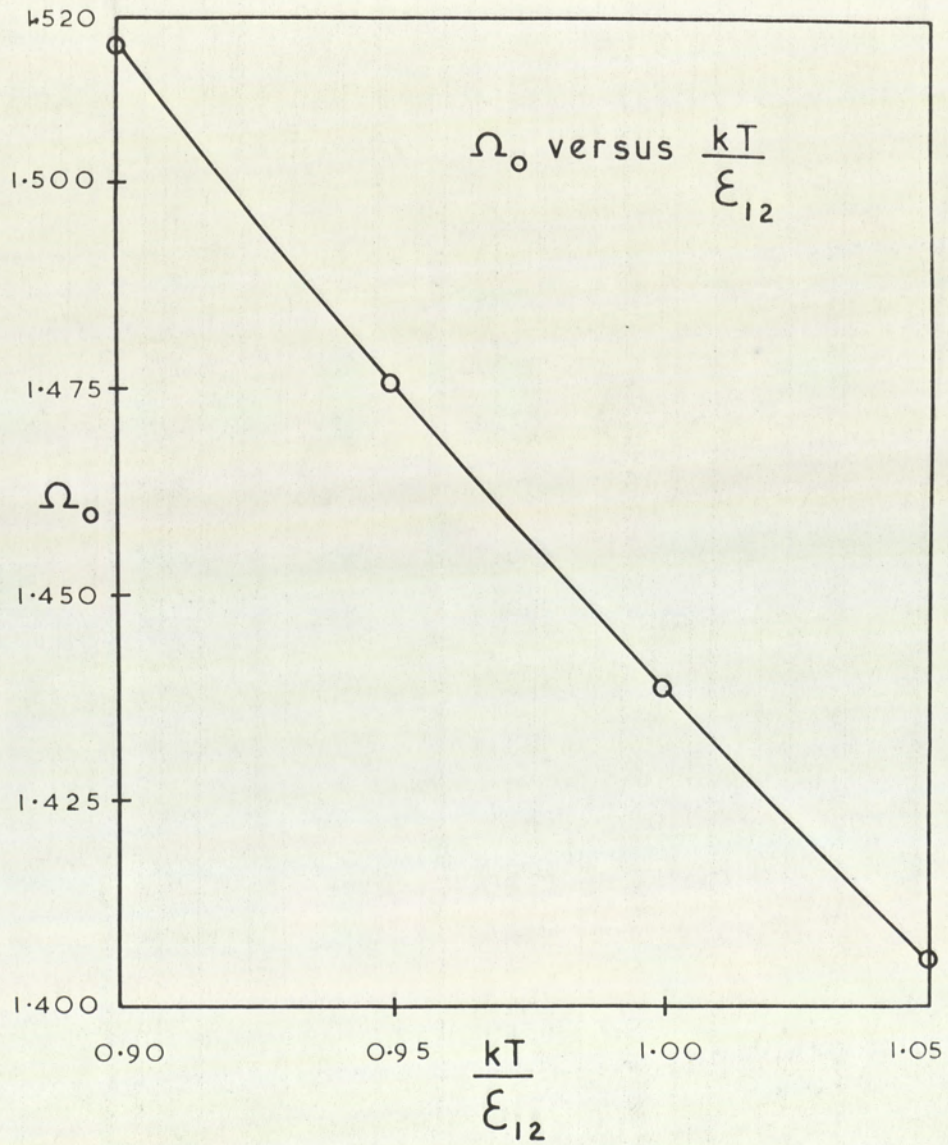
1·520
1·500
1·475
1·450
1·425
1·400
Ω_o
Ω_o versus $\frac{kT}{\varepsilon_{12}}$
0·90
0·95
1·00
1·05
$\frac{kT}{\varepsilon_{12}}$

FIG. 2:1

2 (3) VISCOSITY OF AIR.

This was calculated using the Sutherland Formula (44).

$$\mu = \frac{\mu_o \ (273{\cdot}1 + c)}{T + c} \left(\frac{T}{273{\cdot}1}\right)^{3/2} \text{c.p.}$$

where μ_o = 0·017 c.p. and c = 114. T is in ^{o}K.

Temperature ^{o}C	μ c.p.
10	0·01749
11	0·01754
12	0·01759
13	0·01764
14	0·01768
15	0·01773
16	0·01778
17	0·01783
18	0·01788
19	0·01792
20	0·01797
21	0·01802
22	0·01807
23	0·01812
24	0·01816
25	0·01821

2 (4) DENSITY OF AIR.

At N.T.P. the density of air is 1•2928 gms/litre (45).

Applying the ideal gas laws:-

$$\rho_{760} = 1{\cdot}2928 \times \frac{273{\cdot}1}{T} \text{ gms/litre, where T is in } {}^{\circ}K.$$

Temperature $^{\circ}C$	ρ gms/litre
10	1•2471
11	1•2427
12	1•2384
13	1•2341
14	1•2298
15	1•2255
16	1•2213
17	1•2171
18	1•2129
19	1•2087
20	1•2046
21	1•2005
22	1•1964
23	1•1924
24	1•1884
25	1•1844

APPENDIX 3.

CALCULATION METHODS AND RESULTS.

Calculation of exchanger concentration from the absorptiometer reading.

(1) Correction factor for variations in temperature and pressure between the exchanger and the absorptiometer chamber:-

$$= \left\{ \frac{p_e}{p_A} \cdot \frac{T_A}{T_e} \right\}$$

where T = absolute temperature

p = absolute pressure

suffixes 'A' and 'e' = absorptiometer and exchanger.

Mass balance on flow stream into absorptiometer:-

$$q\, c_e = (q + Q)\, c_A$$

$$c_e = \frac{q + Q}{q} \cdot c_A$$

q = sample flow rate litre/min.

Q = dilution flow rate litre/min.

c_e = exchanger outlet Hg. conc^{n}. $\mu g/m^3$.

c_A = absorptiometer reading $\mu g/m^3$.

(2) Calibration of Absorptiometer:-

$$c_A = \frac{q \cdot c^*}{Q + q}$$

where c^* is the saturated mercury concentration corresponding to the saturator outlet temperature ($\mu g/m^3$).

[See Appendix 2 (1)]

(3) Mass transfer coefficients:-

$R_m = k_c \, S \, \Delta C$ where R_m = mass rate of Hg. evap^n. gms/sec.

k_c = mass transfer coefficient for the rod cm/sec.

S = surface area of rod cm^2.

ΔC = driving force for the rod.

F = flowrate through exchanger in free volumes (L/min.)

c_{sr} = saturated concentration ($\mu g/m^3$) of Hg. vapour, at temperature of probe, at the probe.

$$R_m = \frac{F}{60} \cdot \frac{c_e}{10^9} \text{ gms/sec.}$$

$$= k_c \cdot S \, \Delta C$$

Now $\Delta c = c_{sr}$ $\mu g/m^3 = \frac{c_{sr}}{10^9}$ gms/litre.

$$\therefore \quad k_c S = \frac{F}{60} \cdot \frac{c_e}{c_{sr}} \times 10^3 \text{ cm}^3/\text{sec.}$$

so $$k_c = \frac{F}{S} \times \frac{10^3}{60} \times \frac{c_e}{c_{sr}} \text{ cm/sec.}$$

(4) Mass transfer factor (j_D):-

$$j_D = \frac{k_c}{u} (Sc)^{\frac{2}{3}}$$ where:- u = gas stream velocity cm/sec.

(Sc)= Schmidt number.

A = area available for flow cm^2.

Now $$u = \frac{F \times 10^3}{A \times 60}$$

$$\therefore \quad j_D = \frac{A}{S} \cdot \frac{c_e}{c_{sr}} (Sc)^{\frac{2}{3}}.$$

For individual tube coefficients A = 38·7 cm^2

and S = 58· 75 cms^2 / tube.

(5) Schmidt Number (Sc):-

$$(Sc) = \frac{\mu}{\rho D_v}$$

where:- μ = viscosity of air.

ρ = density of air.

D_v = diffusion coefficient of mercury into air.

At 20°c and 760 mms Hg. :-

μ = 0·01797 c.p., ρ = 1·2046 g/litre, D_v = 0·12254 $cm^2/sec.$

$\therefore$ (Sc) = 1·217

$(Sc)^{\frac{2}{3}}$ = 1·14

Variation in Schmidt Number from 17°c to 23°c is approximately 0·65%

(6) Reynolds Number (Re):-

$$(Re) = \frac{\rho u\, d_t}{\mu}$$

where d_t = tube diameter (0·375").

$$(Re) = \frac{F}{A} \cdot \frac{\rho d_t}{\mu}$$

At 20°c and 760 mms. Hg.:- μ = 0·01797 c.p., ρ = 1·2046 gms/litre.

$\therefore$ $(Re) = \frac{F}{A} \cdot 106{\cdot}6$

Variation of Reynolds Number from 17°c to 23°c is approximately 4%.

APPENDIX 4.

MERCURISATION OF RODS AND GAUZES.

Previous workers (2, 4, 37) had experimented with various ways of obtaining a mercury surface, and Williams (2) had shown that electroplating of the surface with a mercury salt solution produced a better result than amalgaming of the surface. Maugham (37) had shown that a better plating solution was obtained by using a complex ion solution. Haggart (6) had shown that it was possible to obtain constant mercury transfer rates of up to an hour, with nitrogen as the carrier gas, using a freshly flooded mercury surface and he had also investigated the possibility of renewing the mercury surface in situ. (The further development of this technique is described in Chapter III B of the present work.)

The previous methods of obtaining a mercury surface were experimentally assessed, and further work was carried out to optimize the process.

The final method adopted for plating was as follows:-

(a) For plating rods (see also Chapter III C (ii))

(i) Buff the rod in a lathe with Brasso or Bluebell metal polish.

(ii) Immerse in hot Teepol solution, and water rinse.

(iii) Wash in $\frac{N}{4}$ caustic soda solution, and water rinse.

(iv) Wash in 4N sulphuric acid, and water rinse.

(v) Plate at 10-15 amps/ft^2, i.e. 0·4 amps for the rods used in the present work, at 2 volts for one minute, and water rinse. The plating bath is described in Chapter III A (v), and

the plating solution composition is given on page 182.

(vi) Ethanol wash.

(vii) Store under mercury for long periods, or under ethanol for short periods.

Before use the rods must be flushed with clean mercury (Analar grade was used in the present work) to remove surface films. This operation is best carried out using a hypodermic syringe. Extreme cleanliness was found to be essential and the rods were always handled by using crucible tongs with P.V. C. sleeved ends.

New copper rods needed the above plating process repeated at least five times to establish a well bonded surface, before they were used for transfer experiments.

(b) For plating gauzes.

The same system was used for plating gauzes as for plating rods, but as it was not practicable to produce a current density of 10-15 amps/ft.^{2} (140 amps per roll of gauze in this case), the maximum current available from a 5 amp battery charger was used and the plating process continued for an hour.

Before use, clean mercury was allowed to trickle over the rolls of gauze in the saturator column. When not in use the saturator was isolated full of nitrogen to prevent deterioration of the gauzes. It was found that if the gauzes' surfaces deteriorated immersion in 10% nitric acid would restore a bright surface that would "wet" with mercury.

For the gauzes the washing operations were carried out using a pipette cleaner, and the plating path consisted of a length of mild

steel pipe with a plate welded on one end.

(c) The Plating Solution.

The solution composition, which is the subject of a Patent (47), is as follows:-

Mercuric Chloride	1½ ozs.
Sodium Cyanide	4 ozs.
Ammonium Chloride	2 ozs.
Water	1 gallon.

It was found that storing of the solution in brown glass bottles was desirable. After a short time (2 - 3 days) the colourless solution turns brown, which indicates that the solution is spent. As spent solution causes pitting, it is preferable to make up small quantities of the solution as required.

APPENDIX 5.

(1) The Absorptiometer.

A circuit diagram of the absorptiometer is given in Fig.5:1(p.185).

The absorptiometer used in this work was a prototype of the HANOVIA Mercury Vapour Detector (purchased in 1954) which was designed to measure the mercury vapour content of a gas stream by utilising the absorption of ultraviolet light by mercury vapour. A 2 watt low pressure Hanovia mercury resonance tube (type 775/63) provided the source of U.V. radiation and was operated from the A.C. mains supply via a 10 milliamp step up transformer. The wavelength of the U.V. radiation was 2537 Å. To reduce draughts, and allow a temperature equilibrium with the ambient temperature to be achieved, the U.V. tube was housed in a metal container.

{As explained in Chapter III A (vii) the U.V. discharge tube was extremely sensitive to voltage fluctuations and temperature changes. To combat these effects, a constant voltage transformer and a variac were incorporated in the A.C. supply, and the case of the instrument was made into a constant temperature enclosure}.

A photocell (CINTEL QVA 39.S) was used to measure the output of U.V. light from the discharge tube. The photocell and the discharge tube were mounted 10" apart at opposite ends of a cylindrical chamber which had quartz glass windows as endpieces.

Gas was passed through the chamber and checked for mercury vapour present by comparison with the light absorption reading for mercury free gas.

The circuit (Fig. 5 : 1) was basically a bridge fitted with a microammeter to indicate its state of balance. The power to the bridge was supplied via a half wave rectifier with capacitance - resistance - capacitance smoothing.

The same source supplied the photocell via resistance R3 and the current in the photocell developed a voltage across resistors R1 and R2. This voltage was applied to the grid G2 of the valve (6N7), and since it could be varied by resistors R1 and R2 it could be used to balance the bridge. The other grid G1 of the valve was held at a fixed potential by the divider circuit R4 and R5. Thus changes in the photocell current caused by the absorption of mercury vapour into the gas stream produced changes in the balance of the bridge. Resistor R6 controlled the sensitivity of this circuit.

The circuit was set up by adjusting R1 (ADJUST FULL LIGHT) and R2 (BALANCE) to produce zero deflection of the microammeter, when mercury free gas was passed through the absorptiometer chamber. Switches S_1 (CALIBRATE) and S_2 (to simulate increasing the range of the microammeter from 50 μA to 100 μA) were then closed to produce the effect of 100% absorption of the U.V. light, and the microammeter was adjusted to give full scale deflection using resistor R6 (SENSITIVITY).

(2) Calibration of the Absorptiometer (See Fig.5:1).

The calibration of the absorptiometer was carried out by passing mercury/air streams of known concentration through the absorptiometer and noting the corresponding microammeter reading.

The method used was that of Maxwell (4), and entailed passing an air stream through a saturator consisting of a perspex tube of

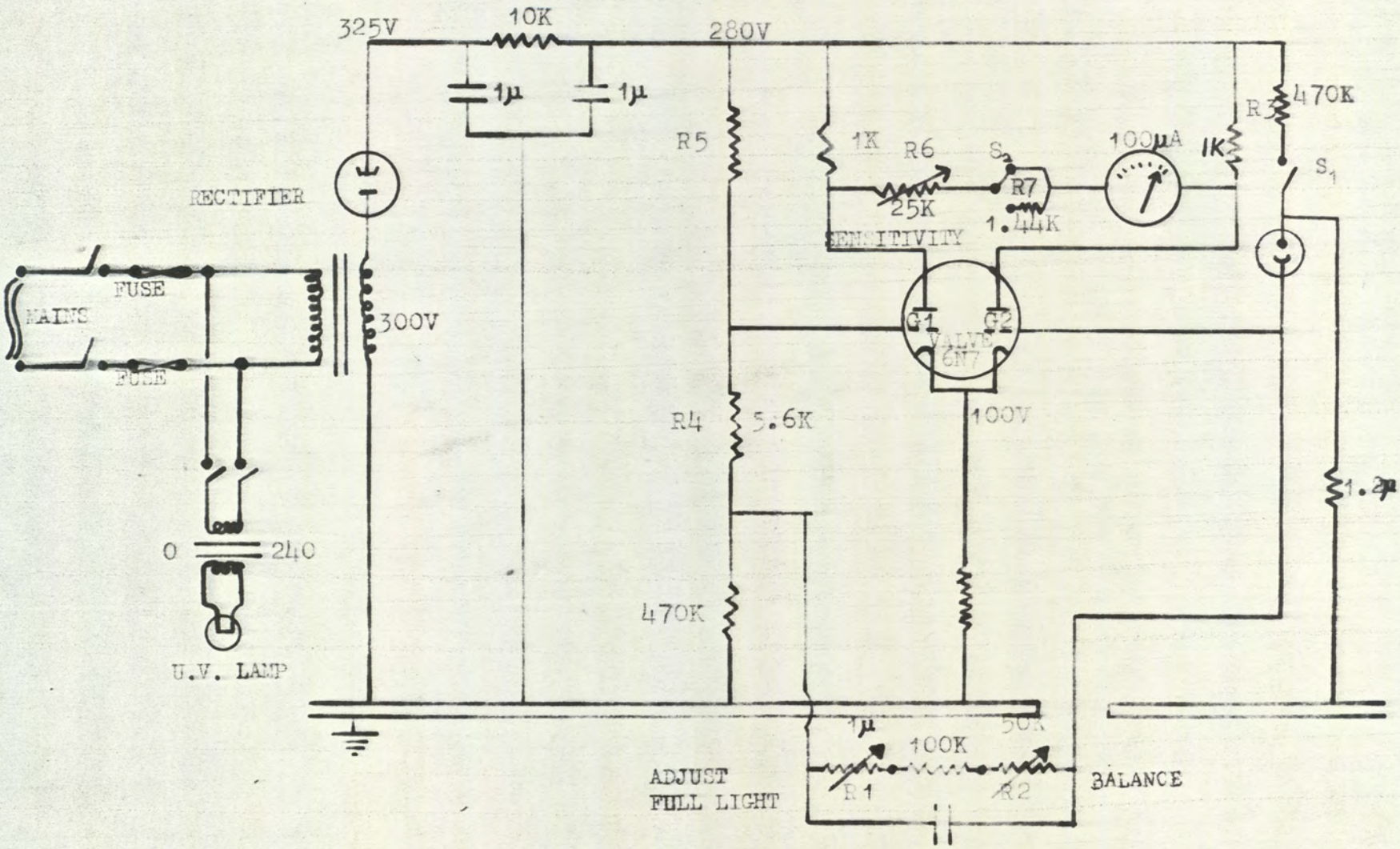

FIG. 5.1 - ABSORPTIOMETER CIRCUIT DIAGRAM

$3\frac{1}{4}$" inside diameter and 30" long which had rolls of mercurized 16 mesh gauze, tightly wound on a 1" diameter perspex rod, inside it. From the vapour pressure of mercury corresponding to the saturator outlet temperature the concentration of mercury in the air stream was calculated (See Appendix 2(1))

Before starting a calibration run the gauzes were mercurized as described in Appendix 4, and after assembly into the saturator clean mercury was allowed to trickle over the gauzes so that they were completely "wetted."

Air was fed via rotameters R4 and R6, and valves V2, V4 and V6 into the absorptiometer and the zero and full scale deflections of the microammeter were set as described in Appendix 5 (1).

Valves V1 and V14 were closed and valve V9 was opened. Valve V10 was then slowly opened to allow air to pass through the saturator, an air flow rate of 0•2 - 1•0 litres/min being used. From the saturator the air/mercury stream passed through rotameter R3 and valve V3 into the absorptiometer, with or without dilution. Dilution of the air/mercury stream was achieved by passing air through rotameters R4 and/or R5, and valves V4 and/or V5, and the two streams then mixed in a Raschig ring filled glass mixer (See Chapter III A).
15 litres/min of this stream was fed to the absorptiometer via rotameter R6 and valve V6, the excess passing to the laboratory extraction system through valve V7.

When conditions were steady the following readings were noted:-

(a) Water level of manometer M3 ($\leq$ 1 cm. of water).

(b) Mercury manometers M_1 and M_2 to allow the flows indicated by the rotameters to be corrected to free volumes.

(c) Rotameters R4, R5 and R7.

(d) Thermocouple emf at the saturator outlet and absorptiometer inlet.

(e) Microammeter reading.

(f) Temperature of the absorptiometer constant temperature enclosure (controlled at $32^{o}c \pm 1^{o}c$).

The above procedure was repeated for different concentrations of mercury vapour in the airstream, obtained by diluting the saturated mercury/airstream, to calibrate the microammeter from 0 - 50 μA.

The results were discarded if a zero shift of the microammeter occurred during a run.

The calibration procedure was followed using one, two, and three rolls of mercurized gauze (each 6" long) in the saturator. No difference in the calibration curve was obtained by using more than one roll of gauze thus demonstrating that the airstream leaving the saturator was saturated with mercury vapour.

Recalibration was carried out every two months, but no change in the calibration curve was found. The calibration curve is presented in Appendix 1 (3) see page 169.

When not in use the saturator column was purged with nitrogen and then isolated full of nitrogen to prevent deterioration of the mercurized gauzes over the period of time between calibration runs.

APPENDIX 6.

The following tables show the values of j_D versus Re_M for the experimental runs carried out in the present work, and a specimen result sheet for an experimental run.

Table 6 : 1 Tubes 58, 64 Old transfer probe drainage system .

$j_{DM} \times 10^3$	Re_M
19.1	68.5
14.25	370
12.8	615
11.85	1100
10.85	1350
10.28	2040
9.67	2950
8.15	3950
7.63	4800
6.48	6150
6.48	6800

Table 6 : 2 Decay Curve for Tube 64. $Re_M = 1122$

Time minutes	Microammeter reading (μA)
0	17.0
1	17.0
2	17.0
3	16.75
4	16.5

Time minutes	Microammeter reading (μA)
5	16.75
6	16.75
7	16.5
8	16.25
9	16.0
10	16.0
11	16.0
12	16.0
13	16.0
14	16.0
15	16.0
16	16.0
17	16.0
18	16.0
19	16.0
20	15.75
25	15.75
30	15.5
35	15.5
40	15.5
45	15.5
50	15.5
55	15.25
60	15.0
65	15.0
70	17.0 REFLUSHED

Table 6 : 2 (Continued)

These results were then repeated twice more and the figures obtained were substantially the same.

After an overnight stand the microammeter reading had fallen to 2.1 but after reflushing the reading returned to 17.0.

Table 6:3 Tube No.64 (New transfer probe drainage system).

$j_{DM} \times 10^3$	Re_M
30.75	55.2
27.0	124
24.4	207
19.5	317
16.0	648
14.5	1105
13.75	1990
13.75	2860
17.75	3780
16.0	6150

Table 6:4 Tube No.64 Extra baffles.

$j_{DM} \times 10^3$	Re_M
31.8	69.5
26.6	126
23.1	210
20.9	328
18.5	477
16.6	762
15.2	1130
14.4	2140
12.75	2980
14.5	4760
12.83	7100

Table 6:5

Tube No.58	
$j_{DM} \times 10^3$	Re_M
26•9	70
22•4	127
20•1	211
17•9	330
15•8	479
14•2	732
12•6	1450
10•7	2140
11•2	3100
8•92	4970
9•85	7360

Table 6:6

Tube No.17	
$j_{DM} \times 10^3$	Re_M
31•3	69.8
26•3	126
21•8	211
18•9	331
17•5	492
15•9	747
13•5	1045
11•6	2150
10•3	3400
7•65	4940
10•7	7560

Table 6:7

Tube No. 23	
$j_{DM} \times 10^3$	Re_M
32.1	69.9
26.0	126
23.1	211
20.3	331
19.2	494
17.0	775
15.1	1180
12.4	2110
11.4	2940
8.7	4720
11.4	7550

Table 6: 8

Tube No.80	
$j_{DM} \times 10^3$	Re_M
21.3	69.8
17.6	127
15.1	211
11.7	331
10.9	497
9.11	790
8.27	1150
7.85	2150
6.57	2920
4.66	5000
4.24	7180

Table 6:9 Decay curve for droplets. $Re_M = 100$

Time (minutes)	Microammeter reading (μA)
0	3·5
$\frac{1}{2}$	3·0
1	2·25
$1\frac{1}{2}$	2·0
2	1·25
$2\frac{1}{2}$	0·75
3	0·75
$3\frac{1}{2}$	0·5
4	0·3
$4\frac{1}{2}$	0·25
5	$< 0·1$

Table 6:10 Decay curve for droplets. $Re_M = 1105$

Time (minutes)	Microammeter reading(μA)
0	2·5
$\frac{1}{2}$	2·0
1	1·25
$1\frac{1}{2}$	0·5
2	0·5
$2\frac{1}{2}$	0·25
3	0·1
$3\frac{1}{2}$	$< 0·1$
4	$> 0·1$

Table 6:11 Decay curve for droplets. $Re_M = 6150$

Time (Minutes	Microammeter reading (μA)
0	2·1
$\frac{1}{2}$	1·5
1	0·8
$1\frac{1}{2}$	0·4
2	0·1
$2\frac{1}{2}$	< 0·1
3	< 0·1

Table 6:12 Specimen Result Sheet. 30/6/67.

Cut down 31% Tube No. 80

Room temp. 21.5°C Barometric pressure Meter temp. 32°C

75.9 cms H_g

R_1 or R_2	M_1	R_6	M_4	TC2	TC3	TC4
1•9	2•0	19•3	1•1	1012	990	986
4•0	2•8	19•3	1•1	1012	990	986
6•0	2•9	19•3	1•1	1012	990	998
8•1	3•8	19•3	1•1	1012	990	998
10•3	4•0	19•3	1•1	1012	990	998
13•4	5•3	19•3	1•1	1012	990	1003
16•4	5•0	19•3	1•1	1012	990	1003
22•0	5•0	19•3	1•1	968	986	1003
26•0	7•0	19•3	1•1	968	986	1003
20•7	21•0	19•3	1•1	968	986	1003
24	26•0	19•3	1•1	968	986	1003

Table 6:12 (Cont) Specimen Result Sheet (Cont)

R_1 or R_2	F {free vols L/min.}	Probe temp. °C	μ^A	c_e	c_{SR}	$j_{DM} \times 10^3$	Re_M
25	25•3	22•6	25	490	17300	21•3	69•8
45	45•8	22•6	21•5	405	17300	17•6	127
75	76•4	22•8	19•5	355	17600	15•1	211
117	120	22•8	16•0	275	17600	11•7	331
175	180	22•8	15•0	255	17600	10•9	497
275	286	22•9	13•0	215	17700	9•11	790
400	415	22•9	12•0	195	17700	8•27	1150
710	735	22•9	11•5	185	17700	7•85	2150
1010	1060	22•9	10•0	155	17700	6•57	2920
1600	1810	22•9	7•5	110	17700	4•66	5000
2250	2600	22•9	7•0	100	17700	4•24	7180

APPENDIX 7.

The table below gives the major dimensions of the model exchangers used in the work of Bergelin et al.(1) and Williams (2) and the present work. The working drawings for the exchanger of Bergelin et al. were not available to Williams but were available to the Author of the present work. As can be seen the differences between the exchangers were very slight.

Dimension	Present Work	Williams (2)	Bergelin et al.(1)	Comments
Minimum clearance available for flow at restrictions in centre row of tubes.	1·55"	1·55"	1·55"	
Baffle cut downs (% of shell diameter).	18·4 31·0 43·7	18·4 31·0 43·7	18·4 31·0 43·7	Bergelin et al. only studied the 43·7 cut downs at this baffle spacing.
Baffle spacing	3·86"	3·89"	3·72"	Williams' exchanger was slightly longer between the end plates, ($16\frac{1}{8}$" not 16") as he did not have a diagram of Bergelin et al.'s exchanger. Bergelin et al. used false

Cont ...

				plastic tube sheets to obtain positioning of pressure tape.
Cross flow area (ft^2)	0.04152	0.04185	0.0398	Williams baffle spacing was fractionally longer than that used in the present work. Bergelin et al. inserted plastic tube sheets.
Window areas (ft^2)				
Baffle cut-down 18.4%	0.01303	0.01303	0.0124	Bergelin used $\frac{3}{16}$" spacer rods not $\frac{1}{8}$" as in the other cases.
Baffle cut-down 31.0%	0.02455	0.02455	0.0239	
Baffle cut-down 43.7%	0.03800	0.03800	0.0365	
Total Heat Transfer Surface (ft^2)				Bergelin only studied the 43.7% case, and the difference was due to 2 dummy tubes and $\frac{1}{8}$" baffles. Williams exchanger was slightly longer than the others.
Baffle cut-down 18.4%	10.13	10.21		
Baffle cut-down 31.0%	10.19	10.27		
Baffle cut-down 43.7%	10.15	10.23	9.59	
Heat transfer surface in the window zone (ft^2)				
Baffle cut-down 18.4%	1.454	1.465		As above.
Baffle cut-down 31.0%	3.781	3.81		
Baffle cut-down 43.7%	6.311	6.36	5.93	

APPENDIX 8

Analysis of the individual tube results of T.A. Williams (2).

Tubes are numbered from 01 to 80 (see Fig. 4 page 36).

For mirror image positions both the numbers are given.

Slopes and constants of the regression line $j_{DM} = cRe_M^{-n}$

Table 8:1 18.4% Baffle Cut Down.

Tube Number	Slope (n)	Constant (c) x 10^3
01	0.3454	311.2
0205	0.4533	734.8
0304	0.4380	671.9
0610	0.4517	661.3
0709	0.4337	631.5
08	0.4534	665.8
1116	0.4828	649.9
1215	0.4531	610.1
1314	0.4265	537.3
1723	0.5579	830.4
1822	0.4204	424.1
1921	0.4340	518.0
20	0.4536	616.8
2429	0.4700	542.1
2528	0.4260	435.8
2627	0.4328	518.9
3036	0.4734	599.8
3135	0.4147	402.7

Tube Number	Slope (n)	Constant (c) x 10^3
3234	0•3942	348•1
33	0•4354	488•1
3744	0•5163	888•9
3843	0•4767	562•2
3942	0•4583	536•0
4041	0•4303	456•1
4551	0•5431	721•4
4650	0•4638	534•8
4749	0•4290	448•9
48	0•4752	569•3
5257	0•5177	657•9
5356	0•4571	558•8
5455	0•4255	417•1
5864	0•5060	677•9
5963	0•4810	536•2
6062	0•4695	539•5
61	0•4652	600•0
6570	0•5016	640•1
6669	0•4417	427•9
6768	0•4369	481•4
7175	0•4871	565•4
7274	0•4868	648•0
73	0•4826	605•9
7679	0•5165	704•5
7778	0•4890	583•5
80	0•4219	367•4

Table 8:2 31% Baffle Cut Down.

Tube Number	Slope (n)	Constant (c) x 10^3
01	0•3920	241•3
0205	0•5077	649•8
0304	0•4682	481•5
0610	0•4860	629•4
0709	0•4919	664•4
08	0•4630	560•3
1116	0•4735	670•8
1215	0•4798	667•6
1314	0•4793	643•3
1723	0•5006	713•4
1822	0•5009	740•3
1921	0•4823	661•0
20	0•4500	535•7
2429	0•5054	701•1
2528	0•5056	681•3
2627	0•4151	443•0
3036	0•5591	857•0
3135	0•4631	559•8
3234	0•4960	608•1
33	0•4411	495•6
3744	0•5811	1092
3843	0•4608	548•4
3942	0•4525	538•2

Tube Number	Slope (n)	Constant (c) x 10^3
4041	0•4238	457•8
4551	0•5896	910•8
4650	0•5009	675•4
4749	0•4385	479•2
48	0•4631	584•0
5257	0•4846	626•6
5356	0•4824	605•1
5455	0•4781	603•4
5864	0•5533	928•4
5963	0•5079	648•8
6062	0•4948	658•9
61	0•4728	594•8
6570	0•5205	737•3
6669	0•4576	493•0
6768	0•4569	518•4
7175	0•4325	314•8
7274	0•4585	430•9
73	0•4855	508•3
7679	0•5058	552•8
7778	0•4678	385•6
80	0•3427	148•4

Table 8:3 43.7% Baffle Cut Down.

Tube Number	Slope (n)	Constant (c) x 10^3
01	0.3594	161.2
0 205	0.5053	509.6
0304	0.4488	342.1
0610	0.4879	518.9
0709	0.4924	505.2
08	0.4780	428.9
1116	0.4755	524.0
1215	0.4682	479.9
1314	0.4262	342.3
1723	0.4877	631.8
1822	0.4532	517.0
1921	0.4642	517.8
20	0.4682	558.2
2429	0.4575	587.2
2528	0.4771	629.3
2627	0.4561	555.8
3036	0.4997	770.3
3135	0.4646	559.2
3234	0.4486	505.4
33	0.4784	613.6
3744	0.5569	1110
3843	0.5166	706.1
3942	0.4431	497.6

Tube Number	Slope (n)	Constant (c) x 10^3
4041	0•4139	382•2
4551	0•4913	680•7
4650	0•4500	521•6
4749	0•4396	492•1
48	0•4317	463•8
5257	0•4637	534•9
5356	0•4569	505•0
5455	0•4148	374•0
5864	0•5333	703•5
5963	0•4373	380•7
6062	0•4376	393•1
61	0•4209	367•2
6570	0•5025	462•4
6669	0•4358	316•1
6768	0•4224	286•0
7175	0•5037	416•8
7274	0•4708	342•2
73	0•4621	319•7
7679	0•5360	492•9
7778	0•4587	253•3
80	0•3679	128•5

TUBE GROUPINGS.

The results of the "t" and "F" tests, with the resultant tube groups, are presented next. Details of the statistical methods employed, and the computer programmes which were developed to carry out these methods are described in Appendix 9.

Comparison of the Bundle Average results obtained by Bergelin et al. (1) with the individual tube results obtained by Williams (2) for the 43·7% baffle cut down case.

Table 8:4.

Tube No.	Slope test			Constant test		
	t	degrees of freedom	significance	t	degrees of freedom	significance
3843	1·917	20	0·95	1·66	21	0·90

Final tube groups resulting from the statistical analysis of the individual tube results of T.A. Williams.

A. Grouping by slope.

In this case a level of significance of less than 0·90 was taken to indicate that the slope of two or more tubes was identical. The special cases for the 31% baffle cut down, whose 3 groups are considered identical, although their levels of significance are 0·90, are covered in the main text of the present work (see Chapter V page 109).

18·4% baffle cut down.

Table 8:5. First Group.

0610 0709 08 7175 7274 73	Average slope of group = 0·466			
	degrees of freedom f_1	degrees of freedom f_2	F	significance
Slope	5	60	1·89	< 0·90

Table 8:6. Second Group.

1723 3744 4551 5257 5864 6570	Average slope of group = 0·524			
	degrees of freedom f_1	degrees of freedom f_2	F	significance
Slope	5	60	1·46	< 0·90

Table 8:7. Third Group.

1215	
1314	
1822	
1921	
20	
2528	Average slope of group = 0.431
2627	
3135	
3234	
33	
3942	
4041	
4749	
5455	

	degrees of freedom f_1	degrees of freedom f_2	F	significance
Slope	13	140	1.23	< 90

Table 8:8. Fourth Group.

1116	
2429	
3036	
3843	
4650	
48	Average slope of grpup = 0•466
5356	
5963	
6062	
61	
6669	
6768	

	degrees of freedom f_1	degrees of freedom f_2	F	significance
Slope	11	120	1•10	< 90

31% baffle cut down.

Table 8:9. First Group.

0205	5864	
0304	5963	
0610	6062	
0709	61	Average slope of group= 0•483
08	6570	
1116	6669	
1215	6768	
1314	7175	
1723	7274	
1822	73	
1921	7679	
20	7778	

	degrees of freedom f_1	degrees of freedom f_2	F	significance
Slope	23	240	1•53	0•90

Table 8:10. Second Group.

	3036 3744 4551	Average slope of group = 0•577		
	degrees of freedom f_1	degrees of freedom f_2	F	significance
Slope	2	30	0•539	$< 0•90$

Table 8:11. Third Group.

	3135 33 3843 3942 4749 48 5257 5356 5455	Average slope of group = 0•463		
	degrees of freedom f_1	degrees of freedom$_2$	F	significance
Slope	8	90	1•61	$< 0•90$

Tube 4650 was included with this group, as outlined in the text (see page 137) because it was part of the identical group (see Table 8:25). With it included the significance became 0•95, and the average slope of the group = 0•467.

Table 8:12. Fourth Group.

2429 2528 3234	Average slope of group = 0.502			
	degrees of freedom f_1	degrees of freedom f_2	F	significance
Slope	2	30	0.065	< 0.90

Table 8:13. Fifth Group.

2627 4041	Average slope of group = 0.419		
	degrees of freedom	t	significance
Slope	20	1.53	0.90

43·7% baffle cut down.

Table 8:14. First Group.

1314 6768	Average slope of group = 0·424		
	degrees of freedom	t	significance
Slope	20	0·557	< 0·75

Table 8:15. Second Group.

3036 4551	Average slope of group = 0·496		
	degrees of freedom	t	significance
Slope	20	1·16	< 0·90

Table 8:16. Third Group.

0304 0709 08 7274 73 7778	Average slope of group = 0·469			
	degrees of freedom f_1	degrees of freedom. f_2	F	significance
Slope	5	60	0,852	< 0·90

Table 8:17. Fourth Group.

1822
1921
2429
2528
3135
3234
33
4650
4749
48
5257
5356
5963
6062

Average slope of group = 0•454

	degrees of freedom f_1	degrees of freedom f_2	F	significance
Slope	13	140	1•59	<90

B. Grouping by slopes and constants.

The following tables are the final groups of tubes of identical transfer characteristics, i.e. identical slopes and constants. N.B. All constants given in the following tables are $\times 10^3$.

18·4% baffle cut down.

Table 8:18. First group.

1921	Average slope of group = 0·433
2627	Average constant of group = 518·5

	degrees of freedom	t	significance
Slope	20	0·186	<0.75
Constant	21	1·05	0·75

Table 8:19. Second Group.

1822 2528 3135 3234 4041 4749 5455	Average slope of group = 0•420 Average constant of group = 419			
	degrees of freedom f_1	degrees of freedom f_2	F	significance
Slope	6	70	0•715	< 0•90
Constant	6	76	2•08	0•90

Table 8:20. Third Group.

3843 3942 4650	Average slope of group = 0•466 Average constant of group = 544			
	degrees of freedom f_1	degrees of freedom f_2	F	significance
Slope	2	30	0•299	< 0•90
Constant	2	32	2•42	< 0•90

31% baffle cut down.

Table 8:21. First Group.

	2627	Average slope of group	= 0.419
	4041	Average constant of group	= 450
	degrees of freedom	t	significance
Slope	20	1.53	0.90
Constant	21	2.46	0.975

N.B. While the constant in this case is significant at the 0.975 level, indicating a borderline relationship, the slope is not borderline and hence doubts about the similarity of the two tubes are removed.

Table 8:22. Second Group.

	2429				
	2528	Average slope of group			= 0.502
	3234	Average constant of group			= 663
	degrees of freedom f_1	degrees of freedom f_2	F	significance	
Slope	2	30	0.0649	$<<$ 0.90	
Constant	2	32	3.42	0.95	

Table 8:23. Third Group.

	7175 7274 7778	Average slope of group = 0•453 Average constant of group = 377		
	degrees of freedom f_1	degrees of freedom f_2	F	significance
Slope	2	30	0•133	< 0•90
Constant	2	32	2•44	< 0•90

Table 8:24. Fourth Group.

	1215 1314 1723 1822 1921	Average slope of group = 0•488 Average constant of group = 685		
	degrees of freedom f_1	degrees of freedom f_2	F	significance
Slope	4	50	1•21	< 0•90
Constant	4	54	2•73	0•95

Table 8:25. Fifth Group.

08
20
3135
33 Average slope of group = 0•468
3843 Average constant of group = 576
3942
4650
4749
48
5257
5356
5455
6062
61

	degrees of freedom f_1	degrees of freedom f_2	F	significance
Slope	13	140	1•57	0•90
Constant	13	153	1•64	0•90

43·7% baffle cut down.

Table 8:26. First Group.

7274	Average slope of group	= 0·466
73	Average constant of group	= 330

	degrees of freedom	t	significance
Slope	20	1·07	0·75
Constant	21	1·69	0·90

Table 8:27. Second Group.

2528		
2627		
3135	Average slope of group	= 0·454
3234	Average constant of group	= 538
33		
3942		
4650		
4749		
48		

	degrees of freedom f_1	degrees of degrees f_2	F	significance
Slope	8	90	1·58	< 0·90
Constant	8	98	1·41	< 0·90

APPENDIX 9.

THE STATISTICAL TECHNIQUES, AND THE COMPUTER PROGRAMMES WHICH CARRIED THEM OUT, USED IN THE ANALYSIS DESCRIBED IN CHAPTER V OF THE PRESENT WORK.

The data were available in the form j_D versus Re_M.

As discussed in Chapter V the relationship between j_D and Re_M is not strictly linear, but to further the analysis it was linearised:-

$$\log j_{DM} = \log c - n \log Re_M$$

(a). The regression lines of the data were determined as follows:- (See Brownlee (38) pages 335 - 337).

The regression equation is $Y = a + b(x - \bar{x})$ (1)

where $\bar{x} = \frac{\sum x}{N}$ N being the number of observations.

The method of least mean squares involves calculating those values of a and b which minimize the run of squares of deviation R between the observed values y_i and the predictions Y_i given by inserting the values of x_i in equation (1).

Thus $$R = \sum\left(y_i - Y_i\right)^2 = \sum\left(y_i - a - b\ x_i - \bar{x}\right)^2$$

The values of a and b which minimize R are given by

$$\frac{\partial R}{\partial a} = -2 \sum\left(y_i - a - b\left(x_i - \bar{x}\right)\right) = 0 \qquad (2)$$

$$\frac{\partial R}{\partial b} = -2 \sum\left(y_i - a - b\left(x_i - \bar{x}\right)\right)\left(x_i - \bar{x}\right) = 0 \qquad (3)$$

These equations can be rewritten as:-

$$\sum\left(y_i - Y_i\right) = 0 \qquad \sum\left(y_i - Y_i\right)\left(x_i - \bar{x}\right) = 0$$

Rearranging equations 2 and 3 gives

$$ka + b \sum\left(x_i - \bar{x}\right) = \sum y_i$$

$$a \sum\left(x_i - \bar{x}\right) + b \sum\left(x_i - \bar{x}\right)^2 = \sum\left(x_i - \bar{x}\right) y_i$$

Since $\sum\left(x_i - \bar{x}\right) = 0$

then $$a = \frac{\sum y_i}{N} = \bar{y}$$

$$b = \frac{\sum\left(x_i - \bar{x}\right) y_i}{\sum\left(x_i - \bar{x}\right)^2}$$

The expression for b may be rewritten as:-

$$b = \frac{\sum x \sum y - \frac{\sum x \sum y}{N}}{\sum x^2 - \frac{\left(\sum x\right)^2}{N}}$$

and this form was chosen for ease of computing.

The slope of the regression line (n) = -b

The constant of the regression line (c) = $e^{(a - b\bar{x})}$

This part of the analysis was performed by computer programme 9:1 (described later in this section) which also carried out various other summations to use as input data in the "t" and "F" tests.

<u>The t test for the comparison of the slopes of two regression lines.</u>

Only the general guide lines will be given for this test and the

full details will be found in Brownlee (pages 338 - 351).

Suppose that we have two sets of observations;

$$\left(x_{1v}, y_{1v}\right), \; i = 1, 2, \; v = 1, \cdots, N_i$$

$$\left(x_{11}, y_{11}\right), \quad \left(x_{12}, y_{12}\right), \; \cdots, \quad \left(x_{1N_1}, y_{1N_1}\right)$$

and $$\left(x_{21}, y_{21}\right), \quad \left(x_{22}, y_{22}\right), \; \cdots, \quad \left(x_{2N_2}, y_{2N_2}\right)$$

Then the problem is to determine whether a common regression line is an adequate fit, or whether separate regression lines

$$Y_1 = a_1 + b_1 \left(x - \bar{x}_1\right)$$

$$Y_2 = a_2 + b_2 \left(x - \bar{x}_2\right)$$

are necessary.

The null hypothesis assumes that the two lines are the same unless proved otherwise.

For this we obtain a value of "t" from:-

$$\frac{b_1 - b_2}{S\left\{\left[\sum_{v}^{N_1}\left(x_{1v} - \bar{x}_1\right)^2\right]^{-1} + \left[\sum_{v}^{N_2}\left(x_{2v} - \bar{x}_2\right)^2\right]^{-1}\right\}^{\frac{1}{2}}} \sim t\left(N_1 + N_2 - 4\right).$$

The purpose of the test is to determine how significant is the difference $b_1 - b_2$.

This gives a value of t k for $\left(N_1 + N_2 - 4\right)$ degrees of freedom $\left(f_1\right)$. By comparing this value of t with the value given in the "Fractional points of t Distribution" (Brownlee page 560) we find the significance of the calculated t. If the cabulated t is

significant at our chosen significance level then the null hypothesis is rejected and the lines differ in slope. (If on the other hand the null hypothesis is accepted then the slope of the common regression line may be found for the true equations of the two parallel lines

$$\eta_1 = \alpha_1 + \beta\left(x - \bar{x}_1\right) \qquad \eta_2 = \alpha_2 + \beta\left(x - \bar{x}_2\right)$$

the common slope b is given by

$$b = \left(\frac{\sum_v^{N_1} y_{1v}\left(x_{1v} - \bar{x}_1\right) + \sum_v^{N_2} y_{2v}\left(x_{2v} - \bar{x}_2\right)}{\sum_v^{N_1}\left(x_{1v} - \bar{x}_1\right)^2 + \sum_v^{N_2}\left(x_{2v} - \bar{x}_2\right)^2} \right)$$

If the null hypothesis were accepted then we next test to determine if the two parallel lines are identical i.e. lie on top of each other.

<u>The t test for comparison of the constants of two regression lines (Brownlee page 351).</u>

If the two lines

$$\eta_1 = \alpha_1 + \beta\left(x - \bar{x}_1\right), \qquad \eta_2 = \alpha_2 + \beta\left(x - \bar{x}_2\right)$$

are identical then $\eta_1 = \eta_2$ and hence

$$\alpha_1 - \beta\bar{x}_1 = \alpha_2 - \beta\bar{x}_2$$

$$\text{and } \left(\alpha_1 - \alpha_2\right) - \beta\left(\bar{x}_1 - \bar{x}_2\right) = 0$$

and so the relevant t value is obtained from

$$\frac{\left(a_1 - a_2\right) - b\left(\bar{x}_1 - \bar{x}_2\right)}{S\left[\frac{1}{N_1} + \frac{1}{N_2} + \left(\bar{x}_1 - \bar{x}_2\right)^2 \Big/ \sum_i^2 \sum_v^{N_i}\left(x_{iv} - \bar{x}_i\right)^2\right]^{\frac{1}{2}}} \sim t\left(N_1 + N_2 - 3\right)$$

This gives a value for t at $\left(N_1 + N_2 - 3\right)$ degrees of freedom $\left(f_2\right)$.

By comparison of the t value with the table of t values the significance of the calculated t is obtained and depending on the level of significance the null hypothesis may be accepted or rejected.

The F test for the comparison of the slopes and constants of families of regression lines.

When we wish to test whether a family of more than two lines may be represented by a common regression line then the F test is used.

The F test is similar in character to the t test but more complex and is described in Brownlee pages 376 - 390.

Assuming k groups of observations (x_{iv}, y_{iv}) , i - 1, ---, k, v = 1, ---, N_i. A separate line can be fitted to each group, $Y = \bar{y}_i + b_i \left(x - \bar{x}_i\right)$ and a sum of squares for variation about each line S_{i1}^2 will be obtained.

If the null hypothesis is accepted then

$$S_1^2 = \frac{\sum_i^k \left(N_i - 2\right) S_{i1}^2}{\sum_i^k \left(N_i - 2\right)}$$

We obtain k individual lines of slope b_i

k parallel lines of average slope $\bar{b}$

the least squares line for the group of slope $\hat{b}$

and the overall regression line of slope b

Then the test may be conveniently summed up in the following table.

Source of variance	degrees of freedom	Mean squares
Between $\hat{b}$ and $\bar{b}$	1	S_4^2
Deviation of the group means about their regression line	$k - 2$	S_3^2
Between the individual slopes b_i	$k - 1$	S_2^2
About the individual line	$\sum_i^k N_i - 2k$	S_1^2

For the present work the requirement was that a single line, the overall regression line, should be an adquate fit to all groups.

To determine this:-

for slope, $F = \frac{S_2^2}{S_1^2}$ at $f_{S1} = (k - 1)$, $f_{S2} = \left(\sum_i^k N_i - 2k\right)$ } degrees of freedom.

If from this the slopes are identical then a more simple form of constant test is obtained by pooling the degrees of freedom of S_4^2 and S_3^2, from which a pooled mean square S_6^2 is obtained. The degrees of freedom of S_2^2 and S_1^2 are then pooled and the error sum of squares S_5^2 is obtained. (Brownlee pages 388 - 390).

Then for the constant, $F = \frac{S_6^2}{S_5^2}$ at $f_{c1} = (k - 1)$, $f_{c2} = \left(\sum_i^k N_i - k - 1\right)$ } degrees of freedom.

Comparison of the calculated F with the F values given in Brownlee (pages 564-569)allowed the null hypothesis to be accepted or rejected.

The computer programmes.

Four computer programmes were employed:

9:1 Analysis of exchanger data.

9:2 t test programme for slope.

9:3 t test programme for constant.

9:4 F test programme for slopes and constants of families of regression lines.

These four programmes are described in the following pages, and a print out is given for each of them.

9:1 Analysis of exchanger data.

This programme calculated the slopes and constants of the regression lines for each set of data of j_D versus Re_M and typed them out. It also calculated various summations and punched a tape of them to be used as input data for the other programmes.

PROGRAMME 9:1

```
PR'5401   INTERPRETER.
RETAIN 1+
0001 INV        0006 C002-      0011 INV        0016 C007-
0002 C000-      0007 C003-      0012 000D+      0017 000S+
0003 INV        0008 C004-      0013 000C+      0018 S000-
0004 C001-      0009 C005-      0014 000S+      0019 C008-
0005 L001-      0010 C006-      0015 INV        0020 INV
```

PROGRAMME 9:1 Cont ....

```
0021 000D+      0043 A006-      0065 000S+      0087 L011-
0022 000C+      0044 C006-      0066 C014-      0088 S020-
0023 LOG        0045 L008-      0067 L002-      0089 EXP
0024 C009-      0046 S000-      0068 M003-      0090 000C+
0025 A002-      0047 C008-      0069 D007-      0091 L003-
0026 C002-      0048 T/J 050    0070 000S+      0092 M003-
0027 INV        0049 JMP 020    0071 C015-      0093 D007-
0028 000C+      0050 L003-      0072 L004-      0094 C018-
0029 LOG        0051 000S+      0073 S015-      0095 L016-
0030 C010-      0052 D007-      0074 000S+      0096 M016-
0031 A003-      0053 C011-      0075 C016-      0097 D014-
0032 C003-      0054 L002-      0076 000D+      0098 000S+
0033 L009-.     0055 000S+      0077 000D+      0099 C019-
0034 M010-      0056 D007-      0078 JMP 082    0100 L006-
0035 A004-      0057 C012-      0079 JMP 078    0101 S018-
0036 C004-      0058 L002-      0080 JMP 079    0102 000S+
0037 L009-      0059 M002-      0081 JMP 080    0103 S019-
0038 M009-      0060 D007-      0082 D014-      0104 000S+
0039 A005-      0061 000S+      0083 000C+      0105 0001+
0040 C005-      0062 C013-      0084 C017-      0106 JMP 005
0041 L010-      0063 L005-      0085 M012-      0107 END
0042 M010-      0064 S013-      0086 C020-
```

The following inputs are fed in:- 1 at step 1, 0 at step 3, the tube number at step 11, the number of pairs of data at step 15, the first Re_M value at 20 and the first j_D value at 27. After performing various calculations the computer returns to 20 for the next Re_M value and so on until the specified number of values have been fed in. When all these values have been fed in the computer performs more calculations before halting for tape to be run out at step 105 and then returning to step 5 for the next tube number.

The computer performs the following calculations:-

Step	Calculation	Step	Calculation
18	N-1	68	$\Sigma x \Sigma y$
23	$\log Re_M = x$	69	$\Sigma x \Sigma y / N$ **
29	$\log j_D = y$	73	$\Sigma x \Sigma y - \frac{\Sigma x \Sigma y}{N}$ **
34	xy	82	$\frac{\Sigma x \Sigma y - \frac{\Sigma x \Sigma y}{N}}{x^2 - \frac{(\Sigma x)^2}{N}} = n$
38	x^2		
42	y^2		
45	N-1, N - 2, ---		
50	Σy **	85	$b\bar{x}$
52	$\bar{y}$	87	$\bar{y}$
54	Σx **	88	$\bar{y} - b\bar{x}$
56	$\bar{x}$	89	C
59	$(\Sigma x)^2$	91	Σy
60	$(\Sigma x)^2 / N$ **	92	$(\Sigma y)^2$
64	$x^2 - \frac{(\Sigma x^2)}{N}$ **	93	$(\Sigma y)^2 / N$

Cont ...

Step	Calculations
96	$\left(\sum x \sum y - \frac{\sum x \sum y}{N}\right)^2$
97	$\frac{\left[\sum x \sum y - \frac{\sum x \sum y}{N}\right]^2}{\sum x^2 - \frac{(\sum x)^2}{N}}$ **
101	$\sum y^2 - \frac{(\sum y)^2}{N}$ **
103	$\left[\sum y^2 - \frac{(\sum y)^2}{N}\right] - \left[\sum x^2 - \frac{(\sum x)^2}{N}\right]$ **

The computer prints out the tube number, a series of values of Re and j_D and the slopes and intercepts of the regression lines (at steps 13, 22, 28, 83 and 90 respectively).

The computer punches out a data tape, for use with the following programmes, containing the tube number, the number of experimental values (N) and the various summations marked with an ** in the above table.

PROGRAMME 9:2

t Test Programme for Slope.

PR 5401 INTERPRETER.

RETAIN 1+

```
0001 INV        0020 INV        0039 INV        0058 000C+
0002 000D+      0021 INV        0040 C010-      0059 C015-
0003 000C+      0022 INV        0041 INV        0060 L006-
0004 INV        0023 C006-      0042 INV        0061 A012-
0005 C000-      0024 L005-      0043 C011-      0062 D015-
0006 D000-      0025 D004-      0044 INV        0063 SQR
0007 C001-      0026 C007-      0045 INV        0064 C016-
0008 A001-      0027 L001-      0046 INV        0065 L008-
0009 C002-      0028 D004-      0047 C012-      0066 A014-
0010 A002-      0029 C008-      0048 L011-      0067 M016-
0011 C003-      0030 0001+      0049 D010-      0068 C017-
0012 INV        0031 INV        0050 C013-      0069 L007-
0013 INV        0032 000D+      0051 L001-      0070 S013-
0014 INV        0033 000C+      0052 D010-      0071 D017-
0015 INV        0034 INV        0053 C014-      0072 000C+
0016 C004-      0035 C009-      0054 L000-      0073 000D+
0017 INV        0036 INV        0055 A009-      0074 000D+
0018 INV        0037 INV        0056 S003-      0075 JMP 030
0019 C005-      0038 INV        0057 000D+      0076 END
```

This programme could be used in two ways:-

(a) It allowed tube "a" to be compared with tubes "b", "c" "d", etc., as was done when the bundle average coefficient of Bergelin et al.(1) was compared with each of Williams (2) individual tube results.

(b) It allowed tube "a" to be compared with "b", "c" with "d", as was done when testing Williams results for identical tubes.

The output tapes from programme 9:1 were used as the input data for this programme. The halt at step 30 was incorporated to allow another input tape to be inserted into the tape reader. The computer carried out the following calculations.

(x,y being the results for tube 1 and x_i, y_i being the results for tube 2.)

Step	Calculation
6	1
8	2
10	4
25	$\left(\sum x \sum y - \frac{\sum x \sum y}{N_1}\right)\left(\sum x^2 - \frac{(\sum x)^2}{N_1}\right)^{-1} = S$
28	$\left(\sum x^2 - \frac{(\sum x)^2}{N_1}\right)^{-1}$
49	$\left(\sum x_i \sum y_i - \frac{\sum x_i \sum y_i}{N_2}\right)\left(\sum x_i^2 - \frac{(\sum x_i)^2}{N_2}\right)^{-1} = S_i$
52	$\left(\sum x_i^2 - \frac{(\sum x_i)^2}{N_2}\right)^{-1}$

Step	Calculation
56	$N_1 + N_2 - 4$ = Number of degrees of freedom.
61	$\dfrac{\left[\sum x \sum y - \dfrac{\sum x \sum y}{N}\right]^2}{\sum x^2 - \dfrac{(\sum x)^2}{N}} + \dfrac{\left[\sum x_i \sum y_i - \dfrac{\sum x_i \sum y_i}{N_2}\right]^2}{\sum x^2 - \dfrac{(\sum x)^2}{N_2}} = \ell + \ell_i$
62	$\dfrac{\ell + \ell_i}{N_1 + N_2 - 4}$
63	$\left(\dfrac{\ell + \ell_1}{N_1 + N_2 - 4}\right)^{\frac{1}{2}}$
66	$\left(\sum x^2 - \dfrac{(\sum x)^2}{N}\right)^{-1} + \left(\sum x_i^2 - \dfrac{(\sum x_i)^2}{N_2}\right)^{-1} = \dfrac{1}{q_v} + \dfrac{1}{q_{vi}}$
68	$\left(\dfrac{1}{q_v} + \dfrac{1}{q_{vi}}\right)\left(\dfrac{\ell + \ell_1}{N_1 + N_2 - 4}\right)^{\frac{1}{2}} = r$
70	$S - S_i$
71	$\dfrac{S - S_i}{r} = t$

The computer prints out the tube numbers being compared at steps 3 and 33, the number of degrees of freedom at step 58 and the value of t at step 72.

PROGRAMME 9:3

t Test Programme for Constant.

```
PR 5401  INTERPRETER.

RETAIN 1+

0001 INV        0020 INV        0039 INV        0058 D014-
0002 000D+      0021 INV        0040 D009-      0059 SQR
0003 000C+      0022 C006-      0041 C010-      0060 C016-
0004 INV        0023 INV        0042 INV        0061 L001-
0005 C000-      0024 INV        0043 D009-      0062 D000-
0006 D000-      0025 C007-      0044 C011-      0063 C017-
0007 C001-      0026 INV        0045 INV        0064 L001-
0008 A001-      0027 C008-      0046 INV        0065 D009-
0009 A001-      0028 0001+      0047 A005-      0066 A017-
0010 C002-      0029 INV        0048 C012-      0067 C018-
0011 INV        0030 000D+      0049 INV        0068 L003-
0012 D000-      0031 000C+      0050 INV        0069 S010-
0013 C003-      0032 INV        0051 A006-      0070 D018-
0014 INV        0033 C009-      0052 D012-      0071 D016-
0015 D000-      0034 A000-      0053 C013-      0072 000C+
0016 C004-      0035 S002-      0054 INV        0073 JMP 028
0017 INV        0036 C014-      0055 INV        0074 END
0018 INV        0037 000D+      0056 INV
0019 C005-      0038 000C+      0057 A008-
```

This programme was used to test pairs of tubes of identical slope obtained by programme 9:2. As with programme 9:2 a halt was incorporated at step 28 to allow input tapes to be fed into the tape reader.

The computer carried out the following calculations using the data tapes from programme 9:1.

Step	Calculation
6	1
8	2
9	3
12	$\frac{\sum y}{N_1}$
15	$\frac{\sum x}{N_1}$
34	$N_1 + N_2$
36	$N_1 + N_2 - 3$ = Number of degrees of freedom.
40	$\frac{\sum y_i}{N_2}$
43	$\frac{\sum x_i}{N_2}$
47	$\sum x^2 - \frac{(\sum x)^2}{N_1} + \sum x_i^2 + \frac{(\sum x_i)^2}{N_2} = q + q_i$
51	$\sum x \sum y - \frac{\sum x \sum y}{N_1} + \sum x_i \sum y_i - \frac{\sum x_i \sum y_i}{N_2} = \omega + \omega_i$

Step	Calculation
52	$\frac{\omega + \omega_i}{q + q_i}$
57	$\ell + \ell_i$ (see step 61 programme 9:2)
58	$\frac{\ell + \ell_i}{N_1 + N_2 - 3}$
59	$\left(\frac{\ell + \ell_i}{N_1 + N_2 - 3}\right)^{\frac{1}{2}}$
66	$\frac{1}{N_1} + \frac{1}{N_2}$
69	$\frac{\sum y}{N_1} - \frac{\sum y_i}{N_2}$
70	$\left(\frac{\sum y}{N_1} - \frac{\sum y_i}{N_2}\right)\left(\frac{1}{N_1} + \frac{1}{N_2}\right)^{-1}$
71	$\frac{\frac{\sum y}{N_1} - \frac{\sum y_i}{N_2}}{\left(\frac{1}{N_1} + \frac{1}{N_2}\right)\left(\frac{\ell + \ell_i}{N_1 + N_2 - 3}\right)^{\frac{1}{2}}} = t.$

The computer prints out the tube numbers being compared at steps 3 and 31, the number of degrees of freedom at step 36 and the value of t at step 72.

PROGRAMME 9:4

F TEST PROGRAMME FOR COMPARISON OF REGRESSION LINES

```
PR5401  INTERPRETER
RETAIN  1+
0001 INV        0022 S001-      0043 M021-      0064 C012-
0002 C000-      0023 C016-      0044 D020-      0065 INV
0003 D000-      0024 C017-      0045 A006-      0066 A013-
0004 C001-      0025 S001-      0046 C006-      0067 C013-
0005 A001-      0026 C018-      0047 INV        0068 INV
0006 C002-      0027 A002-      0048 A007-      0069 A014-
0007 S002-      0028 M002-      0049 C007-      0070 C014-
0008 C003-      0029 C019-      0050 INV        0071 L016-
0009 C004-      0030 0001+      0051 A008-      0072 S001-
0010 C005-      0031 INV        0052 C008-      0073 C016-
0011 C006-      0032 000D+      0053 INV        0074 T/J 076
0012 C007-      0032 000C+      0054 A009-      0075 JMP 030
0012 C008-      0034 INV        0055 C009-      0076 L004-
0014 C009-      0035 C020-      0056 INV        0077 S019-
0015 C010-      0036 A004-      0057 A010-      0078 C022-
0016 C011-      0037 C004-      0058 C010-      0079 L014-
0017 C012-      0038 INV        0059 INV        0080 D022-
0018 C013-      0039 C021-      0060 A011-      0081 C023-
0019 C014-      0040 A005-      0061 C011-      0082 L009-
0020 C015-      0041 C005-      0062 INV        0083 M017-
0021 L000-      0042 L021-      0063 A012-      0084 C034-
```

Programme 9:4 Cont ...

```
0085 L011-
0086 M011-
0087 C035-
0088 L009-
0089 M012-
0090 S035-
0091 D034-
0092 C024-
0093 L005-
0094 M005-
0095 C036-
0096 L006-
0097 M004-
0098 S036-
0099 D004-
0100 C025-
0101 L017-
0102 000D+
0103 000C+
0104 L022-
0105 000C+
0106 L024-
0107 D023-
0108 000C+
0109 L004-
0110 S000-
0111 S001-
0112 C037-
0113 L011-
0114 M011-
0115 D009-
0116 C039-
0117 L013-
0118 S039-
0119 D037-
0120 C038-
0121 L017-
0122 000D+
0123 000C+
0124 L037-
0125 000C+
0126 L025-
0127 D017-
0128 D038-
0129 000C+
0130 END
```

This programme was designed to test for groups of tubes whereas the "t" test only dealt with pairs of tubes.

The number of tubes being tested (k) was typed in by the keyboard at step 1 and the input tapes (from programme 9:1) were then fed in at the halt, step 30.

The computer carried out the following calculations.

Step	Calculations
3	1
5	2
7	0
22	$k - 1$
25	$k - 2$
28	$2k$
36	$N_{i1}, N_{i2}, N_{i3}, \ldots$
40	$\sum y_{i1} + \sum y_{i2} + \sum y_{i3} + \ldots + \sum y_{ik}$
43	$\left(\sum y\right)^2$
44	$\frac{\left(\sum y\right)^2}{N}$
45	$\frac{\left(\sum y_{i1}\right)^2}{N_{i1}} + \frac{\left(\sum y_{i2}\right)^2}{N_{i2}} + \ldots$
49	$\sum x_{i1} + \sum x_{i2} + \ldots$

Step	Calculations
51	$\frac{\left(\sum x_{i1}\right)^2}{N_{i1}} + \frac{\left(\sum x_{i2}\right)^2}{N_{i2}} + \ldots\ldots$
54	$q_1 + q_2 + q_3 + \ldots\ldots + q_k$
57	$\frac{\sum x_{i1} \sum y_{i1}}{N_{i1}} + \frac{\sum x_{i2} \sum y_{i2}}{N_{i2}} + \ldots\ldots$
60	$\omega_1 + \omega_2 + \omega_3 + \ldots\ldots \omega_k$
63	$\frac{\left[\sum x_{i1} \sum y_{i1} - \frac{\sum x_{i1} \sum y_{i1}}{N_{i1}}\right]^2}{\sum x_{i1}^2 - \frac{\left(\sum x_{i1}\right)^2}{N_{i1}}} + \frac{\left[\sum x_{i2} \sum y_{i2} - \frac{\sum x_{i2} \sum y_{i2}}{N_{i2}}\right]^2}{\sum x_{i2}^2 - \frac{\left(\sum x_{i2}\right)^2}{N_{i2}}} + \ldots$
	$= Z_1 + Z_2 + \ldots\ldots + Z_k$
66	$\left[\left(\sum y_{i1}^2 - \frac{\left(\sum y_{i1}\right)^2}{N_{i1}}\right) - \left(\sum x_{i1}^2 - \frac{\left(\sum x_{i1}\right)^2}{N_{i1}}\right)\right] + \ldots\ldots$
	$= h_1 + h_2 \ldots + \ldots\ldots$
69	$l_1 + l_2 + l_3 + \ldots l_k$ (see step 61 programme 9:2)
78	$\sum N_i - 2k$
80	$\frac{l_1 + l_2 + l_3 + \ldots + l_k}{\sum N_i - 2k} = s_1^2$

Step	Calculation
83	$\left(q_1 + q_2 + \ldots\ldots q_k\right)\left(k - 1\right)_1$
86	$\left(\omega_1 + \omega_2 + \ldots\ldots + \omega_k\right)^2$
91	$\dfrac{\left(q_1 + q_2 + \ldots + q_k\right)\left(z_1 + z_2 + \ldots + z_k\right) - \left(\omega_1 + \omega_2 + \ldots + \omega_k\right)}{\left(q_1 + q_2 + q_k\right)\left(k - 1\right)} = s_2^2$
94	$\left(\sum y_{i1} + \sum y_{i2} + \ldots\ldots + \sum y_{ik}\right)^2$
99	$\dfrac{\left(\sum N_i\right)\left(\dfrac{\sum y_{i1}}{N_{i1}} + \dfrac{\sum y_{i2}}{N_{i2}} + \ldots + \dfrac{\sum y_{ik}}{N_{ik}}\right) - \left(\sum y_{i1} + \sum y_{i2} + \ldots + \sum y_{ik}\right)^2}{\sum N_i} = j$
101	$k - 1$ = degrees of freedom f_{S1}
104	$\sum N_i - 2k$ = degrees of freedom f_{S2}
107	$F = \dfrac{s_2^2}{s_1^2}$
111	$\sum N_i - k - 1$
115	$\dfrac{\left(\omega_1 + \omega_2 + \ldots\ldots + \omega_k\right)^2}{\left(q_1 + q_2 + \ldots\ldots q_k\right)} = \sigma$
119	$\dfrac{\left(h_1 + h_2 + \ldots\ldots + h_k\right) - \sigma}{\sum N_i - k - 1} = \sim$

121 $k - 1$ = degrees of freedom f_{c1}

124 $\sum N_i - k - 1$ = degrees of freedom f_{c2}

128 $$\frac{j}{\sim(k - 1)} = F = \frac{S_6^2}{S_5^2}$$

The computer prints out the tube numbers being compared at step 33, the degrees of freedom f_{S1}, f_{S2} and the F value for the slope comparison at steps 103, 105 and 108 respectively. It then prints out the degrees of freedom f_{c1}, f_{c2} and the F value for the constant at steps 123, 125 and 129 respectively.

****
****
**

NOMENCLATURE

			Dimensions
A_C	=	Minimum flow area at centre row of tubes in bundle	L^2
A_W	=	Flow area in baffle window.	L^2
Cp	=	Fluid heat capacity at mean temperature	$L^2T^{-2}\theta^{-1}$
D	=	Mass diffusivity	L^2T^{-1}
d	=	Tube diameter	L
h	=	Heat transfer coefficient	$MT^{-3}\theta^{-1}$
j_D	=	j - factor for mass transfer = $\frac{k_C (Sc)^{\frac{2}{3}}}{u}$	-
j_H	=	j - factor for heat transfer = $\frac{h}{Cp\rho u}(Pr)^{\frac{2}{3}}$	-
k	=	Fluid thermal conductivity at mean temperature	$M L T^{-3} \theta^{-1}$
k_C	=	Mass transfer coefficient	$L T^{-1}$
l	=	Tube transfer length	L
Nu	=	Nusselt number = $\frac{h d}{k}$	-
Pr	=	Prandtl number = $\frac{Cp \mu}{k}$	-

			Dimensions.
Re	=	Reynolds number $= \frac{d u \varrho}{\mu}$	-
Sc	=	Schmidt number $= \frac{\mu}{\varrho D}$	-
S	=	Total transfer area in a baffle compartment	L^2
S_W	=	Transfer area in window zone	L^2
u	=	Average fluid velocity	$L\,T^{-1}$
μ	=	Viscosity at mean fluid temperature	$ML^{-1}T^{-1}$
ϱ	=	Density at mean fluid temperature	$M\,L^{-3}$

Subscripts.

A	=	Bundle average
C	=	Cross flow zone average.
M	=	Fluid velocity based on area A_C
Z	=	Fluid velocity based on window zone flow area $\sqrt{A_C A_W}$
W	=	Window zone average.
O	=	Data for flow normal to a single isolated cylinder.

BIBLIOGRAPHY.

1). O.P. BERGELIN, M.D. LEIGHTON, W.L.LAFFERTY Jr. and R.L.PIGFORD.
"Heat Transfer and Pressure Drop during Viscous and Turbulent Flow across Baffled and Unbaffled Tube Banks",
University of Delaware Engineering Experiments Station Bulletin, No.4, 1957.

2). T.A. WILLIAMS.
Ph.D Thesis, Manchester University, 1962.

3). T.H. CHILTON and A.P. COLBURN.
"Mass Transfer (Absorption) Coefficients".
Ind Engng Chem., ind (int.) Edn, 1934, Vol. 26, pages 1183 - 1187.

4). R.W. MAXWELL and J.A. STORROW.
"Mercury Vapour Transfer Studies - I".
Chem. Eng. Sci. 1957, Vol. 6, pages 204 - 214.

5*). O.E. POTTER.
Ph.D. Thesis, Manchester University, 1957.

6). J.N. HAGGART.
M.Sc. Thesis, Manchester University, 1962.

7). O.L. PIERSON.
"Experimental Investigation of the Influence of Tube Arrangement on Convection Heat Transfer and Flow Resistance in Cross Flow of Gases over Tube Banks.
TRANS. ASME, 1937, Vol, 59, pages 563 - 572.

8). A.P. COLBURN.

"A Method of Correlating Forced Convection Heat Transfer Data and a Comparison with Fluid Friction".

TRANS. ASME 1933, Vol. 29, pages 174 - 210.

9). E. C. HUGE.

"Effect of Equipment Size on Convection Heat Transfer and Flow-Resistance in Cross-Flow of Gases over Tube Banks".

TRANS. ASME, 1949, Vol. 71, pages 27 - 34.

† *
10). G.A. OMOHUNDRO, O.P. BERGELIN and A.P. COLBURN.

"Heat Transfer and Fluid Friction during Viscous Flow across Banks of Tubes".

TRANS. ASME, 1949, Vol. 71, pages 27 - 34.

† *
11). O.P. BERGELIN, E.S. DAVIS and H.L. HULL".

"A Study of three tube arrangements in unbaffled Tubular Heat Exchangers.

TRANS. ASME, 1949, Vol. 71, pages 369 - 374.

† *
12). O.P. BERGELIN, G.A. BROWN, H.L. HULL and F.W. SULLIVAN.

"Heat Transfer and Fluid Friction during Viscous Flow across Banks of Tubes - III".

TRANS. ASME 1950, Vol. 72, pages 881 - 888.

† *
13). O.P. BERGELIN, G.A. BROWN and S.C. DOBERSTEIN.

"Heat Transfer and Fluid Friction during Flow across Banks of Tubes - IV". TRANS. ASME 1952, Vol. 74, pages 953-960.

14). W. M. KAYS, A.L. LONDON and R.K. LO.
"Heat Transfer and Friction Characteristics for Gas Flow Normal to Tube Banks - Use of a Transient - Test Technique".
TRANS. ASME, 1954, Vol. 76, pages 387 - 396.

*15). H. THOMA , HOCHLEISTUNGKESSEL, JULIUS SPRINGER, BER LIN 1921.
(Cited by M. Jakob Heat Transfer. Vol. 1 pp. 605, 1959 Wiley).

16). C.C. WINDING and A.J. CHENEY.
"Mass and Heat Transfer in Tube Banks".
Ind. Eng. Chem. 1948, 40, p.1087

17). I.M. LEADLEY and D.R. OLIVER.
"The Examination of the Heat Transfer Behaviour of Banks of Tubes using a Mass/Heat Transfer Analogy".
Birmingham University Chem. Eng. 1962, 13, p.7.

18). J. WEISMAN.
"Effect of Void Volume and Prandth Modules on Heat Transfer in Tube Banks and Packed Beds".
A.I.Ch.E. Jl. 1955, Vol. I, pages 342 - 348.

19). A.S.T.THOMSON, A.W.SCOTT, A. McK. LAIRD and H.S. HOLDEN.
"Variation in Heat Transfer Rates around Tubes in Cross Flow",
General Discussion on Heat Transfer.
The Institution of Mechanical Engineers, London, 1951, pages 177-180.

20) N.W. SNYDER.
"Heat Transfer in Air from a Single Tube in a Staggered Tube-Bank"
C.E.P. Symposium Series, No.5, 1953, Vol. 49, pages 11-20.

21). T.V. SHEEHAN, R.T. SCHOMER and O.E. DWYER.
"Heat Transfer for Cross Flow of Water through a Tube Bank at Reynolds Numbers up to a million.
Part 1, ASME Paper No.54 - F - 19.

22). E.N. SIEDER and J.E. TATE.
"Heat Transfer and Pressure Drop of Liquids in Tubes".
Ind. Eng. Chem. 1936, 28 p.1429.

23). B. E. SHORT.
"Heat Transfer and Pressure Drop in Heat Exchangers".
University of Texas Publication No.4324/1943.

24). B. E. SHORT.
"The Effect of Baffle Height and Clearance on Heat Transfer and Pressure Drop in Heat Exchangers".
ASME Paper No.47 - A - 105.

25). D.A. DONOHUE.
"Heat Transfer and Pressure Drop in Heat Exchangers".
Ind. Eng. Chem. 1949, 41, pages 2499 - 2511.

26). T. TINKER.
"Shell Side Characteristics of Shell and Tube Heat Exchangers,
Parts 1, 11 and 111, General Discussion on Heat Transfer.
The Institution of Mechanical Engineers, London, 1951, pages 89-116.

27). O.P. BERGELIN, G.A. BROWN and A.P. COLBURN.
"Heat Transfer and Fluid Friction during Flow across Banks of Tubes - V"
TRANS. ASME 1954 Vol. 76, pages 53 - 60.

28). O.P. BERGELIN, K.J. BELL and M.D. LEIGHTON.
"Heat Transfer and Fluid Friction during Flow across Banks of Tubes - VI"
TRANS. ASME. 1958, Vol. 80, 5 pages 53 - 60.

29). K. J. BELL.
"Exchanger Design based on the Delaware Research Programme".
Petroleum Engineer, 1960, Vol. 32, pages C26 - C36, C.40a - C40c.

30). W.H. McADAMS.
"Heat Transmission" (Third Edition) McGraw - Hill Book Company INC. 1954.

31). R.K. GUPTA and D.L. KATZ.
"Flow Patterns for predicting shell-side Heat Transfer Coefficients for Baffled Shell and Tube Exchangers".
Ind. Eng. Chem. 1957, Vol. 49, page 998.

32). T.W. AMBROSE and J.C. KNUDSEN.
"Local Shell-side Heat Transfer Coefficients in Baffled Tubular Heat Exchangers".
A.I.Ch.E. Jl. 1958, 4, page 332.

33). W. H. GIEDT.
"Investigation of variation of point unit heat transfer coefficients around a cylinder normal to an air stream."
TRANS. ASME 1949 Vol. 71, page 375

34). GURUSHANKARIAH and J.G. KNUDSEN.
"Local shell-side heat transfer coefficients in the vicinity of segmental baffles in Tubular Heat Exchangers".
C.E.P. Symposium Series No.29, 1959, Vol. 55, page 29.

35). J. W. STACHIEWICZ and B. SHORT.

"Local shell side heat transfer coefficients in a leak proof Heat Exchanger".

International Developments in Heat Transfer, Colorado, 1961, page 959.

36). R.R. WHITE and S.W. CHURCHILL.

"Experimental foundations of Chemical Engineering".

A.I.Ch.E. Jl. 1959; 5, page 354.

37). R. J. MAUGHAM.

M.Sc. Tech. Thesis, Manchester University, 1961.

38). K.A. BROWNLEE.

"Statistical Theory and Methodology in Science and Engineering, 2nd Edition, J. Wiley, 1965.

39). CALIBRATION DATA for METRIC SERIES ROTAMETER.

Rotameter Manufacturing Co. Ltd., Croydon.

40). J. B. AKERS.

Ph.D. Thesis, Aston University. 1967.

41). F.M. ERNSBERGER and H.W. PITMAN.

Rev . Sci. Inst. 1955, Vol. 26, page 584.

42). J.O. HIRSCHFELDER, C.F. CURTISS and R.B. BIRD.

Molecular Theory of Gases and Liquids J. Wiley 1954.

43). R. C. REID and T.K. SHERWOOD.

"Properties of Gases and Liquids," McGraw-Hill 1958.

44). J. H. PERRY. Page 370.

45). J. H. PERRY. Page 176.

Chemical Engineers Handbook, 3rd Edition, Second Impression.
McGraw Hill 1952.

46). B. GAY and T.A. WILLIAMS.

"Bundle and zonal average heat transfer coefficients".

Trans. I. Ch. E. 1968, 46, No.3, 95.

*47). BRITISH THOMSON HOUSTON COMPANY. B.P.509,965 (1939).

*48). R. HILPERT.

"Experimental study of heat dissipation of heated wire and pipes in an air current".

FORSCHUNG AUF DEM GEBIETE DES INGENIEURWESENS.

Vol. 4, 1933, page 215. (cited by W. H. Giedt (33)).

* Actual references not consulted.

† These references were summarised by Bergelin et al. (1) and Bell (29).

****
****
**